CSCHOLAR Publishing INC

Volume 1 Number 1 2025

Advances in World Medical Research

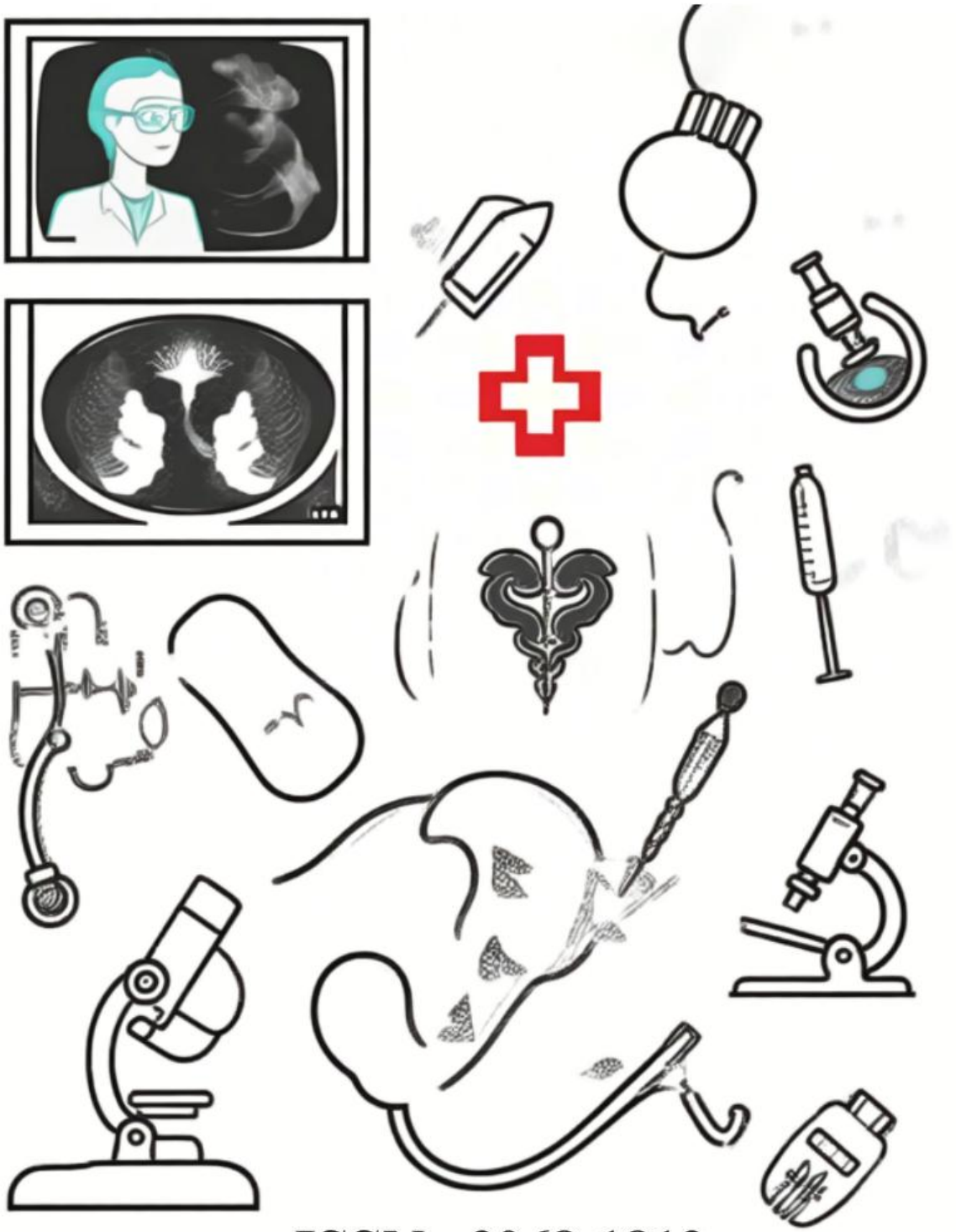

ISSN: 3068-1812

https://awmr.cscholar.com

Advances in World Medical Research

Volume 1, Issue 1, 2025

Quarterly (Issue No. 1)

Cover Design: ConnectSix Scholar Publishing INC

Publishing Unit: ConnectSix Scholar Publishing INC

Publisher's website: http://www.cscholar.com/

Publisher's address:

6547 N Academy Blvd #2265

Colorado Springs CO 80918

US

Website of the journal *Advances in World Medical Research*:

https://awmr.cscholar.com/

Table of contents

Advances in World Medical Research, 2025, 1(1), 1-2
https://doi.org/10.71204/pzd0wr39

Editorial Material

Unveiling the Inaugural Issue of Advances in World Medical Research

Wei Zhang [1, *]

[1] China Academy of Chinese Medical Science Eye Hospital, Beijing 100040, China.

* **Correspondence**:

Wei Zhang

wo_kaoyan@163.com

Received: 13 May 2025/ Accepted: 17 May 2025/ Published online: 20 May 2025

With immense pride and a deep sense of purpose, we are thrilled to present the inaugural issue of Advances in World Medical Research (AWMR). This milestone marks the beginning of a new chapter in the global pursuit of medical knowledge, innovation, and excellence. As an academic journal committed to a rigorous double-blind peer review process, AWMR is dedicated to advancing the frontiers of clinical medicine, healthcare, and related disciplines, fostering collaboration among researchers, clinicians, and scholars worldwide.

The first issue of AWMR showcases a diverse range of high-quality research articles that reflect the journal's broad scope and commitment to interdisciplinary collaboration. We are honored to feature three clinical articles on otorhinolaryngology, delving into the latest diagnostic and treatment approaches for ear, nose, and throat disorders. These studies not only contribute to the understanding of these complex conditions but also provide valuable insights for clinicians seeking to improve patient outcomes.

In addition to the otorhinolaryngology articles, this issue includes two fundamental research papers on oncology, one of which is a comprehensive review. These studies explore the latest advancements in cancer research, from molecular mechanisms to targeted therapies, offering a glimpse into the future of cancer treatment. By publishing these cutting-edge findings, AWMR aims to inspire further research and innovation in the fight against cancer.

Finally, we are delighted to present a clinical case report in ophthalmology, highlighting a rare and challenging case that underscores the importance of multidisciplinary collaboration in diagnosing and treating eye diseases. This article serves as a reminder of the critical role that clinical case reports play in sharing valuable experiences and knowledge among healthcare professionals.

At AWMR, we believe that the exchange of ideas and the dissemination of research findings are essential for the advancement of medical science. Our journal provides a platform for

researchers and clinicians to share their work, engage in scholarly discourse, and contribute to the global medical community. We invite submissions from researchers, clinicians, and scholars worldwide, covering a wide range of topics within the fields of clinical medicine, healthcare, and related disciplines.

As we embark on this exciting journey, we are committed to maintaining the highest standards of academic integrity, quality, and excellence. We look forward to working with you to shape the future of medical research and contribute to the improvement of healthcare worldwide.

Welcome to Advances in World Medical Research. We hope you enjoy reading this inaugural issue and look forward to your continued support and participation in our journal.

Advances in World Medical Research, 2025, 1(1), 3-17
https://doi.org/10.71204/j7y2f615

Role of BAZ2A in Cervical Cancer and Its Effect on Tumor Cell Metabolism

Jiarui Xue [1], Fenglin Dong [1], Yiwei Liu [1], Shuqing Wang [2,3]*, Fen Hu [1], Bin Zhang [4], Guijie Qi [5], Zhihao Shen [5], Rui Guo [5], Panyan Du [5], Ying Zhang [5], Mingjia Zhao [5], Liyuan Han [5], Linfeng Zhou [5], Jinghua Zhang [2,5,6]*, Yan Liu [1,6]*

[1] College of Life Science, North China University of Science and Technology, Tangshan 063210, China

[2] School of Public Health, North China University of Science and Technology, Tangshan 063210, China

[3] Hospital of North China University of Science and Technology, Tangshan 063210, China

[4] Academic Affairs Department, North China University of Science and Technology, Tangshan 063001, China

[5] Department of Clinical Laboratory, North China University of Science and Technology Affiliated Tangshan Maternal and Child Health Hospital, Tangshan 063000, China.

[6] Hebei Key Laboratory of Molecular Oncology, Tangshan 063001, China

*** Correspondence**:

Wang Shuqing

wsq7992023@163.com

Zhang Jinghua

jhzhang_te@163.com

Liu Yan

liuysm@ncst.edu.cn

Received: 2 April 2025/ Accepted: 12 May 2025/ Published online: 20 May 2025

Abstract

This study aims to investigate the role of BAZ2A in cervical cancer and its relationship with cancer development and glycolipid metabolism. BAZ2A knockdown experiments were performed in HeLa cells to study its effects on cell proliferation, invasion, cloning and migration; transcriptome and metabolome sequencing were also performed, and differentially expressed genes and metabolites were analyzed by GO and KEGG enrichment, etc. BAZ2A is highly expressed in cervical cancer, and the knockdown of BAZ2A inhibits the related malignant behaviors in HeLa cells. Transcriptome analysis identified a large number of differentially - expressed genes and related pathways, while metabolome analysis identified a variety of different

metabolites and related pathways. The joint analysis revealed that key genes and metabolites are involved in the BAZ2A regulatory network, affecting the related signaling pathways. Moreover, BAZ2A plays an important role in cervical cancer development and is closely related to glycolipid metabolism. In conclusion, BAZ2A affects cervical cancer development via cell proliferation, cloning, migration, invasion, and energy metabolism.

Keywords: BAZ2A; Cervical Cancer; Transcriptome; Metabolome; Enrichment Analysis

1. Introduction

Cancer has emerged as a global health problem with a continuously increasing morbidity and mortality (Bray et al., 2018; Sung et al., 2021). The development of tumors involves abnormal genetic and molecular mechanisms (Hanahan & Weinberg, 2011). Despite the advancements in research, the action mechanisms of certain key genes remain unclear (Xu et al., 2020; Johnson et al., 2019). Research on tumors mainly focuses on key genes and their underlying mechanisms. Despite the progress in cancer treatment, drug resistance and side - effects significantly affect the treatment efficacy and prognosis (Siegel et al., 2024). Therefore, investigating the pathogenesis of cancer is of crucial importance for the development of novel therapies to improve prognosis (Li et al., 2021).

BAZ2A serves as an epigenetic regulator that influences ribosomal RNA (rRNA) transcription (Dalle Vedove et al., 2022) and participates in rDNA heterochromatin formation by forming a complex with SNF2H (Bevill et al., 2019; Anosova et al., 2015). The PHD - BRD structural domain of BAZ2A is associated with rDNA silencing (Tallant et al., 2015; Bortoluzzi et al., 2017). BAZ2A promotes tumor invasion and cancer progression (GLi et al., 2018; Gu et al., 2015). Notably, it is highly expressed in prostate cancer, and this high expression is predictive of cancer (Pietrzak et al., 2020). The role of BAZ2A in cancer has been extensively investigated, with a focus on specific cancer types.

Our laboratory has been conducting research on the relationship between the BAZ family and tumors. Previously, we published a series of related research findings on this topic. For instance, "KRASG12 mutant induces the release of the WSTF/NRG3 complex and contributes to an oncogenic paracrine signaling pathway" (Gu et al., 2015) revealed the relationship between KRASG12 mutation and the release of the WSTF/NRG3 complex and its contribution to an oncogenic paracrine signaling pathway. "WSTF acetylation by MOF promotes WSTF activities and oncogenic functions" (Pietrzak et al., 2020) explored the acetylation of WSTF by MOF and its impact on WSTF activities and oncogenic functions. "Pan - cancer and multi - omics analyses revealed the diagnostic and prognostic value of BAZ2A in liver cancer" (Liu et al., 2016) demonstrated the diagnostic and prognostic value of BAZ2A in liver cancer through pan - cancer and multi - omics analyses. These research findings have laid the foundation for a further in - depth investigation of the role of the BAZ family in tumors.

Cervical cancer is one of the major malignant tumors in women and poses a serious health threat. Despite the progress in research, its pathogenesis has not been completely clarified (Liu et al., 2020; Liu et al., 2024). These research findings provide a basis for an in - depth exploration of

the role of the BAZ family in tumors. This study focuses on the role of BAZ2A in cervical cancer. It investigates the effects of BAZ2A on the proliferation, invasion, cloning, and migration of cervical cancer cells, as well as its regulatory mechanisms at the gene - expression and metabolic levels and its association with glycolipid metabolism.

2. Materials and Methods

2.1. Cell Culture

Colon cancer cells SW620, human mammary ductal carcinoma cells HCC38, cervical cancer cells HeLa, and human ovarian cancer cells SKOV3 (STR - validated cells) were kindly provided by Xaar Biological Laboratories (Tianjin, China). Cells were cultured in DMEM medium (Thermo, Waltham, MA, USA) supplemented with 10% FBS (Thermo) in an incubator maintained at 37°C with 5% CO2. SiRNAs (si - NC and si - BAZ2A) obtained from Saier Biotechnology Inc (Tianjin, China) were transfected into cells using Lipofectamine 2000 (Thermo). After a 4 - 6 h incubation in serum - free medium, the cells were then switched to serum - supplemented medium. The sequences of the siRNAs are as follows: si - BAZ2A: 5′ - GAG AGUGUC AGA CUA CUA UTT - 3′ and si - NC: 5′ - UUC UCC GAA CGU GUC ACG UTT - 3′.

2.2. RT-qPCR

The RNA of the cells was extracted using Trizol (Thermo) reagent. The FastKing RT kit (Takara, Chuo - ku, Osaka City, Japan) was used to synthesize cDNA from RNA. The SYBR Premix EX Taq Kit (Takara) was used for RT - PCR analysis. The mRNA level of BAZ2A was quantified using the $2^{-\Delta\Delta CT}$ method, with β - actin mRNA serving as an internal reference. The reaction was conducted under the following conditions: an initial denaturation at 94 °C for 30 s, followed by annealing at 58 °C for 30 s and extension at 72 °C for 30 s. This procedure was repeated 40 times.

The primer sequences used are as follows: For β - actin, sense: 5′ - CGT GAC ATT AAG GAG AAG CTG - 3′, antisense: 5′ - CTA GAA GCA TTT GCG GTG GAC - 3′; for BAZ2A, sense: 5′ - GGA GCA GCG GGT TAT CAT - 3′, antisense: 5′ - CAC AGC CAG GTC CAA AGG - 3′.

2.3. CCK8

After being transfected with siRNA, the cells were inoculated into 96 - well plates at a concentration of 2×10^3 cells per well and then incubated for 24 h. Subsequently, the cells were washed with PBS. The cells were treated with CCK8 reagent (Thermo) and incubated for 2 h. Then, the OD value was measured using a microreader.

2.4. Protein Blotting

After lysing the cells, the protein concentration was measured using the BCA Quantitation Kit (Thermo). Subsequently, an equal amount of protein was separated by 6% SDS - PAGE and then transferred onto a nitrocellulose filter membrane. At room temperature, the membrane was incubated in 3% skim milk for 2 h to block non - specific binding. In this study, since incubating

multiple antibodies simultaneously would interfere with each other, resulting in mixed bands, the membrane was cut and then incubated overnight at 4 °C with specific primary antibodies respectively: BAZ2A (ab290639, Abcam, Cambridge, MA, USA), GADPH (ab8245, Abcam), BAX (ab32503, Abcam), Snail (MA5 - 14801, Thermo), p53 (GTX34938, GeneTex, TX, USA), Bcl - 2 (GTX100064, GeneTex), Vimentin (GTX40346, GeneTex), E - cadherin (CSB - RA576116A0HU, CUSABIO, Wuhan, China), and N - cadherin (CSB - RA243509A0HU, CUSABIO). The membrane was incubated with the corresponding secondary antibody (CSB - PA564648/CSB - PA573747, CUSABIO) for 1 h. The ECL chemiluminescence substrate (PerkinElmer, Waltham, MA, USA) was used to visualize the bands.

2.5. Transwell Assay

A suspension of 1×10^5 cells in 100 μL of serum - free medium was added to the upper chamber of a Transwell apparatus, and 750 μL of serum - containing medium was added to the lower chamber. Three biological replicates were included for each condition. The plates were incubated for 12 - 16 h, and then the chambers were removed. The filter was fixed with 4% paraformaldehyde (BL539A, Biosharp, Beijing, China) and then incubated with 800 μL of 0.5% crystal violet (G1063, Solarbio, Beijing, China) solution for 15 min in the dark. The samples were observed using an inverted microscope. Each sample was randomly examined in five different fields of view, and the number of cells passing through the filtration membrane was counted. For invasion assays, Matrigel (Corning, NY, USA), diluted 1:8 with serum - free medium, was added to the lower chamber and incubated for 5 h in a 37 °C incubator. The cells were then evaluated as described above.

2.6. Clone Formation Assay

Cells were seeded into six - well plates at densities of 50, 100, or 200 cells per well and subsequently cultured for 2 - 3 weeks. After the removal of the medium, the plates were rinsed twice with PBS and subsequently fixed in 5 mL of pure methanol for 15 min. Following the removal of the fixative solution, the cells were stained with 0.4% crystal violet for a duration of 10 - 30 min. The plates were washed, air - dried, and subsequently photographed. The number of colonies was counted to quantify them.

2.7. Transcriptome Sequencing Analysis

Samples were collected using Trizol Reagent (Invitrogen, Carlsbad, CA, USA) at a cell density of 5×10^6 cells per mL. Transcriptome sequencing was conducted by Zhongke New Life Biotechnology Co., Ltd (China).

2.8. Metabolome Sequencing Analysis

The constructed cells were expanded, cultured, and subsequently inoculated into T75 cell - culture flasks, with 6 replicates per group and a cell number of 10^7 or above per sample. Then, cell samples were collected. Metabolome sequencing was conducted by Zhongke New Life Biotechnology Co., Ltd (China).

2.9. Statistical Analysis

Statistical analyses were conducted using GraphPad Prism 8.2.1, and group comparisons were performed via Student's t - test. A P - value of less than 0.05 was regarded as statistically significant.

3. Results

3.1. BAZ2A is Highly Expressed in Cervical Cancer and Promotes Malignant Behaviors of Cervical Cancer Cells

We first detected the expression level of BAZ2A in multiple tumor cell lines by qRT-PCR. Results showed that BAZ2A was most highly expressed in colorectal cancer SW620 cells (Figure. 1A). We then designed siRNAs targeting BAZ2A (si-BAZ2A-1, si-BAZ2A-2, si-BAZ2A-3) and validated their interference efficiency in SW620 cells via qRT-PCR and Western blot. qRT-PCR showed a significant reduction in BAZ2A mRNA levels with si-BAZ2A-2 compared to the control group (si-NC) (Figure. 1B). Western blot further confirmed a marked decrease in BAZ2A protein expression after si-BAZ2A-2 treatment (Figure. 1C), indicating that si-BAZ2A-2 had the optimal interference efficiency.

Given the extensive use of HeLa cells in tumor research due to their unique biological properties and our laboratory's stable culture conditions, we selected HeLa cells with intermediate expression levels for subsequent experiments (Masters, 2002). The effects of BAZ2A on cell proliferation, invasion, colony formation, and migration were analyzed using CCK8, Transwell, colony formation, and scratch wound-healing assays. Knockdown of BAZ2A significantly reduced the proliferative capacity of HeLa cells (Figure. 1D), decreased the number of invasive cells (Figure. 1E), reduced colony formation (Figure. 1F), and shortened migration distance (Figure. 1G). These results collectively indicate that BAZ2A knockdown inhibits proliferation, colony formation, migration, and invasion in HeLa cells.

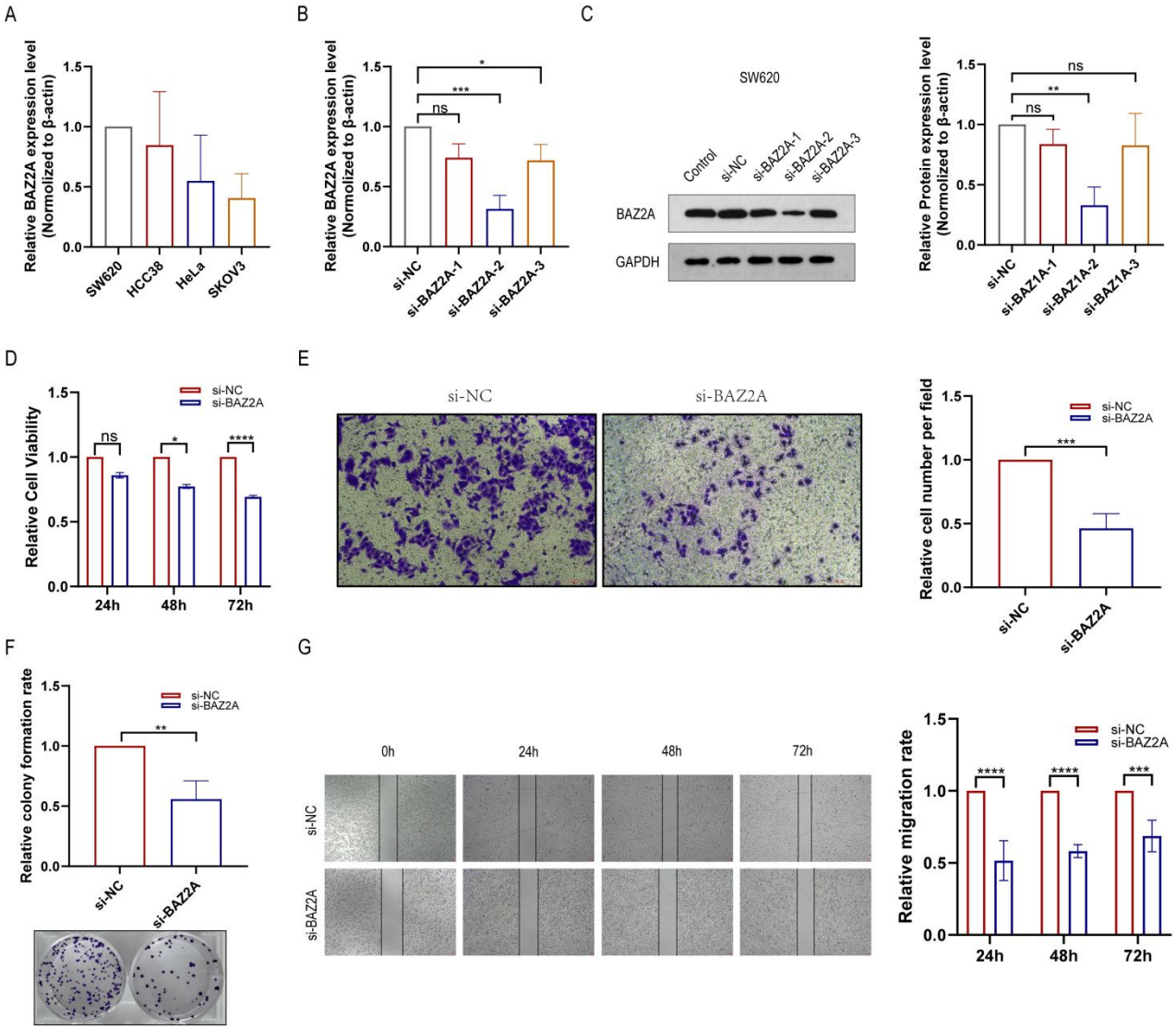

Figure 1. BAZ2A is Upregulated in Cervical Cancer and Promotes Malignant Behaviors in Cervical Cancer Cells

Notes: (A) qRT - PCR Analysis of BAZ2A mRNA Expression in Cervical Cancer Cell Lines. (B) Validation of siRNA Targeting BAZ2A by qRT - PCR in SW620 Cells. (C) Validation of siRNA Targeting BAZ2A by Western Blot in SW620 Cells. (D) The Role of BAZ2A in the Proliferation of HeLa Cells. (E) The Role of BAZ2A in the Invasion of HeLa Cells. (F) The Role of BAZ2A in the Cloning of HeLa Cells. (G) The Role of BAZ2A in the Migration of HeLa Cells. *P < 0.05, **P < 0.005, ***P < 0.001. P - values Less Than 0.05 Were Considered Statistically Significant.

3.2. Transcriptome Analysis of BAZ2A

To investigate the association between BAZ2A and cancer, transcriptome sequencing was performed on cells with BAZ2A knockdown or NC-siRNA transfection. A total of 6,825 differentially expressed genes (DEGs) were identified, including 3,911 upregulated and 2,914 downregulated genes (Figure. 2A). Heatmap analysis showed that DEGs were associated with key processes in tumorigenesis (Figure. 2B).

GO and KEGG enrichment analyses were conducted to annotate DEG functions. GO analysis revealed significant enrichment of 1,689 GO terms ($P < 0.05$), with 81.8% related to biological

processes (BP), including carbohydrate metabolism and lipid metabolic processes (e.g., carbohydrate metabolism, lipid metabolism regulation and transport); 11.6% related to molecular functions (MF), such as anion binding, enzyme binding, and transferase activity; and 6.6% related to cellular components (CC), including plasma membrane, vesicles, ribosomes, and glycogen granules (Liu et al., 2021; Aktary et al., 2017; Stanley, 2011; Jiao et al., 2023; Pecoraro et al., 2021; Neoh et al., 2024) (Figure. 2C-E). These results are illustrated by the directed acyclic plots in Supplementary Figure 1A-C. KEGG analysis showed that DEGs were primarily enriched in tumor progression and metabolic pathways, such as "Pathways in Cancer," "mTOR signaling pathway," and "insulin signaling pathway" (Figure. 2F). the mTOR signaling pathway plays a central role in cellular metabolism (Zou et al., 2020), suggesting that BAZ2A may influence glycolipid metabolism via regulating the mTOR pathway. Detailed information is presented in Supplementary Figure 1D.

Protein-protein interaction network analysis identified ribosomal protein RPS12 as a central node in DEG interactions (Figure. 2G), whose aberrant expression is closely linked to tumorigenesis (Katanaev et al., 2020). Transcription factor annotation revealed enrichment of zf-C2H2 zinc finger proteins, Homeobox, and bHLH family transcription factors in DEGs (Figure. 2H), indicating that BAZ2A may regulate cell differentiation and proliferation by modulating these transcription factors (Zhang et al., 2024; Grier et al., 2005; Putarjunan et al., 2016). Alternative splicing analysis showed that BAZ2A knockdown disrupted mTOR and insulin signaling pathways (Figure. 2I-J), further supporting its role in cellular metabolism and proliferation.

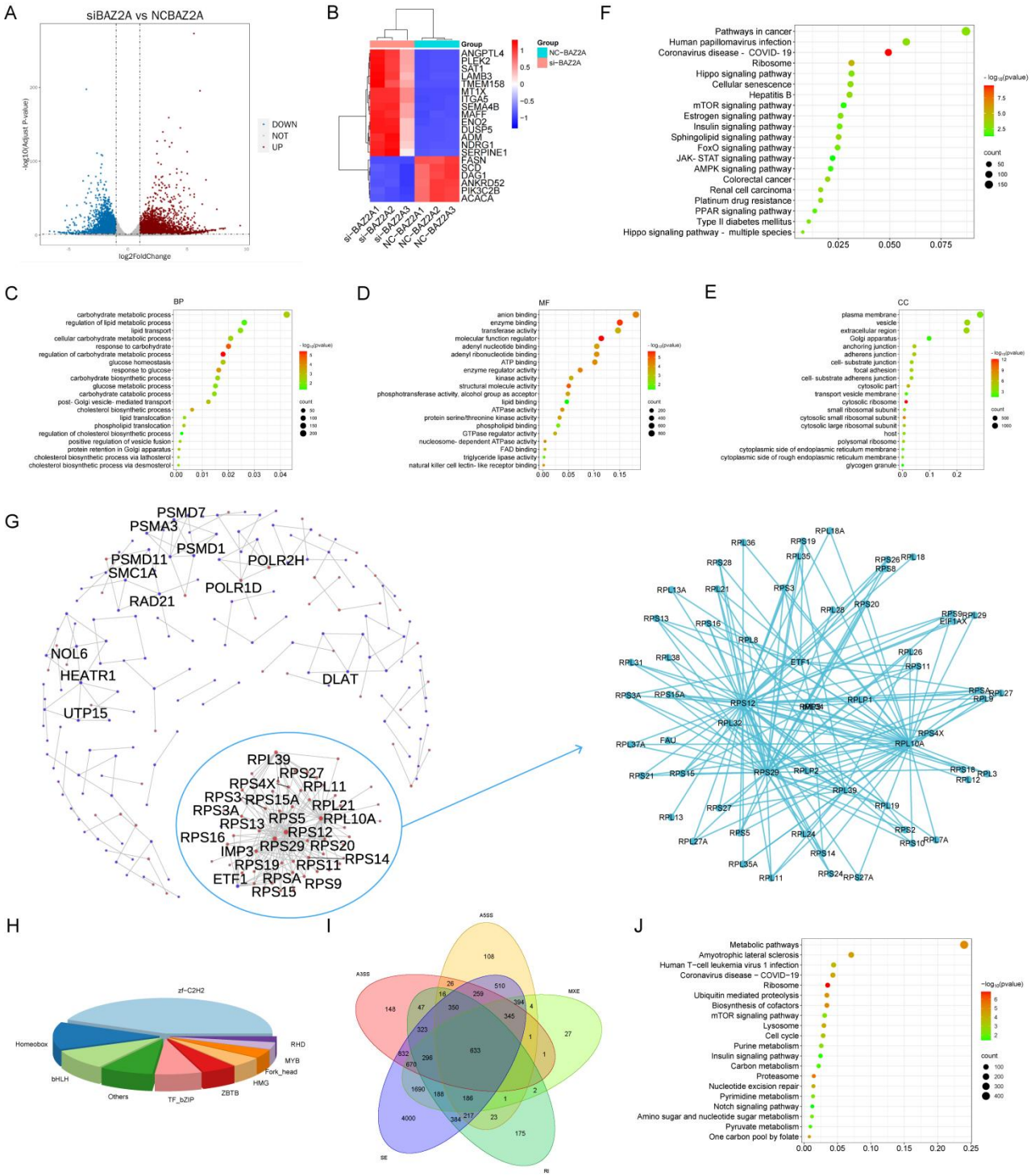

Figure 2. BAZ2A Transcriptome Analysis

Notes: (A) Volcano Plot of Differentially Expressed Genes (DEGs). (B) Heat Map of the Top 20 DEGs. (C - E) GO Enrichment Bubble Diagrams of Differential Genes: (C) Biological Process (BP), (D) Molecular Function (MF), (E) Cellular Component (CC). (F) KEGG Enrichment Bubble Diagram of Differential Genes. (G) Interaction Network Diagram of the Top 300 Differentially Expressed Genes. (H) Pie Chart of Transcription Factor Family Information Statistics. (I) Venn Diagram of Differential Analysis of Alternative Splicing Events (FDR < 0.05 Was Used as the Screening Criterion for Differential AS Events). (J) KEGG Enrichment Bubble Plot of Alternative Splicing Genes.

3.3. Metabolome Analysis of BAZ2A

Metabolome analysis in positive and negative ion modes identified 4,839 (positive ion) and 3,699 (negative ion) differential metabolites, with 1,969/2,870 (positive ion) and 1,464/2,235 (negative ion) metabolites upregulated/downregulated, respectively (Figure. 3A-B). Heatmaps of the top 20 differential metabolites showed their association with tumor development, energy metabolism, and signaling (Figure. 3C-F).

KEGG analysis revealed significant enrichment of differential metabolites in glycolipid metabolism pathways, such as "Central Carbon Metabolism in Cancer" and "Citrate Cycle (TCA Cycle)" (Figure. 3G). Further analysis showed that BAZ2A knockdown enhanced glycolytic activity while inhibiting pyruvate conversion into the TCA cycle, leading to truncation of mitochondrial TCA cycle. Citrate was redirected to extramitochondrial fatty acid synthesis, restricting cis-aconitic acid and isocitric acid synthesis—although isocitric acid accumulated due to upstream substrate buildup. Fumarate synthase dysfunction blocked malate production from fumarate, causing fumarate accumulation (Figure. 3H). These metabolic alterations collectively promoted abnormal cell proliferation and metabolic reprogramming, providing a metabolic basis for cancer cell energy demands.

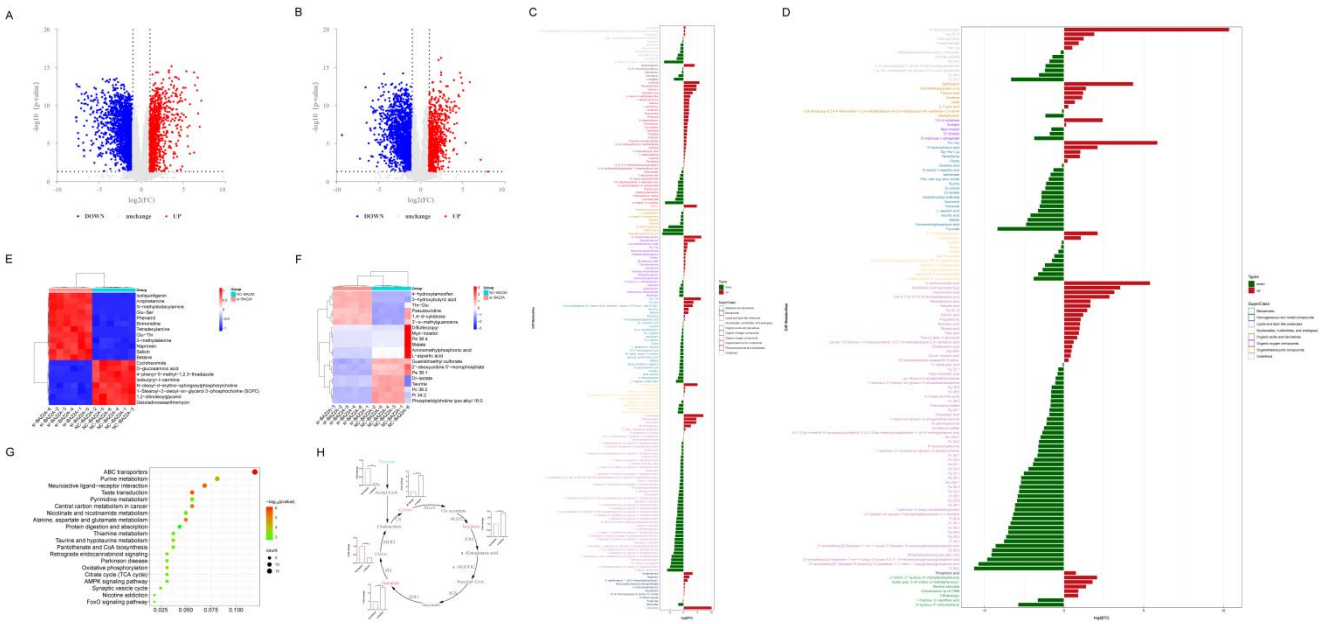

Figure 3. BAZ2A Metabolome Analysis

Notes: (A) Volcano Plot of Differential Metabolites in the Positive Ion Mode (FC > 1.5 or FC < 0.67, P - value < 0.05). (B) Volcano Plot of Differential Metabolites in the Negative Ion Mode (FC > 1.5 or FC < 0.67, P - value < 0.05). (C) Fold - Change Analysis of Significant Differential Metabolites in the Positive Ion Mode. (D) Fold - Change Analysis of Significant Differential Metabolites in the Negative Ion Mode. (E) Heat Map of the Top 20 Differential Metabolites in the Positive Ion Mode. (F) Heat Map of the Top 20 Differential Metabolites in the Negative Ion Mode. (G) KEGG Enrichment Bubble Diagram of Differential Metabolites. (H) The Tricarboxylic Acid Cycle Pathway with Intermediate Metabolites and Response - Regulating Enzymes. Up - regulated Differential Metabolites Are Shown in Red, Down - regulated Metabolites Are Shown in Blue, and Metabolites with Insignificant Changes Are Shown in Black. The Bar Graphs Represent the Statistical Plots of the Metabolites with Significant Differences. *P < 0.05, **P < 0.005, ***P < 0.001. P - values Less Than 0.05 Were Considered Statistically Significant.

3.4. Joint Analysis of Transcriptome and Metabolome for BAZ2A

The PCA plots of Figure 4A, B showed reliable reproducibility. Analysis of the Venn diagram (Figure 4C) revealed that 338 and 154 differentially expressed genes and metabolites were involved in the pathway in the transcriptome and metabolome, respectively, of which six were shared. This finding indicates that there are co - regulated genes and metabolites under BAZ2A regulation. Analysis demonstrated that among the top 10 pathways jointly involved by the transcriptome and metabolome, the “cAMP signaling pathway” (with “cAMP” being cyclic adenosine monophosphate) was highly implicated. This suggests that BAZ2A may synergistically regulate gene expression and metabolism via this pathway, thereby influencing cell physiological processes (Figure 4D). Following the knockdown of BAZ2A, the AMPK, FoxO, and mTOR signaling pathways were affected. This implies that BAZ2A plays a role in cellular energy metabolism and tumor development. Moreover, BAZ2A may indirectly regulate glucose and lipid metabolism by influencing these signaling pathways, which subsequently impact tumor development (Figure 4E).

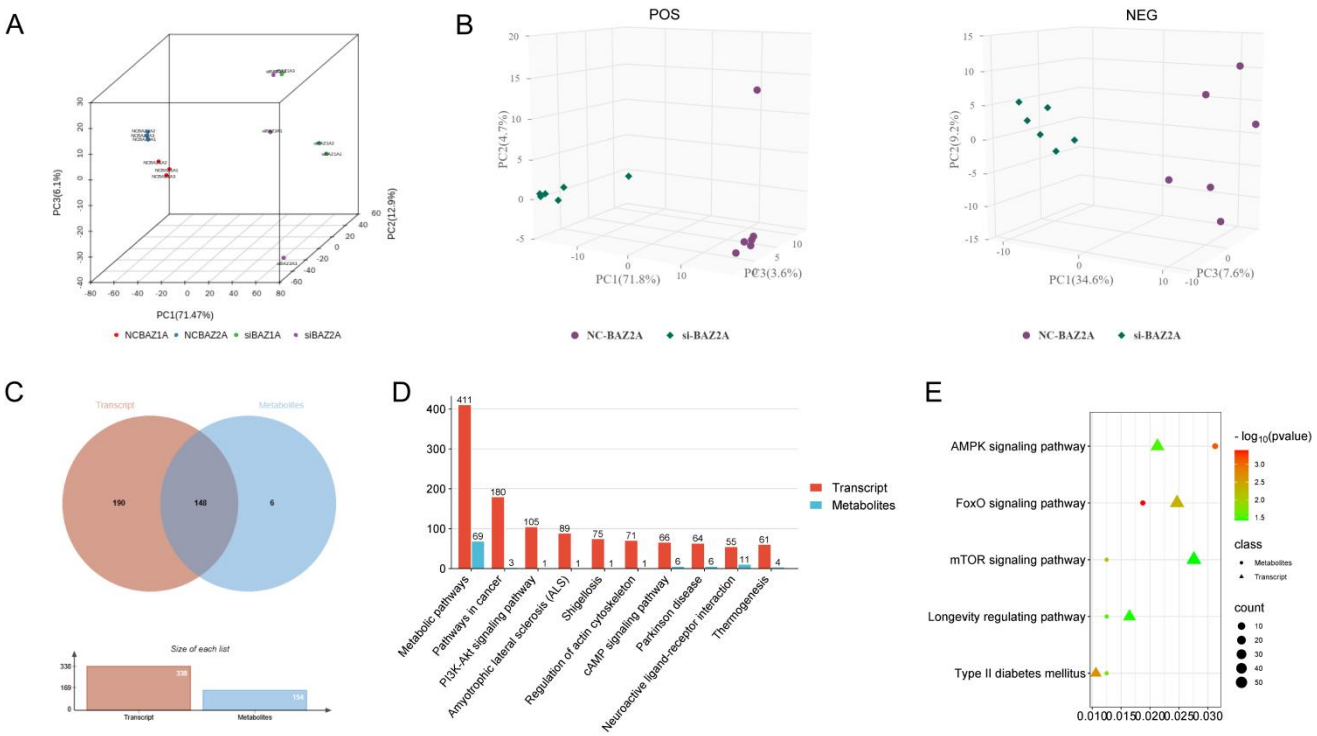

Figure 4. Joint Metabolome and Transcriptome Analysis of BAZ2A

Notes: (A) PCA Plots of Differentially Expressed Genes. (B) PCA Plots of Differential Metabolites. (C) Venn Diagram of Differentially Expressed Genes and Differential Metabolites Involved in the Pathways. (D) The Top 10 Pathways with the Highest Number of Jointly Involved Genes and Metabolites. (E) KEGG Enrichment Bubble Plot of Differential Genes Versus Differential Metabolites.

4. Discussion

In this study, we discovered that BAZ2A is highly expressed in cervical cancer. Moreover, the reduction of BAZ2A levels inhibited multiple malignant behaviors in HeLa cells, indicating that it plays a significant role in the growth and metastasis of cervical cancer cells. Transcriptome

analysis identified 6825 differentially expressed genes, which were significantly enriched in processes related to glycolipid metabolism. Additionally, GO and KEGG analyses unveiled the potential role of BAZ2A in cellular signaling and other aspects.

Metabolomic analysis identified a variety of differential metabolites related to tumor development, energy metabolism, and signaling in both ionic modes. KEGG analysis further revealed an enrichment of glycolipid metabolism - related pathways. These pathways impact cellular energy and material metabolism and furnish a metabolic foundation for cancer cell proliferation and migration.

Joint transcriptome and metabolome analysis demonstrated that key genes and metabolites in both were jointly implicated in the BAZ2A regulatory network, thereby affecting signaling pathways such as AMPK, FoxO, and mTOR. These pathways indirectly regulate glycolipid metabolism and consequently influence tumor development. Therefore, we hypothesize that BAZ2A may influence cell proliferation and migration via metabolic reprogramming, which subsequently impacts tumorigenesis and development.

Appendix

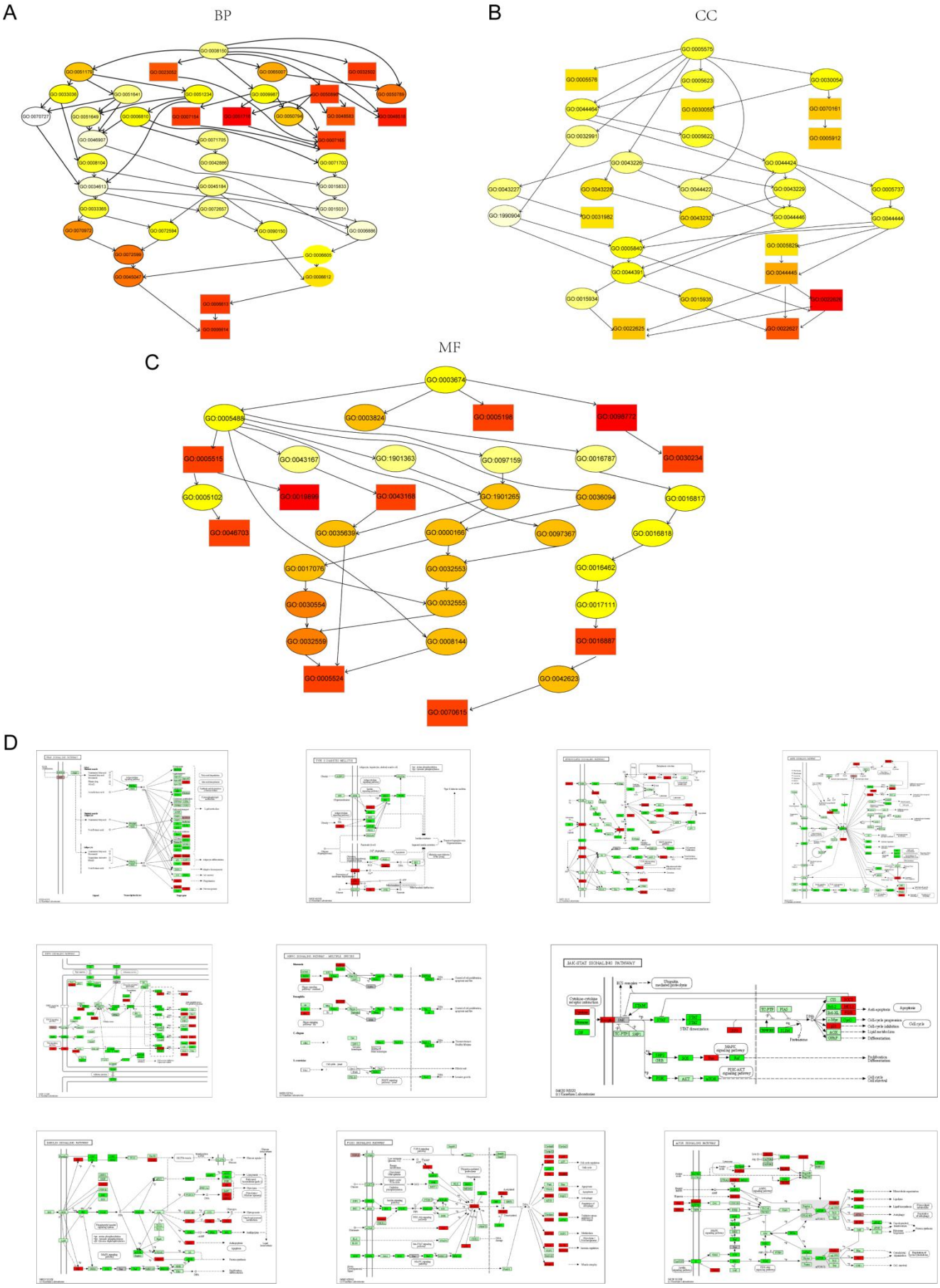

Supplementary figure 1. BAZ2A Transcriptome Analysis

Notes: (A - C) Directed acyclic graphs illustrating GO analysis of differentially expressed proteins (DEP) in biological process (BP) (A), molecular function (MF) (C), and cellular component (CC) (B). (D) KEGG pathway annotation map for differential expression analysis.

Institutional Review Board Statement:

The manuscript does not contain clinical studies or patient data.

Acknowledgments:

The author expresses gratitude for the assistance provided by Shanghai Zhongke New Life Biotechnology Co., Ltd.

Funding:

This work was primarily supported by the Central Government Guides Local Science and Technology Development Fund Projects, China (246Z7740G).

Data Availability Statement::

The data that support the findings of this study are available from the corresponding author upon reasonable request.

Author Contributions:

L. Y, W. Q and Z. H conceived and designed the study. H. F and Z. B prepares experimental materials. X. R analyzed the data. X. R wrote the manuscript. X. R, D. L and L. W confirm the authenticity of all the raw data. All authors read and approved the final manuscript.

Informed Consent Statement:

All patients provided their informed consent.

Conflict of Interest:

The authors declare no competing interests.

References

Aktary, Z., Alaee, M., & Pasdar, M. (2017). Beyond cell-cell adhesion: Plakoglobin and the regulation of tumorigenesis and metastasis . Oncotarget , 8(19), 32270–32291.

Anosova, I., Melnik, S., Tripsianes, K., Kateb, F., Grummt, I., & Sattler, M. (2015). A novel RNA binding surface of the TAM domain of TIP5/BAZ2A mediates epigenetic regulation of rRNA genes . Nucleic Acids Research , 43(10), 5208–5220.

Bevill, S. M., Olivares-Quintero, J. F., Sciaky, N., Golitz, B. T., Singh, D., Beltran, A. S., et al. (2019). GSK2801, a BAZ2/BRD9 Bromodomain Inhibitor, Synergizes with BET Inhibitors to Induce Apoptosis in Triple-Negative Breast Cancer . Molecular Cancer Research , 17(7), 1503–1518.

Bortoluzzi, A., Amato, A., Lucas, X., Blank, M., & Ciulli, A. (2017). Structural basis of molecular recognition of helical histone H3 tail by PHD finger domains . The Biochemical

Journal , 474(10), 1633–1651.

Bray, F., Ferlay, J., Soerjomataram, I., Siegel, R. L., Torre, L. A., & Jemal, A. (2018). Global cancer statistics 2018: GLOBOCAN estimates of incidence and mortality worldwide for 36 cancers in 185 countries . CA: A Cancer Journal for Clinicians , 68(6), 394–424.

Dalle Vedove, A., Cazzanelli, G., Batiste, L., Marchand, J. R., Spiliotopoulos, D., Corsi, J., et al. (2022). Identification of a BAZ2A-Bromodomain Hit Compound by Fragment Growing . ACS Medicinal Chemistry Letters , 13(9), 1434–1443.

GLi, C., Wu, W., Ding, H., Li, Q., & Xie, K. (2018). The transcription factor 7 like 2-binding protein TIP5 activates β-catenin/transcription factor signaling in hepatocellular carcinoma . Molecular Medicine Reports , 17(6), 7645–7651.

Grier, D. G., Thompson, A., Kwasniewska, A., McGonigle, G. J., Halliday, H. L., & Lappin, T. R. (2005). The pathophysiology of HOX genes and their role in cancer . The Journal of Pathology , 205(2), 154–171.

Gu, L., Frommel, S. C., Oakes, C. C., Simon, R., Grupp, K., Gerig, C. Y., et al. (2015). BAZ2A (TIP5) is involved in epigenetic alterations in prostate cancer and its overexpression predicts disease recurrence . Nature Genetics , 47(1), 22–30.

Hanahan, D., & Weinberg, R. A. (2011). Hallmarks of cancer: the next generation . Cell , 144(5), 646–674.

Jiao, L., Liu, Y., Yu, X. Y., Pan, X., Zhang, Y., Tu, J., et al. (2023). Ribosome biogenesis in disease: new players and therapeutic targets . Signal Transduction and Targeted Therapy , 8(1), 15.

Johnson, C. A., James, D., Marzan, A., & Armaos, M. (2019). Cervical Cancer: An Overview of Pathophysiology and Management . Seminars in Oncology Nursing , 35(2), 166–174.

Katanaev, V. L., Kryuchkov, M., Averkov, V., Savitsky, M., Nikolaeva, K., Klimova, N., et al. (2020). HumanaFly: high-throughput transgenesis and expression of breast cancer transcripts in Drosophila eye discovers the RPS12-Wingless signaling axis . Scientific Reports , 10(1), 21013.

Li, H., Fang, H., Chang, L., Qiu, S., Ren, X., Cao, L., et al. (2021). TC2N: A Novel Vital Oncogene or Tumor Suppressor Gene In Cancers . Frontiers in Immunology , 12, 764749.

Liu, J., Ren, L., Li, S., Li, W., Zheng, X., Yang, Y., et al. (2021). The biology, function, and applications of exosomes in cancer . Acta Pharmaceutica Sinica. B , 11(9), 2783–2797.

Liu, Y., Wang, J., Guo, J., Zhang, Q., Wang, S., Hu, F., et al. (2024). *Pan-cancer and multi-omics analyses revealed the diagnostic and prognostic value of BAZ2A in liver cancer*. Scientific Reports , 14(1), 5228.

Liu, Y., Wang, S. Q., Long, Y. H., Chen, S., Li, Y. F., & Zhang, J. H. (2016). KRASG12 mutant induces the release of the WSTF/NRG3 complex, and contributes to an oncogenic paracrine signaling pathway . Oncotarget , 7(33), 53153–53164.

Liu, Y., Zhang, Y. Y., Wang, S. Q., Li, M., Long, Y. H., Li, Y. F., et al. (2020). WSTF acetylation by MOF promotes WSTF activities and oncogenic functions . Oncogene , 39(27), 5056–5067.

Masters, J. R. (2002). HeLa cells 50 years on: the good, the bad and the ugly . Nature Reviews. Cancer , 2(4), 315–319.

Neoh, G. K. S., Tan, X., Chen, S., Roura, E., Dong, X., & Gilbert, R. G. (2024). Glycogen metabolism and structure: A review . Carbohydrate Polymers , 346, 122631.

Pecoraro, A., Pagano, M., Russo, G., & Russo, A. (2021). Ribosome Biogenesis and Cancer: Overview on Ribosomal Proteins . International Journal of Molecular Sciences , 22(11), 5496.

Pietrzak, K., Kuzyakiv, R., Simon, R., Bolis, M., Bär, D., Aprigliano, R., et al. (2020). TIP5 primes prostate luminal cells for the oncogenic transformation mediated by PTEN-loss . Proceedings of the National Academy of Sciences of the United States of America , 117(7), 3637–3647.

Putarjunan, A., & Torii, K. U. (2016). Stomagenesis versus myogenesis: Parallels in intrinsic and extrinsic regulation of transcription factor mediated specialized cell-type differentiation in plants and animals . Development, Growth & Differentiation , 58(4), 341–354.

Siegel, R. L., Giaquinto, A. N., & Jemal, A. (2024). Cancer statistics, 2024 . CA: A Cancer Journal for Clinicians , 74(1), 12–49.

Stanley, P. (2011). Golgi glycosylation . Cold Spring Harbor Perspectives in Biology , 3(4), a005199.

Sung, H., Ferlay, J., Siegel, R. L., Laversanne, M., Soerjomataram, I., Jemal, A., et al. (2021). Global Cancer Statistics 2020: GLOBOCAN Estimates of Incidence and Mortality Worldwide for 36 Cancers in 185 Countries . CA: A Cancer Journal for Clinicians , 71(3), 209–249.

Tallant, C., Valentini, E., Fedorov, O., Overvoorde, L., Ferguson, F. M., Filippakopoulos, P., et al. (2015). Molecular basis of histone tail recognition by human TIP5 PHD finger and bromodomain of the chromatin remodeling complex NoRC . Structure , 23(1), 80–92.

Xu, H. H., Yan, W. H., & Lin, A. (2020). The Role of HLA-G in Human Papillomavirus Infections and Cervical Carcinogenesis . Frontiers in Immunology , 11, 1349.

Zhang, X., Xia, F., Zhang, X., Blumenthal, R. M., & Cheng, X. (2024). C2H2 Zinc Finger Transcription Factors Associated with Hemoglobinopathies . Journal of Molecular Biology , 436(7), 168343.

Zou, Z., Tao, T., Li, H., & Zhu, X. (2020). mTOR signaling pathway and mTOR inhibitors in cancer: progress and challenges . Cell & Bioscience , 10, 31.

Advances in World Medical Research, 2025, 1(1), 18-33
https://doi.org/10.71204/mny7mr80

Research Progress on the Relationship Between WSTF and Cancer

Yunjie Pei [1], Yan Liu [2], Shuqing Wang [3], Yuanyue Zhang [4], Jinghua Zhang [5],*

[1] Affiliated Hospital of North China University of Science and Technology, Tangshan 063000, China

[2] College of Life Science, North China University of Science and Technology, Tangshan 063210, China

[3] Hospital of North China University of Science and Technology, Tangshan 063210, China

[4] Center Laboratory of Nanjing Medical University BenQ hospital Suzhou Campus, Suzhou 215000, China

[5] Department of Tangshan Maternal and Child Health Hospital, Tangshan 063000,China

*** Correspondence**:

Jinghua Zhang

jhzhang_te@163.com

Received: 4 April 2025/ Accepted: 14 May 2025/ Published online: 20 May 2025

Abstract

The Williams syndrome transcription factor (WSTF, alternatively termed BAZ1B) represents a versatile nuclear protein that exerts pleiotropic effects on neurodevelopmental processes, chromatin remodeling, DNA damage repair, as well as transcriptional regulation. Accumulating evidence demonstrates that WSTF is a crucial molecular determinant in the pathogenesis and progression of multiple cancers, positioning it as a viable therapeutic target. This review systematically synthesizes the molecular mechanisms by which WSTF drives oncogenesis across malignancies, focusing on its interplay with regulatory factors and signaling pathways. In breast cancer, WSTF participates in estrogen receptor (ER) signaling and contributes to endocrine therapy resistance by modulating ER-dependent gene expression to promote proliferation and invasion. WSTF also interacts with the vitamin D analog EB1089, suppressing tumor progression through altered promoter binding. In gastric cancer, aberrant WSTF expression disrupts cell adhesion, increasing cancer cell dependency on WSTF. Hyperphosphorylation of WSTF in diffuse gastric cancer further implicates it in tumorigenesis. In cervical, glioblastoma, and lung cancers, WSTF activates the PI3K-Akt signaling cascade, enhancing tumor cell proliferation, migration, and invasion. These findings underscore WSTF's oncogenic role and therapeutic potential. Further investigation into WSTF's functions and regulatory mechanisms will deepen our understanding of tumorigenesis and inform novel therapies targeting this chromatin regulator.

Keywords: WSTF; Malignant Tumors; Transcriptional Regulation; PI3K/Akt Pathway

1. Introduction

1.1. Current Status of Cancer Research

Malignant neoplasms persist as a predominant contributor to global mortality. Epidemiological data from the World Health Organization (2019) indicate that cancer was the primary or secondary cause of premature death (prior to 70 years of age) in 183 nations, while ranking third or fourth in 23 other countries (Sung et al., 2021). Epidemiological studies identify China as the country with the most substantial cancer incidence worldwide, exhibiting a steadily increasing annual caseload (Kamaraju et al., 2020). Globally, 2020 witnessed approximately 19.3 million newly diagnosed cancer cases, of which 4.57 million (23.7%) were recorded within China (Qiu et al., 2022). Despite advancements in medical technology, cancer treatment costs continue to rise, and the disease imposes substantial burdens on societal productivity, labor resources, and economic stability (Stemmer et al., 2013; Yabroff et al., 2011). Thus, early screening, timely diagnosis, and effective treatment are critical to mitigating these losses (Luengo-Fernandez et al., 2013). A paradigm shift has characterized oncological therapeutics since the dawn of the 21st century, transitioning sequentially from empirical clinical practice to evidence-based practice approaches, and currently progressing toward individualized precision medicine strategies. (Powell et al., 2022).

1.2. Structure o*f WSTF*

The Williams syndrome transcription factor (WSTF), encoded by the *BAZ1B* gene (HGNC:963; chr7q11.23), is a chromatin-modifying protein that regulates genomic architecture. The BAZ1B gene spans 80 kilobases in length and contains a 4,449-base pair open reading frame. As a member of the BAZ/WAL protein family, the Williams syndrome transcription factor (WSTF) is a large nuclear protein comprising 1,425 amino acid residues with an approximate molecular mass of 171 kilodaltons. This multidomain protein features two evolutionarily conserved functional modules: a plant homeodomain (PHD)-type zinc finger motif and a bromodomain, both of which mediate critical chromatin interactions (Chris Barnett & Jocelyn E. Krebs, 2011; Liu et al., 2020; Sharif et al., 2021; Zanella et al., 2019). Williams syndrome (WS; OMIM 194050) is a contiguous gene deletion syndrome, resulting in a complex developmental disorder characterized by multisystem defects. Common clinical features of WS patients include intellectual disability, distinctive facial features, unique cognitive profiles, congenital heart disease, infantile hypercalcemia, and growth deficiencies (Allegri et al., 2020; Bellugi et al., 1990; Serrano-Juárez et al., 2023). Functionally, WSTF serves as a versatile atypical tyrosine kinase that coordinates multiple essential biological processes. It participates in chromatin organization through nucleosome remodeling, regulates transcription via RNA polymerase I- and III-dependent mechanisms, modulates vitamin D3-dependent signaling pathways, and contributes to genomic stability maintenance through its involvement in DNA damage repair systems (Chris Barnett & Jocelyn E. Krebs, 2011; Sharif et al., 2021). Remarkably, WSTF demonstrates substantial overexpression in malignant lesions relative to adjacent normal tissues, underscoring its promise as an emerging molecular target for anticancer therapy.

2. Biological Functions of WSTF

2.1. Neurodevelopmental Regulation

WSTF serves as a key regulator of neurodevelopment. Haploinsufficiency of the WSTF in neural progenitor populations induces genome-wide transcriptional perturbations and impairs cellular differentiation programs, resulting in dysregulation of multiple downstream genetic networks critical for neurodevelopment. WSTF-targeted genes are enriched in the Wnt signaling pathway, which balances neuronal progenitor proliferation and differentiation. Intriguingly, WSTF can rescue differentiation impairments caused by its haploinsufficiency by attenuating hyperactive Wnt signaling in neural stem cells (Lalli et al., 2016; Zhou et al., 2022).

2.2. Chromatin Remodeling

The WSTF serves as an essential structural and functional element within ATP-dependent chromatin remodeling machinery, particularly within two key complexes: the WSTF-ISWI chromatin regulatory complex (WICH) and the B-WICH complex (Goto et al., 2024; Li et al., 2021; Maga & Hubscher, 2003; Poot et al., 2005; Poot et al., 2004). Research demonstrates that: The WICH complex prevents heterochromatin protein 1 (HP1) from binding to newly replicated DNA (Poot et al., 2004). Biochemical studies reveal that WICH's targeting to nascent replication foci is mediated by high-affinity binding to the Proliferating cell nuclear antigen (PCNA) trimer, facilitating chromatin remodeling at active replication forks.By temporarily maintaining chromatin in a transcriptionally accessible state, WICH delays post-replicative chromatin maturation, thereby preserving chromatin structure (Maga & Hubscher, 2003; Poot et al., 2005).

2.3. Role in DNA Damage Repair

H2A.X represents a specialized variant of histone Histone H2A (H2A)(Dibitetto et al., 2024) that is functionally indispensable for DNA damage response pathways. The distinctive WAC (WSTF/Acf1/cbp146) domain within WSTF exhibits intrinsic tyrosine kinase capability, specifically catalyzing phosphorylation at tyrosine residue 142 (Y142) of H2A.X, generating the γH2AX(a form of H2AX with a phosphate group added at position S139)-pY142 epigenetic mark (Broering et al., 2015; Xiao et al., 2009). This phosphorylation event facilitates molecular interactions with RNA polymerase II (Pol II), establishing a functional linkage between DNA damage signaling and transcriptional regulation in actively cycling cell populations.The DNA damage response involves a sophisticated regulatory mechanism:Upon DNA damage, ATM (a PI3-K-like kinase)-dependent EYA1/3 (eyes absent homologs 1 and 3) phosphatases initially remove pre-existing γH2AX-pY142 modifications, leading to transcriptional silencing at damage sites requiring repair(Yuan et al., 2010). Subsequently, WSTF translocates to DNA lesion sites to restore γH2AX-pY142. This molecular mechanism promotes transcription-coupled homologous recombination (TC-HR) in G1-phase cells, where RNA polymerase II-generated transcripts serve as template donors for precise DNA repair, ensuring preservation of genomic stability (Chris Barnett & Jocelyn E. Krebs, 2011; Ji et al., 2019; Oppikofer et al., 2017).

2.4. Transcriptional Regulation

Emerging evidence demonstrates that nuclear myosin 1 (NM1), WSTF, and SWI/SNF-related

matrix-associated actin-dependent regulator of chromatin subfamily A member 1 (SNF2H) associate with RNA polymerase I (Pol I) and ribosomal DNA (rDNA) loci (Percipalle et al., 2006; Venit et al., 2020). The molecular interplay between NM1 and the WSTF orchestrates the coordinated recruitment of two functionally distinct chromatin remodeling complexes—WICH and the WSTF-containing nucleosome assembly complex (WINAC)—to specific genomic loci. At these target sites, these multi-protein assemblies collaboratively execute chromatin structure modifications that ultimately drive transcriptional activation(Percipalle et al., 2006; Sarshad et al., 2013). The dynamic interplay between NM1 and actin filaments generates biophysical forces that activate kinase-dependent phosphorylation of WSTF at specific regulatory residues (Tyr/Ser). This post-translational modification acts as a molecular switch that induces conformational changes in WSTF, leading to the structural destabilization and subsequent disassembly of the B-WICH chromatin remodeling complex. As a consequence, this regulatory cascade terminates B-WICH-mediated chromatin reorganization at ribosomal DNA loci, thereby modulating rDNA transcriptional output. This dissociation event subsequently prevents the binding of Pol I to gene promoters, thereby effectively inhibiting transcriptional activation (Aydin Ö et al., 2014; Sarshad et al., 2013).

As a critical transcriptional regulator, WSTF performs diverse biological functions under normal physiological conditions. However, emerging evidence has demonstrated the essential role of WSTF in malignant tumor progression, generating substantial research interest in its oncogenic functions. Subsequent sections will systematically review mechanistic insights into WSTF's contributions to cancer pathogenesis.

3. Advances in WSTF Research in Malignant Tumors

3.1. WSTF Promotes Malignant Tumor Development and Progression

Emerging evidence highlights the multifaceted role of the WSTF in oncogenesis, with its involvement spanning transcriptional regulation, immune modulation, and epigenetic remodeling.

3.1.1. RUNX2-Dependent Transcriptional Regulation

Studies show that Runt-related transcription factor 2 (RUNX2) and WSTF form a functional complex in the nuclear matrix, working together to regulate DNA damage response (DDR) through three main mechanisms. First, RUNX2 helps bring WSTF to DNA damage sites, which increases the production of γ-H2AX. This process improves the ability to repair DNA. Second, WSTF usually increases apoptosis by adding phosphate groups to H2AX at position Y142. However, RUNX2 reduces this effect by controlling WSTF's activity, which helps cancer cells avoid programmed cell death. Third, this complex lowers the acetylation levels of histone H3 lysine 9 (H3K9) and Histone H3 lysine 56 (H3K56). These changes modify chromatin structure, which affects DNA repair efficiency and how genes are expressed (Yang et al., 2015). This pathway underscores WSTF's role in promoting cancer progression through cooperation with the RUNX family of transcription factors.

3.1.2. Immunomodulatory Functions in the Tumor Microenvironment

L-Arginine potentiates T cell-mediated anti-tumor responses through metabolic reprogramming, a process orchestrated by the L-arginine-responsive transcriptional regulators BAZ1B, Positive Coactivator 4 (PC4) and Splicing Factor, Arginine/Serine-rich 1 (SFRS1) Interacting Protein 1 (PSIP1), and Translin (TSN). These factors sense intracellular L-arginine concentrations. They dynamically modulate the expression of genes involved in DNA repair, chromatin remodeling, and cell survival, thereby augmenting T cell effector functions. Structural proteomics analysis (limited proteolysis-mass spectrometry LiP-MS) identified early conformational changes in WSTF following L-arginine stimulation, suggesting its potential involvement in the initial signaling cascade. However, genetic ablation of WSTF did not impair L-arginine-induced metabolic adaptation or survival advantages in T cells, whereas depletion of BAZ1B, PSIP1, or TSN markedly attenuated these effects. These findings demonstrate that while WSTF may participate in the early L-arginine response network, BAZ1B and its associated factors serve as the core molecular machinery sustaining T cell anti-tumor activity (Geiger et al., 2016). This study establishes the L-arginine-BAZ1B/PSIP1/TSN axis as a critical regulatory node in tumor immunity, while revealing WSTF's non-essential yet potentially modulatory role in this immunometabolic network.

3.1.3. Epigenetic Control of Tumorigenesis

Extensive research has demonstrated that WSTF contributes to cancer progression through several distinct but interconnected biological processes. The first major mechanism involves post-translational modifications, where males absent on the first (MOF)-mediated acetylation at the K426 residue significantly enhances WSTF's ability to regulate gene expression. Importantly, this acetylation event also facilitates subsequent phosphorylation at the S158 position. Together, these molecular modifications work synergistically to promote aggressive tumor behaviors, including enhanced cell proliferation, increased migratory capacity, and greater invasive potential (Liu et al., 2020).

In cancers harboring $KRAS^{G12}$ mutations, WSTF participates in a unique pathogenic cascade. The mutant KRAS protein induces specific epigenetic alterations at the neuregulin-3 (*NRG3*) gene promoter region, resulting in transcriptional activation. This leads to the formation of stable WSTF/NRG3 protein complexes that are secreted through non-classical pathways. Once released into the extracellular environment, these complexes function as potent signaling molecules that can stimulate nearby wild-type cells through paracrine mechanisms. The activated pathways include several well-characterized oncogenic signaling networks such as RAS, Neurogenic locus notch homolog protein 1 (NOTCH1), and Janus Kinase (JAK) which collectively contribute to microenvironmental changes favorable for tumor progression (Liu et al., 2016).

At the genomic level, comprehensive studies utilizing advanced sequencing technologies have revealed that elevated WSTF expression exerts widespread effects on cellular homeostasis. Specifically, WSTF overexpression leads to the transcriptional repression of critical cell cycle inhibitors including Cyclin-Dependent Kinase Inhibitor 1A (CDKN1A) and Mouse Double Minute 2 (MDM2). Concurrently, it downregulates essential components of the proteasomal

degradation machinery, specifically Proteasome Activator Subunit 3 (PSME3) and Proteasome Activator Subunit 4 (PSME4). This coordinated suppression disrupts both upstream signaling pathways and downstream protein degradation cascades, thereby compromising critical cell cycle checkpoints and fostering a molecular microenvironment conducive to dysregulated proliferation and neoplastic progression (Grochowska et al., 2022).

WSTF has emerged as a central regulator in malignant tumor development and progression, orchestrating diverse oncogenic processes through transcriptional control, immune modulation, and epigenetic remodeling. Its interactions with key factors like RUNX2 and NRG3, modulation of L-arginine metabolism, and influence on tumor suppressors (CDKN1A, MDM2) and proteasomal degradation (PSME3/4) collectively drive cancer cell survival, proliferation, and metastasis. These effects are mediated via two core mechanisms: molecular complex formation and epigenetic regulation, highlighting WSTF's multifaceted role in tumorigenesis. Deeper WSTF research could lead to precise cancer treatments, particularly for resistant cases. Combining lab research with clinical applications strongly supports using WSTF both to predict cancer and to develop targeted drugs.

3.2. WSTF in Breast Cancer Signaling

Estrogen receptor (ER) signaling constitutes a fundamental pathway in breast cancer pathogenesis and therapeutic intervention, with approximately 80% of breast malignancies exhibiting ER-positive status and consequent estrogen-dependent proliferative capacity (Bulun et al., 2009; Lundqvist et al., 2018; Nelson & Bulun, 2001; Sammons et al., 2020; Simpson, 2004; Will et al., 2023).Current clinical strategies predominantly employ endocrine-based therapeutics, including selective estrogen receptor modulators (SERMs) such as tamoxifen and aromatase inhibitors, which effectively attenuate ER signaling cascades to achieve tumor growth suppression (Salvati et al., 2022).

The aromatase enzyme, encoded by *CYP19A1*, catalyzes estrogen synthesis (Lin et al., 2023), and its inhibition by vitamin D analogs like EB1089—which downregulates *CYP19A1* expression and aromatase activity-effectively suppresses growth in aromatase-dependent breast cancer cells (Bulun et al., 2009; Lundqvist et al., 2018). Mechanistically, EB1089 alters nuclear receptor/cofactor interactions at the CYP19A1 promoter, enabling vitamin D receptor (VDR) binding while displacing WSTF, thereby impeding breast cancer progression (Lundqvist et al., 2013). Notably, 1α,25-dihydroxyvitamin D3 and its analogs exhibit antiproliferative and prodifferentiation effects, highlighting their therapeutic potential (Bajbouj et al., 2022; Dennis et al., 2023; Hill et al., 2015). In estrogen-dependent breast cancer, targeting ER signaling remains central, with WSTF identified as an activator of CYP19A1 and ERα promoters, while 1,25(OH)2D3 disrupts WSTF-promoter binding to abolish this activation (Bajbouj et al., 2022). These findings position vitamin D analogs as promising therapeutic agents.

Emerging evidence indicates that Dot1L and Menin (encoded by MEN1) colocalize within the cytoplasmic compartment to cooperatively regulate critical pathways involved in breast cancer progression. These pathways include estrogen signaling, p53 activity, HIF1α-mediated responses, death receptor signaling, as well as cell cycle control and epithelial-mesenchymal transition (EMT)

regulation (Liu et al., 2020; Saatci et al., 2021; Salvati et al., 2022). Dot1L and Menin have been shown to influence estrogen signaling through interactions with nuclear chaperone complexes, particularly the BAZ1B-containing B-WICH and WINAC complexes. Experimental reduction of *BAZ1B* expression in both antiestrogen-sensitive and resistant breast cancer cell lines consistently results in significant suppression of ERα expression, impaired proliferative capacity, and transcriptomic reprogramming affecting estrogen response, Myc signaling, mTOR activity, PI3K/AKT pathway, and metabolic processes. The functional interplay between ERα, Dot1L, Menin and BAZ1B - and their coordinated inhibition - exerts profound effects on the proliferation and survival of endocrine-resistant breast cancer cells. These findings support the potential therapeutic strategy of combined pharmacological targeting of these factors to overcome endocrine resistance in ERα-positive breast malignancies (Liu et al., 2020; Saatci et al., 2021; Salvati et al., 2022).

Research findings demonstrate that WSTF can interact with two key acetyltransferases, p300/CBP-Associated Factor (PCAF) and MOF, to co-regulate the acetylation levels at histone sites H3K9 and Histone H4 lysine 16 (H4K16) (Vintermist et al., 2011). The molecular mechanism can be delineated into three critical steps:First, activation of the Ras signaling pathway induces phosphorylation at serine 158 (S158) of the WSTF protein. This post-translational modification serves as a molecular switch that enhances WSTF's binding affinity for PCAF while simultaneously reducing its interaction with MOF.Second, the altered binding dynamics lead to functional consequences: PCAF enzymatic activity becomes elevated, resulting in increased H3K9 acetylation (H3K9ac). Conversely, MOF activity is diminished, causing decreased H4K16 acetylation (H4K16ac).Third, these coordinated changes in histone acetylation patterns directly modulate the expression of tumor-related genes, including Breast tumor kinase (Brk) and p21. Ultimately, these molecular events promote breast cancer cell proliferation, migration, and enhanced tumorigenic potential in vivo, as evidenced by animal studies.This study reveals WSTF functions as a molecular sensor that transduces Ras signaling to differentially regulate PCAF and MOF activities, thereby establishing a novel epigenetic mechanism controlling oncogene expression. These findings not only advance our understanding of breast cancer pathogenesis but also identify potential therapeutic targets for intervention (Li et al., 2016; Liu et al., 2020).

In summary, WSTF has been identified as a central player that: (1) activates *CYP19A1/ERα* genes, (2) cooperates with PCAF/MOF acetyltransferases to regulate histone marks (H3K9ac/H4K16ac), and (3) integrates Ras pathway signals. Ras-mediated phosphorylation at S158 alters WSTF's binding preferences - increasing PCAF but decreasing MOF interaction - ultimately affecting oncogenes (Brk, p21) to drive cancer progression. Vitamin D compounds counteract this by blocking WSTF's binding to CYP19A1/ERα promoters. These findings establish WSTF as both an epigenetic regulator and therapeutic target. Moving forward, studies should clarify WSTF's regulation mechanisms and explore combination therapies pairing WSTF inhibitors with vitamin D analogs for more precise breast cancer treatment.

3.3. WSTF in Gastric Cancer Signaling Pathways

Dysregulation of cell adhesion represents a hallmark feature across multiple cancer types

(Schnell et al., 2013). In gastric cancer, the adhesion protein Claudin-4 (CLDN4), which mediates intercellular adhesion and maintains cell polarity - shows significant upregulation (Tsukita et al., 2019). Notably, the DNA repair protein MutS Homolog 2 (MSH2) is enriched in cell adhesion-related pathways, where it regulates CLDN4 expression through modulating enhancer-promoter interactions, thereby controlling invasive growth of gastric cancer cells. MSH2 deficiency leads to adhesion pathway dysregulation, rendering aggressive gastric cancer cells dependent on WSTF and consequently sensitive to bromodomain/ Bromodomain and Extra-Terminal motif inhibitors (BET) (extra-terminal motif) inhibition, ultimately promoting gastric carcinogenesis (Nargund et al., 2022; Nargund et al., 2023).

Comprehensive studies show that diffuse gastric cancer develops when several cellular pathways malfunction, including c-MYC signaling, EMT processes, and semaphorin communication. In these cancers, the BAZ1B, With No lysine (K) kinase 1 (WNK1) and myosin light chain kinase (MLCK) show excessive phosphorylation activity, while Adaptor-Associated Kinase 1 (AAK1) activity decreases. The WSTF contributes by phosphorylating BAZ1B at Ser699/705 sites, which activates PI3K/Akt and IL-6/ signal transducer and activator of transcription 3 (STAT3) pathways to promote EMT and invasion. lamin A/C (LMNA) phosphorylation at S392 strongly associates with metastasis. WSTF also influences cancer progression through its roles in maintaining chromatin structure and DNA repair, potentially affecting genetic stability. These multiple mechanisms make WSTF an important factor in diffuse subtype of gastric cancer (DGC) development and potential treatment target (Singh et al., 2024).

In summary, dysregulation of cell adhesion plays a pivotal role in gastric cancer, with WSTF driving tumor progression through coordinated multi-pathway mechanisms: (1) phosphorylating BAZ1B to activate PI3K/Akt and STAT3 pathways, thereby promoting EMT; (2) inducing LMNA hyperphosphorylation to enhance metastatic potential; and (3) compromising genomic stability. Notably, the functional coupling between WSTF and the MSH2-CLDN4 axis establishes it as a promising therapeutic target—WSTF inhibition synergistically enhances the efficacy of BET inhibitors when MSH2 is deficient. These findings elucidate WSTF's critical role in gastric cancer and identify novel therapeutic targets and strategies. Future investigations should focus on elucidating the functional mechanisms of WSTF and its associated signaling pathways, which will deepen our understanding of gastric cancer pathogenesis and inform the development of innovative treatment approaches.

3.4. WSTF Promotes Malignant Tumor Development Through the PI3K/Akt Signaling Pathway

A growing body of research evidence clearly indicates that WSTF commonly contributes to cancer progression in multiple tumor types, primarily by activating the important PI3K/AKT cell signaling pathway. In the specific case of cervical cancer (CC), detailed laboratory studies have demonstrated significantly higher levels of WSTF protein in both patient tumor samples and cultured cancer cell lines when compared to normal healthy tissues. Furthermore, these investigations showed that WSTF expression levels gradually increase in parallel with disease progression, suggesting its potential role in driving more advanced stages of cervical cancer development. Studies demonstrate that WSTF knockdown suppresses CC cell proliferation,

invasion, and migration through PI3K/Akt pathway inhibition, establishing WSTF as a key driver of CC malignancy (Jiang et al., 2021).

Consistent with these observations, the research team led by Liyuan Yang reported similar findings in glioblastoma, an aggressive form of brain cancer. Their study demonstrated that elevated WSTF protein expression in tumor cells promotes key oncogenic processes: accelerated cell proliferation and enhanced migratory capacity. This tumor-promoting effect is mediated through a specific molecular mechanism in which WSTF induces AKT protein phosphorylation, thereby initiating an activation cascade of the PI3K/Akt signaling pathway. Ultimately, this pathway activation drives the characteristic uncontrolled growth and metastatic behavior of glioblastoma cells (Yang et al., 2021).

In lung cancer, Jin Meng's studies revealed that WSTF acts like a cancer-causing gene. It works by switching on two important pathways at the same time - the PI3K/Akt pathway and the IL-6/STAT3 pathway. When both pathways are active, they change how cells behave, making them more likely to undergo EMT (Jiang et al., 2021; Meng et al., 2016). This process helps lung cancer cells in several ways: they grow faster, move more easily, and invade other tissues more effectively. As a result, the cancer spreads quicker and becomes more aggressive (Kim et al., 2006; Mittal, 2016; Zeisberg et al., 2007).

Cumulative evidence demonstrates that WSTF exhibits pleiotropic oncogenic functions across multiple malignancies, notably cervical carcinoma, glioblastoma multiforme, and lung cancer. Mechanistically, WSTF consistently activates the PI3K/AKT signaling cascade, thereby promoting hallmark cancer phenotypes including enhanced proliferative capacity, increased invasive potential, and metastatic dissemination via EMT(Jiang et al., 2021; Meng et al., 2016; Yang et al., 2021). Because multiple studies have now confirmed how important WSTF is in these different cancers, it has become clear that this protein could be a good target for new cancer treatments. The next important step for researchers will be to figure out exactly how WSTF causes these cancer-promoting effects at the molecular level. Understanding these detailed mechanisms could lead to new targeted therapies that might work against several types of cancer.

4. Summary and Perspectives

Scientific research has clearly shown that WSTF encodes an essential protein involved in cancer processes. WSTF has been identified as a crucial cancer-associated gene, with its expression level in malignant cells showing direct associations with neoplastic transformation, disease advancement, and therapeutic responses in diverse malignancies. WSTF exerts its oncogenic effects through pleiotropic mechanisms, including modulation of key cellular signaling pathways, epigenetic regulation of gene expression programs, and chromatin remodeling. These coordinated actions collectively promote tumorigenesis by enhancing malignant cell proliferation and metastatic potential. Although we have learned much about WSTF's cancer roles, future studies should address key questions regarding through additional research.

4.1. Molecular Mechanisms of WSTF in other Malignancies

Although we know that WSTF is involved in cancer development, its exact mechanisms are not yet fully understood. WSTF plays important roles in regulating gene expression, modifying chromatin structure, and repairing DNA damage—all of which are closely linked to cancer initiation and progression. By studying WSTF's functions in greater detail, we may uncover new therapeutic targets for cancer treatment.

4.2. Developing Targeted Therapies Against WSTF

As a promising therapeutic target, WSTF shows potential for inhibiting tumor growth and metastasis. Future research should focus on developing more selective and effective WSTF inhibitors to enhance treatment efficacy while minimizing side effects. Researchers should also explore combination therapies with existing treatments like conventional chemotherapy and immune checkpoint inhibitors to potentially improve therapeutic outcomes.

4.3. The Interaction of WSTF with the Tumor Immune Microenvironment

Recent studies show that the immune cells and molecules around tumors (called the tumor microenvironment) significantly influence cancer growth. Future investigations should focus on two key aspects of WSTF's role in tumor immunology: first, elucidating its mechanisms of immune cell regulation within the tumor microenvironment; and second, determining whether malignant cells utilize WSTF-mediated pathways to evade immune surveillance. These critical questions will help establish WSTF's immunomodulatory functions in cancer pathogenesis. Answers to these questions may lead to new combination therapies that make immunotherapies work better for more patients.

In summary, WSTF is an important transcription factor that contributes significantly to cancer development and progression. Current studies continue to investigate exactly how WSTF works at the molecular level in different cancers. Researchers are also examining whether targeting WSTF could lead to new cancer treatments. The findings from these studies may help scientists develop better therapies and improve outcomes for cancer patients.

Author Contributions:

Writing—original draft preparation,Yunjie Pei; writing—review and editing,Yan Liu, Shuqing Wang, Jinghua Zhang; visualization:Yuanyue Zhang

Funding:

No funding was received for this study.

Institutional Review Board Statement:

Not applicable

Informed Consent Statement:

Not applicable

Data Availability Statement:

Not applicable

Acknowledgments:

We apologize to the colleagues whose work could not be cited here due paper length restraints.

Conflict of Interest Statement:

All authors declare no competing interests.

References

Allegri, L., Baldan, F., Mio, C., De Felice, M., Amendola, E., & Damante, G. (2020). BAZ1B is a candidate gene responsible for hypothyroidism in Williams syndrome. Eur J Med Genet, 63(6), 103894.

Aydin Ö, Z., Marteijn, J. A., Ribeiro-Silva, C., Rodríguez López, A., Wijgers, N., Smeenk, G., van Attikum, H., Poot, R. A., Vermeulen, W., & Lans, H. (2014). Human ISWI complexes are targeted by SMARCA5 ATPase and SLIDE domains to help resolve lesion-stalled transcription. Nucleic Acids Res, 42(13), 8473-8485.

Bajbouj, K., Al-Ali, A., Shafarin, J., Sahnoon, L., Sawan, A., Shehada, A., Elkhalifa, W., Saber-Ayad, M., Muhammad, J. S., Elmoselhi, A. B., Guraya, S. Y., & Hamad, M. (2022). Vitamin D Exerts Significant Antitumor Effects by Suppressing Vasculogenic Mimicry in Breast Cancer Cells. Front Oncol, 12, 918340.

Barnett, C., & Krebs, J. E. (2011). WSTF does it all: a multifunctional protein in transcription, repair, and replication. Biochem Cell Biol, 89(1), 12-23.

Barnett, C., & Krebs, J. E. (2011). WSTF does it all: a multifunctional protein in transcription, repair, and replicationThis paper is one of a selection of papers published in a Special Issue entitled 31st Annual International Asilomar Chromatin and Chromosomes Conference, and has undergone the Journal's usual peer review process. Biochemistry and Cell Biology, 89(1), 12-23.

Bellugi, U., Bihrle, A., Jernigan, T., Trauner, D., & Doherty, S. (1990). Neuropsychological, neurological, and neuroanatomical profile of Williams syndrome. Am J Med Genet Suppl, 6, 115-125.

Broering, T. J., Wang, Y. L., Pandey, R. N., Hegde, R. S., Wang, S. C., & Namekawa, S. H. (2015). BAZ1B is dispensable for H2AX phosphorylation on Tyrosine 142 during spermatogenesis. Biol Open, 4(7), 873-884.

Bulun, S. E., Lin, Z., Zhao, H., Lu, M., Amin, S., Reierstad, S., & Chen, D. (2009). Regulation of aromatase expression in breast cancer tissue. Ann N Y Acad Sci, 1155, 121-131.

Dennis, C., Dillon, J., Cohen, D. J., Halquist, M. S., Pearcy, A. C., Schwartz, Z., & Boyan, B. D. (2023). Local production of active vitamin D(3) metabolites in breast cancer cells by CYP24A1 and CYP27B1. J Steroid Biochem Mol Biol, 232, 106331.

Dibitetto, D., Liptay, M., Vivalda, F., Dogan, H., Gogola, E., González Fernández, M., Duarte, A., Schmid, J. A., Decollogny, M., Francica, P., Przetocka, S., Durant, S. T., Forment, J. V.,

Klebic, I., Siffert, M., de Bruijn, R., Kousholt, A. N., Marti, N. A., Dettwiler, M., . . . Rottenberg, S. (2024). H2AX promotes replication fork degradation and chemosensitivity in BRCA-deficient tumours. Nat Commun, 15(1), 4430.

Geiger, R., Rieckmann, J. C., Wolf, T., Basso, C., Feng, Y., Fuhrer, T., Kogadeeva, M., Picotti, P., Meissner, F., Mann, M., Zamboni, N., Sallusto, F., & Lanzavecchia, A. (2016). L-Arginine Modulates T Cell Metabolism and Enhances Survival and Anti-tumor Activity. Cell, 167(3), 829-842.

Goto, N., Suke, K., Yonezawa, N., Nishihara, H., Handa, T., Sato, Y., Kujirai, T., Kurumizaka, H., Yamagata, K., & Kimura, H. (2024). ISWI chromatin remodeling complexes recruit NSD2 and H3K36me2 in pericentromeric heterochromatin. J Cell Biol, 223(8), e202310084.

Grochowska, A., Statkiewicz, M., Kulecka, M., Cybulska, M., Sandowska-Markiewicz, Z., Kopczynski, M., Drezinska-Wolek, E., Tysarowski, A., Prochorec-Sobieszek, M., Ostrowski, J., & Mikula, M. (2022). Evidence supporting the oncogenic role of BAZ1B in colorectal cancer. Am J Cancer Res, 12(10), 4751-4763.

Hill, N. T., Zhang, J., Leonard, M. K., Lee, M., Shamma, H. N., & Kadakia, M. (2015). 1α, 25-Dihydroxyvitamin D_3 and the vitamin D receptor regulates ΔNp63α levels and keratinocyte proliferation. Cell Death Dis, 6(6), e1781.

Ji, J. H., Min, S., Chae, S., Ha, G. H., Kim, Y., Park, Y. J., Lee, C. W., & Cho, H. (2019). De novo phosphorylation of H2AX by WSTF regulates transcription-coupled homologous recombination repair. Nucleic Acids Res, 47(12), 6299-6314.

Jiang, D., Ren, C., Yang, L., Li, F., Yang, X., Zheng, Y., Ji, X., & Tian, Y. (2021). Williams syndrome transcription factor promotes proliferation and invasion of cervical cancer cells by regulating PI3K/Akt signaling pathway. J Obstet Gynaecol Res, 47(7), 2433-2441.

Kamaraju, S., Drope, J., Sankaranarayanan, R., & Shastri, S. (2020). Cancer Prevention in Low-Resource Countries: An Overview of the Opportunity. American Society of Clinical Oncology Educational Book, (40), 72-83.

Kim, K. K., Kugler, M. C., Wolters, P. J., Robillard, L., Galvez, M. G., Brumwell, A. N., Sheppard, D., & Chapman, H. A. (2006). Alveolar epithelial cell mesenchymal transition develops in vivo during pulmonary fibrosis and is regulated by the extracellular matrix. Proc Natl Acad Sci U S A, 103(35), 13180-13185.

Lalli, M. A., Jang, J., Park, J. H., Wang, Y., Guzman, E., Zhou, H., Audouard, M., Bridges, D., Tovar, K. R., Papuc, S. M., Tutulan-Cunita, A. C., Huang, Y., Budisteanu, M., Arghir, A., & Kosik, K. S. (2016). Haploinsufficiency of BAZ1B contributes to Williams syndrome through transcriptional dysregulation of neurodevelopmental pathways. Hum Mol Genet, 25(7), 1294-1306.

Li, C., Y, Liu, Y., Deng, Y., Wang, S., Q, Song, M., Z, Chen, S., Chang, J., F, & Yang, Z., Y. (2016). H3K9ac and H4K16ac were Regulated Through PCAF/WSTF/MOF Com

plex in Breast Cancer Cells. Genomics and Applied Biology, 35(05), 1008-1012.

Li, Y., Gong, H., Wang, P., Zhu, Y., Peng, H., Cui, Y., Li, H., Liu, J., & Wang, Z. (2021). The emerging role of ISWI chromatin remodeling complexes in cancer. J Exp Clin Cancer Res, 40(1), 346.

Lin, C. H., Zahid, M., Kuo, W. H., Hu, F. C., Wang, M. Y., Chen, I. C., Beseler, C. L., Mondal, B., Lu, Y. S., Rogan, E. G., & Cheng, A. L. (2023). Estrogen-DNA Adducts and Breast Cancer Risk in Premenopausal Asian Women. Cancer Prev Res (Phila), 16(3), 153-161.

Liu, Y., Wang, S. Q., Long, Y. H., Chen, S., Li, Y. F., & Zhang, J. H. (2016). KRASG12 mutant induces the release of the WSTF/NRG3 complex, and contributes to an oncogenic paracrine signaling pathway. Oncotarget, 7(33), 53153-53164.

Liu, Y., Zhang, Y.-Y., Wang, S.-Q., Li, M., Long, Y.-H., Li, Y.-F., Liu, Y.-K., Li, Y.-H., Wang, Y.-Q., Mi, J.-S., Yu, C.-H., Li, D.-Y., Zhang, J.-H., & Zhang, X.-J. (2020). WSTF acetylation by MOF promotes WSTF activities and oncogenic functions. Oncogene, 39(27), 5056-5067.

Luengo-Fernandez, R., Leal, J., Gray, A., & Sullivan, R. (2013). Economic burden of cancer across the European Union: a population-based cost analysis. Lancet Oncol, 14(12), 1165-1174.

Lundqvist, J., Hansen, S. K., & Lykkesfeldt, A. E. (2013). Vitamin D analog EB1089 inhibits aromatase expression by dissociation of comodulator WSTF from the CYP19A1 promoter—a new regulatory pathway for aromatase. Biochimica et Biophysica Acta (BBA) - Molecular Cell Research, 1833(1), 40-47.

Lundqvist, J., Kirkegaard, T., Laenkholm, A. V., Duun-Henriksen, A. K., Bak, M., Feldman, D., & Lykkesfeldt, A. E. (2018). Williams syndrome transcription factor (WSTF) acts as an activator of estrogen receptor signaling in breast cancer cells and the effect can be abrogated by 1α,25-dihydroxyvitamin D(3). J Steroid Biochem Mol Biol, 177, 171-178.

Maga, G., & Hubscher, U. (2003). Proliferating cell nuclear antigen (PCNA): a dancer with many partners. J Cell Sci, 116(Pt 15), 3051-3060.

Meng, J., Zhang, X. T., Liu, X. L., Fan, L., Li, C., Sun, Y., Liang, X. H., Wang, J. B., Mei, Q. B., Zhang, F., & Zhang, T. (2016). WSTF promotes proliferation and invasion of lung cancer cells by inducing EMT via PI3K/Akt and IL-6/STAT3 signaling pathways. Cell Signal, 28(11), 1673-1682.

Mittal, V. (2016). Epithelial Mesenchymal Transition in Aggressive Lung Cancers. Adv Exp Med Biol, 890, 37-56.

Nargund, A. M., Xu, C., Mandoli, A., Okabe, A., Chen, G. B., Huang, K. K., Sheng, T., Yao, X., Teo, J. M. N., Sundar, R., Kok, Y. J., See, Y. X., Xing, M., Li, Z., Yong, C. H., Anand, A., A, I. Z., Poon, L. F., Ng, M. S. W., . . . Tan, P. (2022). Chromatin Rewiring by Mismatch Repair Protein MSH2 Alters Cell Adhesion Pathways and Sensitivity to BET Inhibition in Gastric Cancer. Cancer Res, 82(14), 2538-2551.

Nargund, A. M., Xu, C., Mandoli, A., Okabe, A., Chen, G. B., Huang, K. K., Sheng, T., Yao, X., Teo, J. M. N., Sundar, R., Kok, Y. J., See, Y. X., Xing, M., Li, Z., Yong, C. H., Anand, A., Bin Adam Isa, Z. F., Poon, L. F., Ng, M. S. W., . . . Tan, P. (2023). Correction: Chromatin Rewiring by Mismatch Repair Protein MSH2 Alters Cell Adhesion Pathways and Sensitivity to BET Inhibition in Gastric Cancer. Cancer Res, 83(5), 804.

Nelson, L. R., & Bulun, S. E. (2001). Estrogen production and action. J Am Acad Dermatol, 45(3 Suppl), S116-124.

Oppikofer, M., Sagolla, M., Haley, B., Zhang, H. M., Kummerfeld, S. K., Sudhamsu, J., Flynn, E. M., Bai, T., Zhang, J., Ciferri, C., & Cochran, A. G. (2017). Non-canonical reader modules of BAZ1A promote recovery from DNA damage. Nat Commun, 8(1), 862.

Percipalle, P., Fomproix, N., Cavellán, E., Voit, R., Reimer, G., Krüger, T., Thyberg, J., Scheer, U., Grummt, I., & Farrants, A. K. (2006). The chromatin remodelling complex WSTF-SNF2h interacts with nuclear myosin 1 and has a role in RNA polymerase I transcription. EMBO Rep, 7(5), 525-530.

Poot, R. A., Bozhenok, L., van den Berg, D. L., Hawkes, N., & Varga-Weisz, P. D. (2005). Chromatin remodeling by WSTF-ISWI at the replication site: opening a window of opportunity for epigenetic inheritance? Cell Cycle, 4(4), 543-546.

Poot, R. A., Bozhenok, L., van den Berg, D. L., Steffensen, S., Ferreira, F., Grimaldi, M., Gilbert, N., Ferreira, J., & Varga-Weisz, P. D. (2004). The Williams syndrome transcription factor interacts with PCNA to target chromatin remodelling by ISWI to replication foci. Nat Cell Biol, 6(12), 1236-1244.

Powell, K., Haslam, A., & Prasad, V. (2022). An Empirical Analysis of Precision Previvorship: Are Familial and High-Risk Cancer Preventive Programs Evidence Based? Am J Med, 135(2), 179-183.

Qiu, X., Zhang, K., Zhang, Y., & Sun, L. (2022). Benefit Finding and Related Factors of Patients with Early-Stage Cancer in China. International Journal of Environmental Research and Public Health, 19(7), 4284.

Saatci, O., Huynh-Dam, K. T., & Sahin, O. (2021). Endocrine resistance in breast cancer: from molecular mechanisms to therapeutic strategies. J Mol Med (Berl), 99(12), 1691-1710.

Salvati, A., Melone, V., Sellitto, A., Rizzo, F., Tarallo, R., Nyman, T. A., Giurato, G., Nassa, G., & Weisz, A. (2022). Combinatorial targeting of a chromatin complex comprising Dot1L, menin and the tyrosine kinase BAZ1B reveals a new therapeutic vulnerability of endocrine therapy-resistant breast cancer. Breast Cancer Res, 24(1), 52.

Sammons, S., Sedrak, M. S., & Kimmick, G. G. (2020). The Evolving Complexity of Treating Hormone Receptor-Positive, Human Epidermal Growth Factor Receptor-2 (HER2)-Negative Breast Cancer: Special Considerations in Older Breast Cancer Patients-Part I: Early-Stage Disease. Drugs Aging, 37(5), 331-348.

Sarshad, A., Sadeghifar, F., Louvet, E., Mori, R., Böhm, S., Al-Muzzaini, B., Vintermist, A., Fomproix, N., Östlund, A. K., & Percipalle, P. (2013). Nuclear myosin 1c facilitates the chromatin modifications required to activate rRNA gene transcription and cell cycle progression. PLoS Genet, 9(3), e1003397.

Schnell, U., Cirulli, V., & Giepmans, B. N. (2013). EpCAM: structure and function in health and disease. Biochim Biophys Acta, 1828(8), 1989-2001.

Serrano-Juárez, C. A., Prieto-Corona, B., Rodríguez-Camacho, M., Sandoval-Lira, L., Villalva-Sánchez Á, F., Yáñez-Téllez, M. G., & López, M. F. R. (2023). Neuropsychological Genotype-Phenotype in Patients with Williams Syndrome with Atypical Deletions: A Systematic Review. Neuropsychol Rev, 33(4), 891-911.

Sharif, S. B., Zamani, N., & Chadwick, B. P. (2021). BAZ1B the Protean Protein. Genes (Basel), 12(10), 1541.

Simpson, E. R. (2004). Aromatase: biologic relevance of tissue-specific expression. Semin Reprod Med, 22(1), 11-23.

Singh, S., Parthasarathi, K. T. S., Bhat, M. Y., Gopal, C., Sharma, J., & Pandey, A. (2024). Profiling Kinase Activities for Precision Oncology in Diffuse Gastric Cancer. OMICS: A Journal of Integrative Biology, 28(2), 76-89.

Stemmer, S. M., Mahal, A., Karan, A., Fan, V. Y., & Engelgau, M. (2013). The Economic Burden of Cancers on Indian Households. PLoS One, 8(8), e71853.

Sung, H., Ferlay, J., Siegel, R. L., Laversanne, M., Soerjomataram, I., Jemal, A., & Bray, F. (2021). Global Cancer Statistics 2020: GLOBOCAN Estimates of Incidence and Mortality Worldwide for 36 Cancers in 185 Countries. CA: A Cancer Journal for Clinicians, 71(3), 209-249.

Tsukita, S., Tanaka, H., & Tamura, A. (2019). The Claudins: From Tight Junctions to Biological Systems. Trends Biochem Sci, 44(2), 141-152.

Venit, T., Mahmood, S. R., Endara-Coll, M., & Percipalle, P. (2020). Nuclear actin and myosin in chromatin regulation and maintenance of genome integrity. Int Rev Cell Mol Biol, 355, 67-108.

Vintermist, A., Böhm, S., Sadeghifar, F., Louvet, E., Mansén, A., Percipalle, P., & Ostlund Farrants, A. K. (2011). The chromatin remodelling complex B-WICH changes the chromatin structure and recruits histone acetyl-transferases to active rRNA genes. PLoS One, 6(4), e19184.

Will, M., Liang, J., Metcalfe, C., & Chandarlapaty, S. (2023). Therapeutic resistance to anti-oestrogen therapy in breast cancer. Nat Rev Cancer, 23(10), 673-685.

Xiao, A., Li, H., Shechter, D., Ahn, S. H., Fabrizio, L. A., Erdjument-Bromage, H., Ishibe-Murakami, S., Wang, B., Tempst, P., Hofmann, K., Patel, D. J., Elledge, S. J., & Allis, C. D. (2009). WSTF regulates the H2A.X DNA damage response via a novel tyrosine kinase activity. Nature, 457(7225), 57-62.

Yabroff, K. R., Lund, J., Kepka, D., & Mariotto, A. (2011). Economic burden of cancer in the United States: estimates, projections, and future research. Cancer Epidemiol Biomarkers Prev, 20(10), 2006-2014.

Yang, L., Du, C., Chen, H., & Diao, Z. (2021). Downregulation of Williams syndrome transcription factor (WSTF) suppresses glioblastoma cell growth and invasion by inhibiting PI3K/AKT signal pathway. Eur J Histochem, 65(4), 3255.

Yang, S., Quaresma, A. J., Nickerson, J. A., Green, K. M., Shaffer, S. A., Imbalzano, A. N., Martin-Buley, L. A., Lian, J. B., Stein, J. L., van Wijnen, A. J., & Stein, G. S. (2015). Subnuclear domain proteins in cancer cells support the functions of RUNX2 in the DNA damage response. J Cell Sci, 128(4), 728-740.

Yuan, J., Adamski, R., & Chen, J. (2010). Focus on histone variant H2AX: to be or not to be. FEBS Lett, 584(17), 3717-3724.

Zanella, M., Vitriolo, A., Andirko, A., Martins, P. T., Sturm, S., O'Rourke, T., Laugsch, M., Malerba, N., Skaros, A., Trattaro, S., Germain, P. L., Mihailovic, M., Merla, G., Rada-Iglesias, A., Boeckx, C., & Testa, G. (2019). Dosage analysis of the 7q11.23 Williams region

identifies BAZ1B as a major human gene patterning the modern human face and underlying self-domestication. Sci Adv, 5(12), eaaw7908.

Zeisberg, E. M., Tarnavski, O., Zeisberg, M., Dorfman, A. L., McMullen, J. R., Gustafsson, E., Chandraker, A., Yuan, X., Pu, W. T., Roberts, A. B., Neilson, E. G., Sayegh, M. H., Izumo, S., & Kalluri, R. (2007). Endothelial-to-mesenchymal transition contributes to cardiac fibrosis. Nat Med, 13(8), 952-961.

Zhou, J., Zheng, Y., Liang, G., Xu, X., Liu, J., Chen, S., Ge, T., Wen, P., Zhang, Y., Liu, X., Zhuang, J., Wu, Y., & Chen, J. (2022). Atypical deletion of Williams-Beuren syndrome reveals the mechanism of neurodevelopmental disorders. BMC Med Genomics, 15(1), 79.

Advances in World Medical Research, 2025, 1(1), 34-49
https://doi.org/10.71204/cp3e9n39

Observation on the Efficacy of Self-formulated Huatan Chushi Zhuyu Decoction in the Treatment of Adenoid Hypertrophy in Children and Literature Research on Traditional Chinese Medicine Treatment

Ying Wang [1], Changwen Che [2], Mingsheng Zhang [2], Zhonghai Xin [3,*]

[1] Department of Otorhinolaryngology, Changping District Integrated Traditional Chinese and Western Medicine Hospital, Beijing 102208, China

[2] Department of Otorhinolaryngology, Dongzhimen Hospital, Beijing University of Chinese Medicine, Beijing 100007, China

[3] Department of Otorhinolaryngology, Wangjing Hospital, China Academy of Chinese Medical Sciences, Beijing 100102, China

*** Correspondence**:

Zhonghai Xin

xzh_d716@163.com

Received: 8 April 2025/ Accepted: 14 May 2025/ Published online: 20 May 2025

Abstract

To observe the clinical efficacy of the self-formulated Huatan Chushi Zhuyu Decoction (HCZ Decoction) combined with basic Western medical treatment in children with moderate to severe adenoid hypertrophy (AH) accompanied by allergic rhinitis (AR), and to explore the theoretical basis by referring to traditional Chinese medicine (TCM) literature. A retrospective analysis was conducted. A total of 64 children with moderate to severe AH admitted to the outpatient department from January 2022 to December 2024 were included and divided into the decoction group (43 cases) and the non-decoction group (41 cases) according to the treatment regimen. The non-decoction group was treated with mometasone furoate nasal spray (100 μg/d) + montelukast (4-5 mg/d) for 2 weeks, combined with cetirizine (5-10 mg/d) for anti-allergy. On this basis, the decoction group was additionally given the HCZ Decoction (including tangerine peel, Poria cocos, Pinellia ternata, licorice, Arisaema cum Bile, peach kernel, Spina Gleditsiae, etc.), one dose per day, taken after breakfast and dinner, with a treatment course of 2 weeks. Baseline data such as age, gender, and BMI of the children in the two groups were collected. The differences in nasal symptom scale, pediatric sleep disorder scale, polysomnography (PSG) parameters, and the degree of AH before and after treatment were compared. The t-test and chi-square test were performed using SPSS 27.0 statistical software, with a significance level of $P < 0.05$. Chinese databases such as CNKI and Wanfang (from 2014 to 2024) were systematically searched. Using the Citespace 6.3 literature processing tool, the hotspots and clustering information of keywords,

institutions, and co-authors related to the TCM treatment of AH in Chinese literature were analyzed. There were no statistical differences in general data and clinical baseline data between the two groups ($P > 0.05$), indicating comparability. The scores of various items in both the decoction group and the non-decoction group decreased after treatment, confirming the effectiveness of the treatment. The total score of OSA-18 was at the moderate to severe level, and there were differences in the total score and the changes of various scores between the decoction group and the non-decoction group, with the scores of the decoction group being lower. There was a difference in the change score of the total nasal symptom score (TNSS) between the two groups, mainly manifested in nasal obstruction and sneezing. There were no differences in the changes of OAHI and LSaO2 scores between the two groups. The literature study showed that the core therapeutic methods of TCM treatment for AH are "resolving phlegm, removing dampness, and promoting blood circulation to remove blood stasis", which highly coincides with the compatibility of the self-formulated decoction. The HCZ Decoction combined with basic Western medical treatment can significantly improve the nasal symptoms and sleep quality of children with moderate to severe AH accompanied by AR. Its curative effect may be achieved by regulating the local inflammatory response rather than reducing the volume of the adenoids. TCM literature supports that ‘the intermingling of phlegm, blood stasis, and dampness’ is the core pathogenesis of AH. This decoction provides a safe and effective non-surgical treatment option for clinical practice.

Keywords: Adenoid Hypertrophy; Allergic Rhinitis; Decoction

1. Introduction

AH is a common disease in pediatric otorhinolaryngology, which has a high incidence during the physiological AH period of children aged 4 to 6 years. Epidemiological surveys show that its incidence rate is as high as 30%-40% (Tse et al., 2023). The occurrence of this disease is closely related to AR, recurrent upper respiratory tract infections, obesity, atopic constitution, and genetic factors (Niedzielski et al., 2023). In addition to local symptoms such as nasal obstruction, rhinorrhea, and sinusitis, the most serious complication of AH is obstructive sleep apnea hypopnea syndrome (OSA), which can lead to the disruption of children's nighttime sleep structure. Consequently, it can trigger attention deficit hyperactivity disorder (ADHD) during the day, abnormal emotional behaviors, and disorders of nighttime growth hormone secretion, affecting neurocognitive development and physical growth (Shivnani et al., 2023). Moreover, the long-term state of mouth breathing can lead to abnormal maxillofacial development (adenoid facies), increase the difficulty of orthodontic treatment, and induce secretory otitis media through eustachian tube dysfunction, thus affecting auditory function (Shivnani et al., 2023; Zhang et al., 2024).

With the transformation of the modern medical model and the update of health concepts, the standardized diagnosis and treatment of AH have increasingly received attention. As the gold standard treatment method, adenoidectomy's curative effect is influenced by factors such as the age of the child patient, atopic constitution, and the mucosal repair ability after surgery (Randall,

2020). Conservative drug treatment (nasal glucocorticoids + leukotriene receptor antagonists) has a certain curative effect on children with AH complicated by AR (Eldegeir et al., 2023). However, studies have shown that about 9% of cases require secondary surgical intervention (Schupper et al., 2018). In clinical practice, some parents refuse surgery due to concerns about surgical risks or ethical issues, and simply using Western medicine treatment often fails to achieve the expected results (Zwierz et al., 2024). Therefore, exploring a safe and effective integrated traditional Chinese and Western medicine treatment plan is of great clinical significance.

Based on the TCM pathogenesis theory of "intermingling of phlegm and blood stasis", this study proposes the therapeutic method of "resolving phlegm, removing dampness, and promoting blood circulation to remove blood stasis". It is planned to combine a self-formulated TCM decoction with Western medicine treatment to improve the clinical symptoms of children patients. The aim of this study is to verify the clinical efficacy of this decoction through a retrospective study. With the support of bibliometric research, this study aims to provide evidence support for the TCM clinical non-surgical treatment of AH.

2. Materials and Methods

2.1. General Information

Children's cases that met the diagnostic criteria for AH and AR (Ahmad et al., 2023; Cheng et al., 2024), were treated at the outpatient department of the Otolaryngology Department of our hospital from January 2022 to December 2024, had complete information, and were under 12 years old were collected. A total of 84 cases that met the inclusion criteria and exclusion criteria were included in the study. The general information of the cases, including age, gender, body mass index (BMI), the degree of AH, etc., was collected.

2.2. Clinical Information

2.2.1 Inclusion and Exclusion Criteria

Inclusion Criteria:

① Children who meet the diagnostic criteria for OSA and AR, do not meet the surgical indications such as adenoidectomy and need to receive conservative treatment as evaluated by doctors, as well as children who meet the surgical indications but whose guardians insist on choosing conservative treatment and are willing to follow the research protocol for TCM intervention; ② Children under 12 years old; ③ Children who meet the syndrome type of deficiency of qi in the spleen and lung with intermingling of phlegm and blood stasis; ④ The guardians of the children have a full understanding of the research purpose, methods, possible benefits and risks, and voluntarily sign the informed consent form; ⑤ Children who are willing to accept the TCM treatment plan and are willing to cooperate with the requirements of various examinations, follow-ups during the entire research process.

Exclusion Criteria:

① Children suffering from serious diseases of important organs such as the heart, liver, kidney, and lung, or suffering from malignant tumors and hematological diseases; ② Children with a clear history of allergy to the traditional Chinese medicine or related drug components to be used in the study; ③ Children who have received other systemic treatments that may affect the results of this study within 4 weeks before the start of the study; ④ Children or their guardians who cannot cooperate well with the study, such as being unable to take medicine on time or attend follow-ups on time; ⑤ Children with mental diseases who are unable to cooperate with the treatment, or those who are in the acute infection period and are not suitable for the study of traditional Chinese medicine treatment.

2.2.2. Research Grouping

The study was conducted in a retrospective analysis and parallel control manner. According to whether the self-formulated decoction was taken or not, the cases were divided into two groups: the non-decoction group (41 cases) and the decoction group (43 cases). The non-decoction group was treated with mometasone furoate nasal spray (100 μg/d) + montelukast (4-5 mg/d) for 2 weeks, combined with cetirizine (5-10 mg/d) for anti-allergy. On this basis, the decoction group was additionally given the HCZ Decoction (including tangerine peel, Poria cocos, Pinellia ternata, licorice, Arisaema cum Bile, peach kernel, Spina Gleditsiae, etc.), one dose per day, taken after breakfast and dinner, with a treatment course of 2 weeks.

2.2.3. Observation Indicators

Baseline clinical data within one week before the start of treatment and outcome clinical data at the end of treatment were collected for the enrolled cases, including the degree of AH under endoscopy, OSA - 18 score, TNSS score, and PSG test results.

Endoscopic evaluation: Nasal fibro – nasopharyngoscopy was used for examination. The color and swelling degree of the nasal mucosa, the size of the turbinate, the condition of secretions in the nasal passages, the degree of obstruction of the posterior nasal choanae by the adenoids, and the characteristics of the surface secretions of the adenoids were systematically and carefully observed. The degree of obstruction of the posterior nasal choanae by the adenoids was determined using a percentage as a quantitative index. Specifically, when the adenoids obstructed 50% of the posterior nasal choanae, it was defined as mild obstruction; when the obstruction ratio was between 50% (exclusive) and 75% (inclusive), it was classified as moderate obstruction; if the obstruction ratio was greater than or equal to 75%, it was determined as severe obstruction (Varghese et al., 2016).

OSA-18 score: As an evaluation method for pediatric snoring, it is divided into five aspects: sleep impact, physical symptoms, emotional impact, daytime state, and impact on guardians, with a total of 18 items (Alimoglu et al., 2020). In this study, an evaluation rule of 1-7 points was adopted. 1 point indicated no such problem, 2 points indicated almost none, 3 points indicated rarely, 4 points indicated sometimes, 5 points indicated often, 6 points indicated mostly, and 7 points indicated definitely. A score <= 60, 60 - 80, >= 80 points represented mild, moderate,

and severe impacts on the child's life, respectively. The total OSA-18 score was the sum of the scores of the five aspects, ranging from 7 to 126 points. The evaluation times were within one week before treatment and at the end of treatment.

TNSS score: It is used for the evaluation of nasal symptoms of AR. In this study, it was used for the evaluation of nasal symptoms of AH complicated by AR. The evaluation was divided into four dimensions: nasal congestion, nasal itching, runny nose, and sneezing. Each dimension used a scoring range of 0-3 points. The more severe, the higher the score of the symptoms. 0 points corresponded to no such symptoms; 1 point corresponded to mild symptoms that did not trouble daily life; 2 points corresponded to moderate symptoms that made the patient feel troubled but did not interfere with normal activities or sleep; 3 points corresponded to severe symptoms that seriously affected daily activities and sleep status (Cheng et al., 2024). The total TNSS score was the sum of the scores of the four dimensions, ranging from 0 to 12 points. The evaluation time points were set within one week before treatment and at the end of treatment.

Sleep evaluation: PSG testing was used for the objective evaluation of OSA. The whole - night sleep monitoring method was adopted for PSG, with a monitoring time of more than 7 hours. Information such as nasal airflow, blood oxygen, heart rate, respiratory movement, body position, and snoring was collected. Two people manually interpreted the monitoring data to obtain a report. With OAHI ＞＝ 1 as the diagnostic standard for OSA (Ahmad et al., 2023), the OAHI and LSaO2 indicators were collected. The evaluation time points were set within one week before treatment and at the end of treatment.

2.3. Bibliometric Research Method

The bibliometric analysis of the literatures retrieved from CNKI and Wanfang databases was carried out using the tool Citespace 6.3. The search terms were "adenoid hypertrophy", the search scope was set as "title", the search time range was set from January 2000 to December 2024, and the literature type was set as journal articles. Manually, the articles that met the requirements related to the traditional Chinese medicine treatment of adenoid hypertrophy were selected according to the titles and abstracts.

The bibliographic citation information of the literatures in ref format was exported and then imported into the Citespace software. Duplicate literatures were screened out, and a total of 2,237 literatures were finally counted. Appropriate time slices, node types, and threshold parameters were set in the software interface. The network visualization effect and analysis precision were adjusted, and the analysis was run to generate a knowledge graph. The co-citation relationships among the "keywords" of the literatures, the ranking of hotspots, the time series of article publication, and the relationships among the publishing institutions and authors were presented.

2.4. Statistical Method

The SPSS 24.0 software was used. For the comparison of continuous variables between groups, one-way analysis of variance was adopted, and the test level was set as $\alpha = 0.05$. A P value less than 0.05 indicated that the difference was statistically significant. The general linear model repeated measures test was used for the detection of repeated measurement data in the two groups.

3. Results

3.1. Comparison of General Information between the Decoction Group and the Non-decoction Group

A total of 84 cases were included in the study, with 43 cases in the decoction group and 41 cases in the non-decoction group. The average ages of the two groups were 6.37 years old and 5.65 years old respectively. According to the BMI values of the cases, they were divided into two categories: normal and overweight. Among them, the overweight cases in the decoction group accounted for 11.63% (5/43), and those in the non-decoction group accounted for 17.07% (7/34). The body weights of the cases in both groups were mainly within the normal range. The degrees of adenoid hypertrophy in both groups were mainly moderate to severe, accounting for 79.07% (34/43) in the decoction group and 82.93% (34/41) in the non-decoction group.

There were no significant differences in age, gender composition, body weight characteristics, and the degree of adenoid hypertrophy between the cases in the decoction group and the non-decoction group (p ＞＝ 0.05, see Table 1). The general information levels between the groups were consistent, indicating comparability.

Table 1. Comparison of the general data between the decoction group and the non-decoction group

	cases	gender		age	BMI		AH		
		male	female		normal	Over weight	0	1	2
decoction group	43	22	21	6.37±2.39	38	5	9	16	18
non-decoction group	41	24	17	5.65±2.09	34	7	7	13	21
P value	-	0.519		0.150	0.544		0.689		

3.2. Comparison of Baseline Data of Clinical Observations between the Decoction Group and the Non-decoction Group

The baseline statistics of clinical data for the decoction group and the non-decoction group included the total OSA-18 score, the total TNSS score, and the values of OAHI and LSaO2 from PSG. There were no significant differences in the above-mentioned scores and values between the two groups (p＞＝0.05, see Table 2). The levels of clinical observation data between the groups were consistent, indicating comparability. The OSA-18 scores were mainly at the moderate level, suggesting that AH had a moderate impact on the lives and daily activities of the children. The enrolled children mainly had mild to moderate OSA.

Table 2. Comparison of the baseline data before treatment between the decoction group and the non-decoction group

	OSA-18	TNSS(total)	OAHI	$LSaO_2$
decoction group	70.58±2.71	7.27±1.29	5.06±1.65	88.12±1.87
non-decoction group	70.90±2.93	6.92±1.31	4.87±1.66	88.26±1.92
P value	0.604	0.219	0.598	0.757

3.3. Comparison of Observation Indicators of Adenoid Hypertrophy between the Decoction Group and the Non-decoction Group

The scores of the five aspects of OSA-18, namely sleep impact, physical symptoms, emotional impact, daytime state, and impact on guardians, were statistically analyzed respectively. It was found that after treatment, the scores of all items and the total score of all cases were lower than the baseline scores before treatment. The results of the test using the general linear model for repeated measures are shown in Table 3.

Between-group effect: There was a significant between-group difference in the total OSA-18 score between the two groups ($p < 0.001$); specifically, in terms of the four aspects of treatment's impact on sleep, body symptoms, daytime state, and impact on guardians, there were between-group differences in the scores ($p < 0.001$, $p < 0.001$, $p = 0.002$, $p < 0.001$).

Time effect: The total OSA-18 score and the scores of all five aspects decreased after treatment, and there were significant differences in the scores of the cases before and after treatment ($p < 0.001$).

Interaction effect between group and time: There were differences in the changing trends of the total OSA-18 score and the scores of all five aspects before and after treatment between the two groups ($p < 0.001$, $p < 0.001$, $p = 0.008$, $p = 0.004$, $p = 0.004$, $p < 0.001$), indicating an interaction effect. There were differences in the treatment scores between the decoction group and the non-decoction group.

Table 3. Comparison of the OSA-18 scores before and after treatment between the decoction group and the non-decoction group

	sleeping		Body symptom		mood		daytime		guidians		Total	
	before	after	before	after	before	after	before	after	before	after	before	after
decoction grou	16.93 ±1.54	6.60± 1.23	16.20 ±1.42	8.20± 0.96	6.34± 1.25	4.53± 0.63	10.86 ±1.31	5.25± 0.95	20.23 ±1.37	11.88 ±1.19	70.58 ±2.71	36.46 ±2.59

p												
non-decoction group	12.60±1.61	9.46±1.38	16.41±1.46	9.46±1.14	6.58±1.30	4.75±0.85	10.95±1.49	6.41±1.04	20.34±1.29	14.04±1.70	70.90±2.93	44.14±3.31
treatment												
P value	＜0.001		＜0.001		＜0.001		＜0.001		＜0.001		＜0.001	
η^2	0.947		0.938		0.949		0.907		0.938		0.981	
treatment*grouping interaction												
P value	＜0.001		0.008		0.004		0.004		＜0.001		＜0.001	
η^2	0.372		0.082		0.000		0.097		0.230		0.429	
grouping												
P balue	＜0.001		＜0.001		0.246		0.002		＜0.001		＜0.001	
η^2	0.290		0.144		0.016		0.109		0.237		0.517	

3.4. Comparison of Nasal Symptoms of Allergic Rhinitis between the Decoction Group and the Non-decoction Group

The scores of the four dimensions of TNSS, namely nasal congestion, nasal itching, runny nose, and sneezing, were statistically analyzed respectively. It was found that after treatment, the scores of all items and the total score of all cases were lower than the baseline scores before treatment. The results of the test using the general linear model for repeated measures are shown in Table 4.

Between-group effect: The total TNSS score and the scores of all four dimensions decreased after treatment, and there were no significant differences in the scores of the cases before and after treatment between the two groups ($p \geq 0.05$).

Time effect: The total TNSS score and the scores of all four dimensions decreased after treatment, and there were significant differences in the scores of the cases before and after treatment ($p < 0.001$).

Interaction effect between group and time: There were differences in the changing trends of the total TNSS score and the scores of nasal congestion and sneezing before and after treatment between the two groups ($p < 0.001$, $p < 0.001$, $p = 0.006$), indicating an interaction effect. There were differences in the total TNSS score, the scores of nasal congestion and sneezing treatment

between the decoction group and the non-decoction group, while there were no differences in the symptoms of nasal itching and rhinorrhea.

Table 4. Comparison of the TNSS scores before and after treatment between the decoction group and the non-decoction group

	Nasal obstruction		itching		rhinorrhea		sneezing		total	
	before	after	before	after	before	after	before	after	before	after
decoction group	2.53±0.50	0.69±0.70	1.02±0.85	0.23±0.47	2.00±0.65	1.32±0.47	1.72±0.59	10.9±0.29	7.27±1.29	3.34±1.13
non-decoction group	2.34±0.57	1.24±0.66	1.07±0.78	0.48±0.59	2.02±0.68	1.31±0.47	1.48±0.55	1.19±0.40	6.92±1.31	4.24±1.13
Treatment										
P value	＜0.001		＜0.001		＜0.001		＜0.001		＜0.001	
η^2	0.778		0.480		0.527		0.420		0.855	
Treatment*grouping interaction										
P value	＜0.001		0.198		0.820		0.006		＜0.001	
η^2	0.182		0.020		0.0.001		0.088		0.173	
grouping										
P value	0.092		0.244		0.939		0.441		0.221	
η^2	.034		.017		0.000		0.007		0.018	

3.5. Comparison of Sleep Observation Indicators between the Decoction Group and the Non-decoction Group

The scores of the two dimensions of PSG, namely OAHI and LSaO2, were statistically analyzed. It was found that after treatment, the OAHI scores of all cases were lower than the baseline values, and the LSaO2 scores were higher than the baseline values. The results of the test using the general linear model for repeated measures are shown in Table 5.

Between-group effect: The OAHI score decreased after treatment, and the LSaO2 score increased after treatment. There were no significant differences in the scores of the cases before and after treatment between the two groups (p ＞＝ 0.05).

Time effect: The OAHI score decreased after treatment, and the LSaO2 score increased after treatment. There were significant differences in the scores of the cases before and after treatment ($p < 0.001$).

Interaction effect between group and time: There were no differences in the changing trends of the scores of the two dimensions of OAHI and LSaO2 before and after treatment between the two groups (for the scores of the two dimensions of OAHI and LSaO2), indicating no interaction effect. There were no differences in the scores of the two dimensions of OAHI and LSaO2 between the decoction group and the non-decoction group before and after treatment.

Table 5. Comparison of the PSG-related scores before and after treatment between the decoction group and the non-decoction group

	OAHI		$LSaO_2$	
	before	after	before	after
decoction group	5.06±1.65	0.53±0.63	87.72±2.02	96.02±2.09
non- decoction group	4.87±1.66	046±0.55	88.43±1.89	96.14±2.18
Treatment				
P value	＜0.001		＜0.001	
η^2	0.882		0.895	
treatment*grouping interaction				
P value	0.740		0.330	
η^2	0.001		0.0.012	
grouping				
P value	0.518		0.207	
η^2	0.005		0.019	

3.6. Bibliometric Analysis of Traditional Chinese Medicine Treatment for Adenoid Hypertrophy

According to the bibliometric analysis and statistics, the keywords in terms of citation quantity and ranked by time are as follows: Yu Jingmao, deficiency of qi in the lung and spleen, nasal obstruction, TCM clinical practice, children, review, curative effect, external treatment method, pediatric tuina, and data mining.

Pediatric tuina and data mining are relatively hot keywords in recent years (Figure 1, A). In terms of the results of keyword clustering hotspots, the top 10 ranked keywords are: clinical experience, children, deficiency of qi in the spleen and lung, pediatric tuina, snoring and sleeping, data mining, experience of famous doctors, review, curative effect, intermingling of phlegm and blood stasis, Erchen Decoction, TCM, staged treatment, Yu Jingmao and children (Figure 1, B, C).

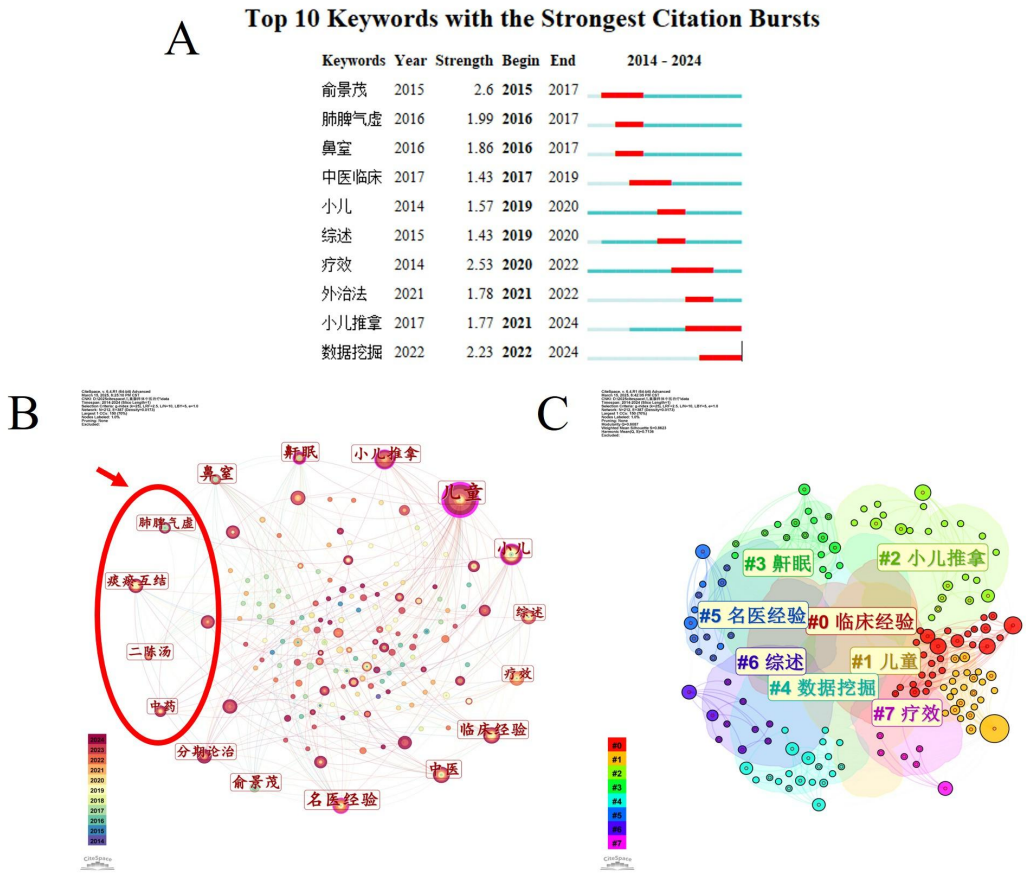

Figure 1. Cluster Analysis and Hotspot Analysis of Keywords in the Treatment of AH in Children with TCM

Arranged in chronological order, the articles summarizing the clinical experience of TCM treatment for AH in children have the longest citation time span, showing a uniform distribution from 2014 to 2024. The citations of articles on data mining of TCM treatment for AH in children have increased significantly in the past five years.

Among the authors of the published articles, the top three most cited are Jiang Zhiyan, Liu Zhuyun, and Ren Xianzhi. Among the institutions of the published articles, the top three most cited are Longhua Hospital Affiliated to Shanghai University of Traditional Chinese Medicine, Shanghai University of Traditional Chinese Medicine, and the Seventh Hospital Affiliated to Shanghai University of Traditional Chinese Medicine.

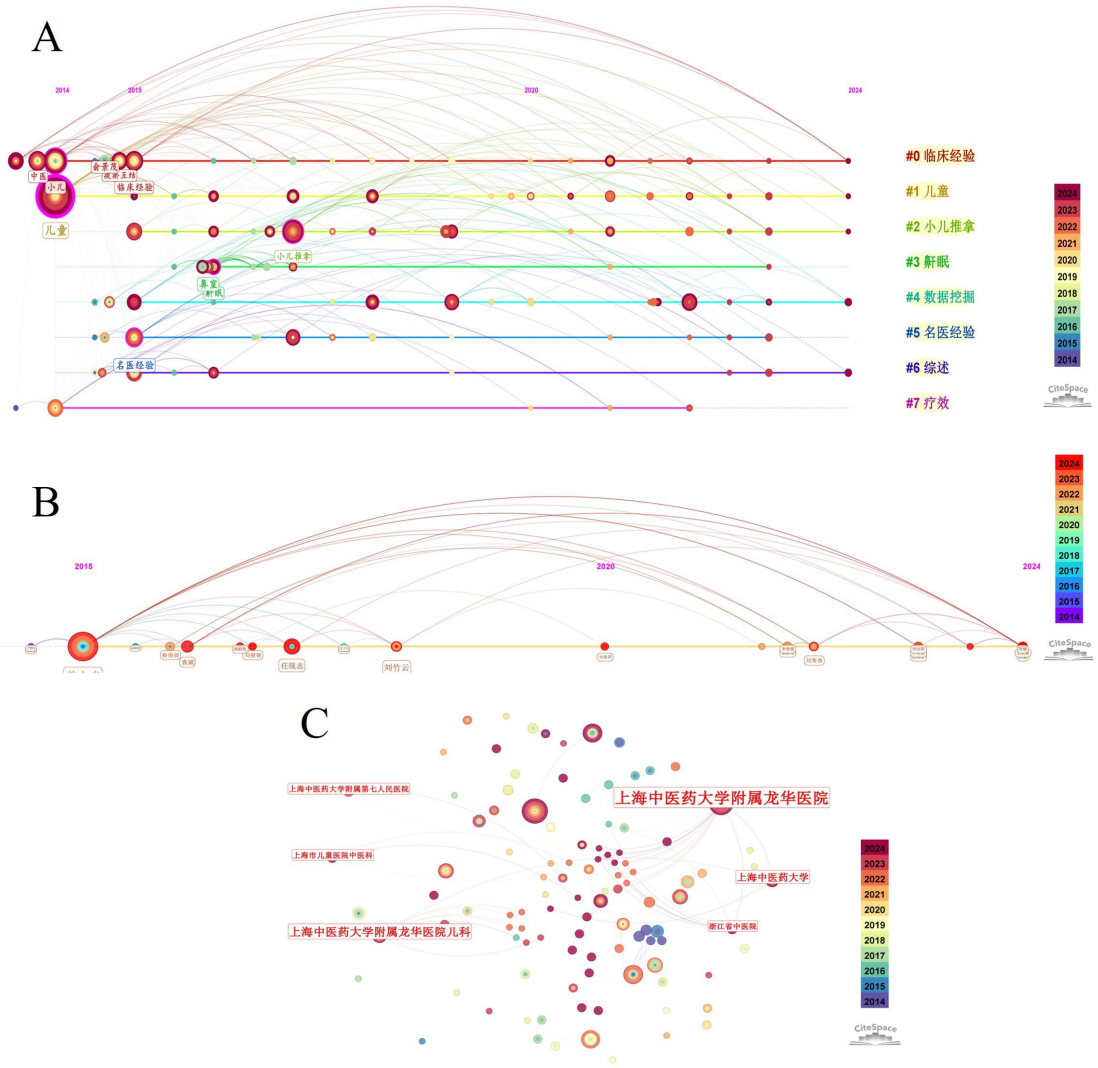

Figure 2. Arrangement of Keywords and author citation in Chronological Order and Co-occurrence of Institutional Co-citations

4. Discussion

According to modern medical concepts and relevant guidelines (Ahmad et al., 2023; Joseph et al., 2025), for AH, the conservative treatment methods mainly focus on the application of nasal glucocorticoids and leukotriene receptor antagonists. In addition, some research reports have pointed out that second-generation antihistamine drugs play a certain role in controlling nasal symptoms and ear complications (Velentza et al., 2020). In the field of treating AR in children, nasal glucocorticoids and second-generation antihistamine drugs have been clearly listed as the preferred treatment options. At the same time, the importance of immunotherapy, health education, and nursing has also been emphasized (Pavon-Romero et al., 2021).

However, in clinical practice, even if children meet the surgical indications for AH, some parents still prefer conservative treatment. Behind this phenomenon, there are both subjective factors such as cultural differences and many objective factors. For example, surgery cannot completely cure AR, and it may be complicated by chronic sinusitis after surgery. There may even be a situation where the AH again and require reoperation. Relevant studies have shown that

factors such as the first surgical age being less than 2 years old, frequent upper respiratory tract infections, suffering from AR, and genetic factors are all risk factors for secondary adenoidectomy (Lee et al., 2018). Moreover, eustachian tube dysfunction after surgery is relatively common, and it often requires repeated tympanic membrane puncture or even tube insertion to improve hearing (Diksha et al., 2022).

It can be seen that relying solely on modern medical drug treatment is difficult to fully meet the clinical needs of conservative treatment for AH. Therefore, exploring new treatment options to further improve the treatment effect and meet the actual clinical needs is of great practical significance. Traditional medicine has shown significant advantages in the treatment of AH and AR and has gained widespread cultural recognition in China. Many domestic research reports have shown that TCM and non-drug external treatment methods of TCM can effectively improve the symptoms of AH and the clinical manifestations of AR (Sun et al., 2019; Zhang et al., 2020).

Based on a systematic summary of previous research reports and personal clinical experience, this study uses a self-formulated HCZ Decoction to treat children with AH complicated by AR, aiming to observe the clinical efficacy of this decoction on the basis of standard modern drug treatment.

The results of this study showed that the clinical symptoms of OSA in all the included cases improved after treatment. The OSA-18 score decreased from moderate to mild after treatment, indicating that both the treatment in the decoction group and the non-decoction group was effective, and the treatment effect of the decoction group was better than that of the non-decoction group, with a between-group difference. This superiority was manifested in five aspects: sleep impact, body symptoms, mood impact, daytime state, and impact on guardians. The conclusion of this study is consistent with the viewpoints reported in previous studies (Zhang et al., 2020; Zhao et al., 2023).

In terms of the improvement of nasal symptoms, although the decoction group did not show superiority compared with the non-decoction group, the improvement trends of nasal obstruction and sneezing symptoms were different from those of the non-decoction group, suggesting that the decoction group still had advantages in the treatment of nasal symptoms, which was in line with the viewpoints in the previous literatures on the treatment of AR in children with TCM (Zhang et al., 2020). However, there were no differences in the trends and effects of improving OAHI and LSaO2 between the two groups, indicating that the treatment with this decoction may not have shown advantages in improving objective scores.

The bibliometric study suggested that the treatment of AH with TCM focused more on the experience summary of famous veteran Chinese medicine doctors and the mining of clinical data. The clinical syndrome differentiation mainly focused on deficiency of qi in the spleen and lung and the intermingling of phlegm and blood stasis. Taking Erchen Decoction as an example, the medication focused on removing dampness, resolving phlegm, and promoting blood circulation to remove blood stasis, providing literature support for the composition of the decoction in this study.

The innovation of this study lies in combining clinical observation with bibliometric research, analyzing the clinical impact of the method of resolving phlegm, removing dampness, and

promoting blood circulation to remove blood stasis in the treatment of AH, and providing a reference basis for the conservative treatment of AH complicated by AR with traditional medicine in clinical practice. The deficiency is that further follow-up was not carried out to explore the long-term effects of AH treatment. The sample size of this study still needs to be expanded to clarify the impact of treatment on objective evaluation results.

Author Contributions:

Ying Wang and Zhonghai Xin designed the work; Ying Wang, Changwen Che contributed to the acquisition, analysis, and interpretation of data; Ying Wang wrote the main manuscript and prepared all the figures. Mingsheng Zhang and Zhonghai Xin revised the manuscript. All authors reviewed the manuscript.

Funding:

This work was supported by the grant of Science and Technology Innovation Project of the China Academy of Chinese Medicine Science (CACMS Innovation Fund, No.CI2021A02707).

Institutional Review Board Statement:

The studies were reviewed and approved by the Ethics Committee of the Wangjing Hospital, China Academy of Chinese Medical Sciences.

Informed Consent Statement:

Not applicable.

Data Availability Statement:

Not applicable.

Acknowledgments:

The authors acknowledge for the support and technical comments of all reviewers.

Conflict of Interest Statement:

All authors declare no competing interests.

References

Ahmad, Z., Krüger, K., Lautermann, J., Lippert, B., Tenenbaum, T., Tigges, M., Tisch, M. (2023). Adenoid hypertrophy-diagnosis and treatment: the new S2k guideline. HNO, 71(Suppl 1), 67-72.

Alimoglu, Y., Altin, F., Yorguner, N. E., Acikalin, R. M., & Yasar, H. (2020). Predicting the outcome after adenoidectomy-alone for adenoid hypertrophy causing sleep disordered breathing. American Journal of Otolaryngology, 41(6), 102646.

Cheng, M., Dai, Q., Liu, Z., Wang, Y., Zhou, C. (2024). New progress in pediatric allergic rhinitis. Front Immunol, 15, 1452410.

Diksha, Singhal, S. K., Gupta, N., Gupta, R., & Verma, R. R. (2022). Radiological and audiological assessment in patients with adenoid hypertrophy undergoing adenoidectomy. Indian Journal of Otolaryngology and Head & Neck Surgery, 74(Suppl 2), 1527-1531.

Eldegeir, M., Marry, N. A., Awami, F., Alsada, F. (2023). The combination of nasal steroids and anti-leukotriene to reduce adenectomy in children with OSA and adenoid hypertrophy. Qatar Med J, (2), 31.

Joseph, M., Krishna, M. M., Franco, A. J., Jekov, L., Sudo, R. Y. U., & Cabral, T. D. D. (2025). Efficacy of combination therapy with mometasone and montelukast versus mometasone alone in treatment of adenoid hypertrophy in children: A systematic review and meta-analysis. American Journal of Otolaryngology, 46(1), 104566.

Lee, D. J., Chung, Y. J., Yang, Y. J., & Mo, J. H. (2018). The impact of allergic rhinitis on symptom improvement in pediatric patients after adenotonsillectomy. Clinical and Experimental Otorhinolaryngology, 11(1), 52-57.

Niedzielski, A., Chmielik, L. P., Mielnik-Niedzielska, G., Kasprzyk, A., Bogusławska, J. (2023). Adenoid hypertrophy in children: a narrative review of pathogenesis and clinical relevance. BMJ Paediatr Open, 7(1), e001710.

Pavon-Romero, G. F., Larenas-Linnemann, D. E., Xochipa Ruiz, K. E., Ramirez-Jimenez, F., & Teran, L. M. (2021). Subcutaneous allergen-specific immunotherapy is safe in pediatric patients with allergic rhinitis. International Archives of Allergy and Immunology, 182(6), 553-561.

Randall, D. A. (2020). Current Indications for Tonsillectomy and Adenoidectomy. J Am Board Fam Med, 33(6), 1025-1030

Schupper, A. J., Nation, J., Pransky, S., et al. (2018). Adenoidectomy in Children: What Is the Evidence and What Is its Role?. Curr Otorhinolaryngol Rep, 6, 64–73.

Shivnani, D., Kobal, M. R., Raman, E. V., Shruthi, M. S. (2023). Impact of Chronic Adenoid Hypertrophy on Quality of Life Index in Children and Role of Adenoidectomy. Indian J Otolaryngol Head Neck Surg, 75(4), 3396-3401.

Sun, Y. L., Zheng, H. T., Tao, J. L., Jiang, M. C., Hu, C. C., Li, X. M., & Yuan, B. (2019). Effectiveness and safety of Chinese herbal medicine for pediatric adenoid hypertrophy: A meta-analysis. International Journal of Pediatric Otorhinolaryngology, 119, 79-85.

Tse, K. L., Savoldi, F., Li, K. Y., McGrath, C. P., Yang, Y., Gu, M. (2023). Prevalence of adenoid hypertrophy among 12-year-old children and its association with craniofacial characteristics: a cross-sectional study. Prog Orthod, 24(1), 31.

Varghese, A. M., Naina, P., Cheng, A. T., Asif, S. K., & Kurien, M. (2016). ACE grading—A proposed endoscopic grading system for adenoids and its clinical correlation. International Journal of Pediatric Otorhinolaryngology, 83, 155-159.

Velentza, L., Maridaki, Z., Blana, E., & Miligkos, M. (2020). Antihistamines in the management of pediatric allergic rhinitis: A systematic review. Paediatric Drugs, 22(6), 673-683.

Zhang, J., Fu, Y., Wang, L., Wu, G. (2024). Adenoid facies: a long-term vicious cycle of mouth breathing, adenoid hypertrophy, and atypical craniofacial development. Front Public Health, 12, 1494517.

Zhang, M., Fan, Y., Tian, C., Xie, Y., Huang, Y., Yang, S., & Zhang, Q. (2020). The efficacy and safety of Chinese herbal compound in pediatric patients with allergic rhinitis: A protocol for systematic review and meta-analysis. Medicine, 99(32), e21643.

Zhao, X., Xu, J., Wang, M. Y., Hou, Z. W., Shi, H. S., & Zhang, X. X. (2023). Effect of oral Xiao-xian decoction combined with acupoint application therapy on pediatric adenoid hypertrophy: A randomized trial. Medicine, 102(5), e32804.

Zwierz, A., Domagalski, K., Masna, K., Burduk, P. (2024). Maximal medical treatment of adenoid hypertrophy: a prospective study of preschool children. Eur Arch Otorhinolaryngol, 281(5), 2477-2487.

Advances in World Medical Research, 2025, 1(1), 50-60
https://doi.org/10.71204/7agtqd88

Scleritis Caused by Eosinophilic Granulomatosis with Polyangiitis: A Case Report

Wenbo Hou [1,*], Xin Li [1], Xuguang Sun [2]

[1] DepartmentIIof Ophthalmology, The Eye Hospital, China Academy Of Chinese Medical Sciences, Beijing 100040, China

[2] Department of Ocular Microbiology, Beijing Institute of Ophthalmology, Beijing Tongren Hospital, Capital Medical University, Beijing 100730, China

*** Correspondence**:

Wenbo Hou

susie2001@126.com

Received: 10 April 2025/ Accepted: 12 May 2025/ Published online: 20 May 2025

Abstract

To report a case of an 81-year-old female with scleritis due to eosinophilic granulomatosis with polyangiitis (EGPA) and emphasize the importance of accurate diagnosis and appropriate management. The patient's initial symptoms, including scleritis and systemic manifestations such as recurrent fever, were observed. Laboratory tests, imaging studies, ANCA testing, and bone marrow biopsy were performed for diagnosis. Treatment with methylprednisolone and cyclophosphamide was administered, and the response was monitored by observing the resolution of scleritis and normalization of blood parameters. The patient was initially misdiagnosed. However, through comprehensive examinations, the EGPA diagnosis was confirmed. The treatment was effective, with the scleritis being resolved and blood parameters returning to normal. EGPA is a rare ANCA-associated vasculitis with complex and non-specific manifestations. ANCA is a significant biomarker, and comprehensive laboratory testing is crucial for accurate diagnosis. Treatment consists of induction and maintenance phases. Ophthalmologists should be aware of the possibility of systemic autoimmune diseases in scleritis patients, especially those with eosinophilia and systemic symptoms, and cooperate with internal medicine specialists for optimal patient management.

Keywords: Eosinophilic Granulomatosis with Polyangiitis; ANCA; Scleritis; Autoimmune Disease; ANCA-associated Vasculitis

1. Introduction

Eosinophilic Granulomatosis with polyangiitis (EGPA), formerly known as Churg-Strauss syndrome, is the rarest form of antineutrophil cytoplasmic antibody (ANCA)-associated vasculitis

(AAV) (Churg & Strauss, 1951; Jennette et al., 2012; Kitching et al., 2020). It is characterized by eosinophil-rich granulomatous inflammation and vasculitis affecting small to medium-sized vessels, with an annual prevalence ranging from 10.7 to 17.8 cases per million[4]. As an uncommon disease, EGPA is distinguished by a wide range of clinical symptoms that might change at different points in the disease's natural history. Systemic vasculitis frequently progresses quickly, and in about half of patients, systemic symptoms are accompanied by clinical signs of a vasculitis process, including purpura, scleritis, alveolar hemorrhage, extracapillary glomerulonephritis, and involvement of the peripheral nervous system (Furuta et al., 2019; Lutalo et al., 2014).

Since EGPA can progress to organ- or life-threatening diseases, we must be on the lookout for patients who have scleritis along with systemic symptoms, particularly those who have elevated eosinophils and ANCA levels. In this report, we present a case of scleritis caused by granulomatosis with EGPA, although the local features of scleritis in this case are not specific, the findings of pertinent tests can aid in the early diagnosis of EGPA.

2. Case Presentation

An 81-year-old female patient presented with the chief complaints of recurrent fever for half a year and redness in the right eye accompanied by decreased visual acuity for more than one month. The patient had a history of hypothyroidism and sinusitis in the past. In the recent half year, she had experienced fatigue, recurrent low fever, numbness in the limbs, and weight loss. She denied a family history of trauma and hereditary diseases.

At the time of consultation, the best corrected visual acuity (BCVA) of the right eye was 0.25, and the intraocular pressure was 15 mmHg (1 mmHg = 0.133 kPa). The sclera was congested with a dark red color (Figure 1), and the lens was opaque (C2N2PO). The optic disc in the fundus had a normal color and a clear border, with the cup-to-disc ratio (C/D) approximately 0.3 and the arteriovenous ratio (A:V) approximately 1:2. The reflection of the fovea centralis was unclear.

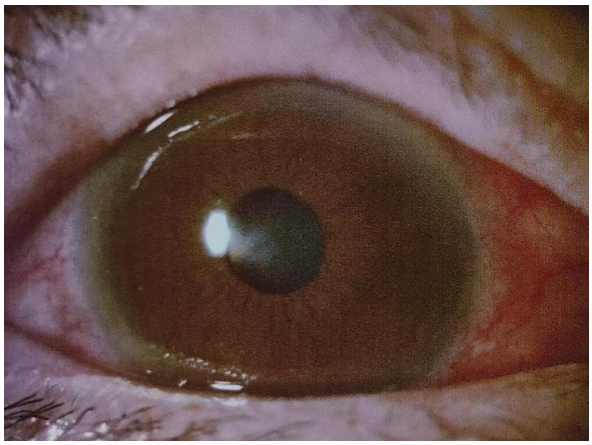

Figure 1. This is an anterior segment photograph of the patient taken at the time of presentation. The sclera is dark red with edema and there is a decrease in vision.

The results of auxiliary examinations were as follows:

(1) Blood routine: The white blood cell count (WBC) was 11.4 × 10^9/L (elevated), the percentage of neutrophils (NEUT%) was 78.6% (elevated), the percentage of lymphocytes (LYM%) was 9.6% (decreased), the neutrophil count (NEUT) was 8.96 × 10^9/L (elevated), and the eosinophil count was 0.53 × 10^9/L (elevated).

(2) Comprehensive biochemistry: The rheumatoid factor (RF) was 32.4 IU/ml, and the C-reactive protein (CRP) was 67.21 mg/L.

(3) Coagulation panel: The fibrinogen (Fib) was 4.6 g/L, the D-dimer was 1.8 mg/L, and the fibrinogen degradation products (FDP) were 7.1 mg/L.

(4) Seven items of thyroid function: Triiodothyronine (TT3) was 0.85 nmol/L, free triiodothyronine (FT3) was 2.66 pmol/L, thyroid-stimulating hormone (TSH) was 6.00 mIU/L, anti-thyroglobulin antibody (TG-Ab) was 222.4 IU/ml, and anti-thyroid peroxidase antibody (TPO-Ab) was 360.54 IU/ml.

(5) Screening for rheumatic immune diseases: Anti-centromere antibody (CENP-B) was 93.17 RU/ml.

(6) Detection of respiratory viruses: Antibodies to common respiratory viruses were all negative.

(7) Inflammatory panel: Interleukin-6 (IL-6) measurement was 25.5 pg/ml.

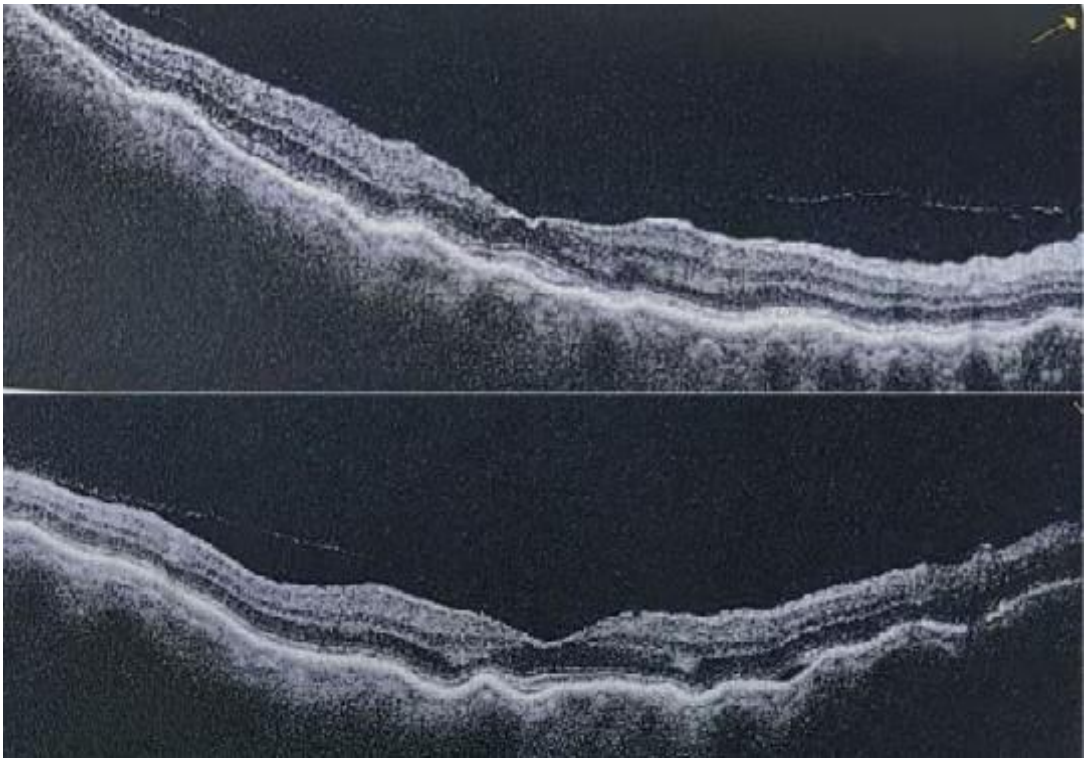

Figure 2. The patient was found to have a cuspidate wave-like folding of the choroid and retina in the macula by OCT examination.

(8) Tests for eight items of infectious diseases, hepatitis A antibody, and hepatitis E antibody were all negative.

(9) Electrocardiogram showed sinus rhythm, right ventricular conduction delay, moderate left axis deviation, and no other significant abnormalities.

(10) Optical coherence tomography (OCT) of both eyes: The choroid in the macular area was thickened, and there were wavy folds in the retina and choroid (Figure 2).

(11) Fluorescein fundus angiography (FFA) and indocyanine green angiography (ICGA) indicated choroidal edema in the right eye and scleritis in the right eye.

(12) Ocular B-ultrasound showed thickening of the right sclera with the "T" sign (Figure 3).

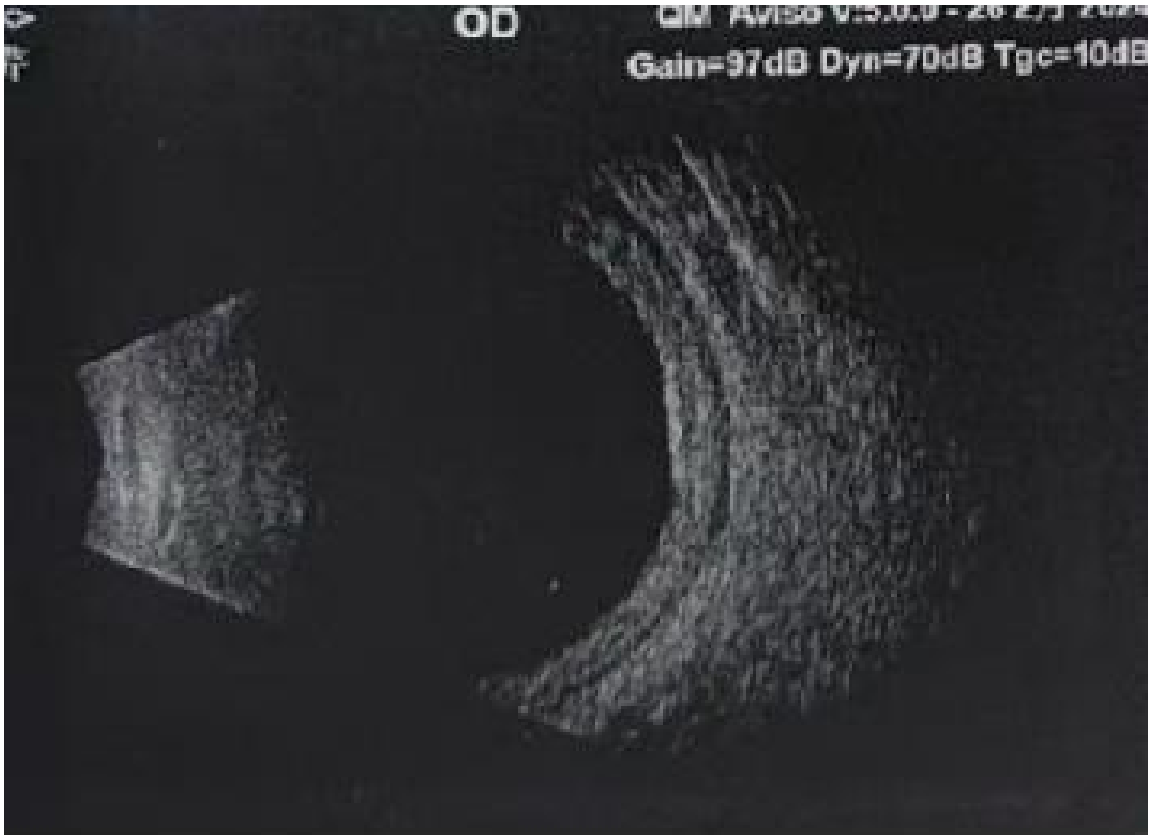

Figure 3. The patient presents with the classic "T-sign"

(13) Plain CT scan of the paranasal sinuses: The mucous membranes of the bilateral maxillary sinuses, part of the ethmoid sinuses, and sphenoid sinuses were thickened.

(14) Color Doppler ultrasound of organs and blood vessels throughout the body: There were no significant abnormalities in the liver, gallbladder, pancreas, and spleen; there were bilateral renal cysts; the uterus was in the postmenopausal state; the bilateral lower extremity arteries showed atherosclerotic changes accompanied by plaques. Echocardiography showed aortic valve regurgitation (mild), mitral and tricuspid valve regurgitation (mild), and decreased left ventricular diastolic function.

(15) Enhanced orbital MRI scan: The ring of the right eye was thickened with enhancement, and there were abnormal enhancements in the right lacrimal gland, right orbital apex, and posterior ethmoid sinuses; there was partial empty sella turcica; there was a slight inflammation in the bilateral maxillary sinuses; and there was inflammation in the bilateral mastoid processes.

Based on the above examination results, the patient was diagnosed with scleritis in the right eye, sinusitis, and hypothyroidism. She was treated with prednisolone acetate eye drops, 6 times a day, tobramycin and dexamethasone eye ointment, once a night, pranoprofen eye drops, 4 times a day for the right eye, and retrobulbar injection of triamcinolone acetonide injection 20 mg + dexamethasone sodium phosphate injection 2.5 mg + lidocaine injection 0.5 ml for the right eye. Additionally, a trial treatment was carried out using Cefoperazone sodium 1.5g was administered intravenously, and Diclofenac sodium pills were taken orally on a daily basis. This regimen consisted of systemic antibiotics and nonsteroidal anti-inflammatory drugs due to the persistent uncertainty regarding the cause of the recurrent fever. After three weeks of treatment, the scleritis in the patient's right eye substantially subsided, and the visual acuity improved. The best corrected visual acuity of the right eye was 0.6. OCT reexamination showed that the choroidal folds had mostly disappeared, and the fever had abated. Subsequently, the patient was discharged. However, two weeks after discharge, the fever recurred, reaching a maximum of 39.2°C. Consequently, the patient was readmitted to the hospital. After being hospitalized again, laboratory examinations were conducted. It was found that the level of MPO-ANCA was 246.00 AU/ml (elevated), and the titer of P-ANCA was 1:20. Flow cytometry of bone marrow demonstrated an increased proportion of eosinophils. Bone marrow biopsy revealed that the bone marrow hyperplasia was generally normal, with the proliferation of granulocyte, erythrocyte, and megakaryocyte lineages accompanied by easily observable eosinophils (Figure 4). The screening results for bone marrow proliferative neoplasm (MPN) gene mutations were negative. No clonal abnormalities were detected in the bone marrow chromosome examination.

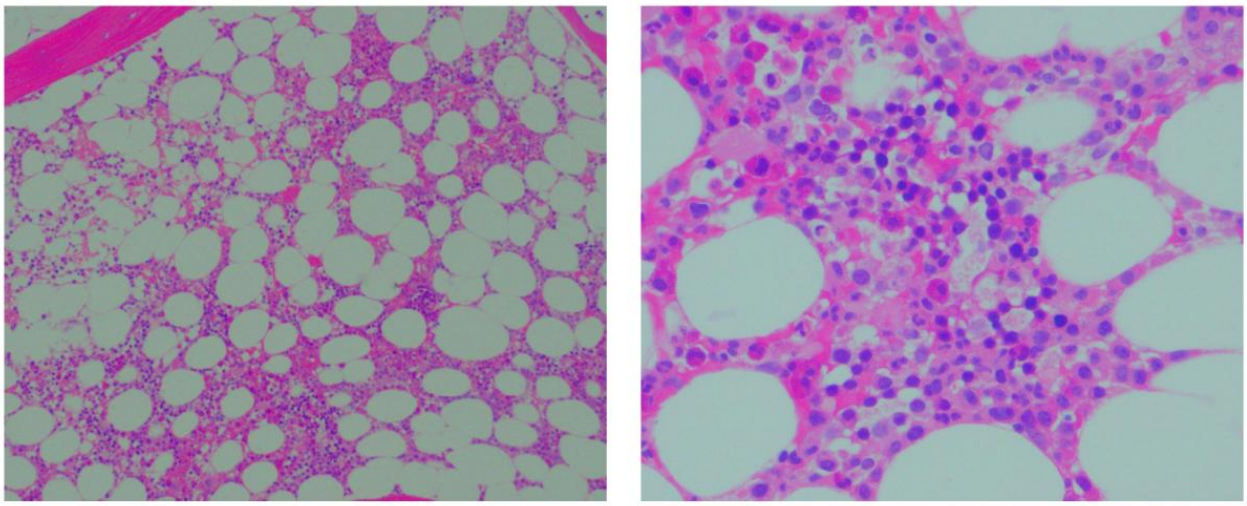

Figure 4. Bone marrow aspiration: There is a marked increase in the activity of bone marrow cell morphogenesis, with an increase in the proportion of granulocytes and an increase in the proportion of acidophilic granulocytes.

Based on the patient's past medical history, symptoms, physical signs, laboratory test results, and imaging findings, a diagnosis of eosinophilic granulomatous vasculitis (EGPA) was confirmed. After the diagnosis was clear, methylprednisolone at a dose of 40 mg once daily was administered by intravenous infusion, combined with cyclophosphamide at a dose of 0.2 g every other day. In addition, low-molecular-weight heparin at a prophylactic dose was used for anticoagulation, and cotrimoxazole was given for infection prevention. After one month of treatment, the patient's systemic symptoms such as fever and fatigue completely disappeared, scleritis was completely cured, and both blood routine parameters and immune indexes returned to normal. The best corrected visual acuity (BCVA) of the right eye improved to 0.8, and no significant abnormalities were found in the ocular examination. Prednisolone tablets at a dose of 40 mg once daily and cyclophosphamide at a dose of 0.1 g every other day were used for maintenance treatment, along with liver protection and anticoagulation therapies. During the follow-up period, the patient's condition remained stable, and there was no recurrence.

3. Discussion

Scleritis is a relatively rare eye disease in clinical practice, accounting for only about 0.5% of all eye diseases. Its etiology is complex and not fully understood at present. It may be related to exogenous infection, endogenous infection, and autoimmune diseases (Vergouwen et al., 2020; Nevares et al., 2020). Scleritis can occur during the onset or before the onset of potentially fatal systemic autoimmune diseases, therefore, early diagnosis and treatment of scleritis, especially thorough screening for patients with systemic symptoms, is particularly important.

This case is an example of an autoimmune disease - eosinophilic granulomatous vasculitis (EGPA) causing scleritis. The patient initially presented with scleritis, but because the systemic symptoms were mild and presented only low-grade fever, the true underlying cause of the scleritis was not investigated.

EGPA is a rare clinical disease. The pathological changes mainly involve small and medium-sized blood vessels, manifesting as systemic necrotizing vasculitis, and it belongs to antineutrophil cytoplasmic antibody (ANCA)-associated vasculitis (AAV) (Churg & Strauss, 1951). It was first described by Churg and Strauss in 1951 (Churg & Strauss, 1951). It often presents initially with asthma, sinusitis, and eosinophilia. After an average period of 3 to 9 years, it progresses to the vasculitis stage, and the pathological changes can involve multiple tissues and organs throughout the body. Due to the lack of specificity in its clinical manifestations, it is prone to misdiagnosis and missed diagnosis (Szczeklik et al., 2011; Keogh et al., 2006).

Currently, there is no formal diagnostic criteria for EGPA. Historically, Lanham et al. published a set of diagnostic criteria in 1984, but it did not include ANCA testing and had poor sensitivity for a limited number of disease patients (Lanham et al., 1984). The 2012 revision of the Chapel Hill Consensus Conference (CHCC) vascular disease nomenclature classified EGPA as a disease characterized by eosinophilic and necrotizing granulomatous inflammation, typically involving the respiratory tract, with necrotizing vasculitis predominating, primarily affecting small to medium-sized vessels, and accompanied by asthma and eosinophilia (Jennette et al., 2013;

Wechsler et al., 2017). Recently, a practical diagnostic criteria set was proposed by a joint working group supported by the European Respiratory Society (ERS) and Groupe d'Etudes et de Recherche sur les Maladies Orphelines Pulmonaires (GERM'O'P), limiting the term EGPA to patients with positive ANCA tests or those with true vascular inflammation features (Cottin et al., 2016).

EGPA is usually divided into three overlapping stages: a prodromal period, which may last for several years, characterized by respiratory symptoms with asthma and sinusitis; the second stage, accompanied by an increase in blood eosinophils, tissue infiltration of eosinophils, and organ damage caused by eosinophils; and the third stage, characterized by systemic necrotizing vasculitis. Once diagnosed with EGPA, the clinical course can progress from an acute, self-limiting process to multi-organ dysfunction, with a high morbidity and mortality rate (Berti et al., 2020).

EGPA presented as heterogeneous clinical manifestations that may change at different stages of the natural course of the disease. Most patients have systemic symptoms such as fever, muscle and joint pain, and weight loss. Skin involvement manifests as purpura, subcutaneous nodules, urticaria, skin infarction, reticular purpura, and tense vesicles. The literature reports that 62% of patients with EGPA have cardiac involvement, but only 26% have clinical symptoms. Cardiac involvement is the leading cause of death in EGPA (Hazebroek et al., 2015). Peripheral neuropathy is the most important clinical manifestation of the vasculitis phase of EGPA, affecting about 2/3 of patients, and presents as multiple mononeuritis, affecting both motor and sensory nerves (Koike et al., 2012).

ANCA is an important vascular inflammation biomarker in EGPA. The positive rate of ANCA in granulomatous vasculitis and microscopic polyangiitis can reach 75%-95%. The positive rate of ANCA in EGPA is 30%-40%, mainly positive for p-ANCA and MPO-ANCA. The prognosis of EGPA is good, with a 7-year survival rate of 90%. MPO-ANCA positivity, peripheral blood eosinophilia $<3\times10^9$/L at diagnosis, and peripheral neuropathy may be risk factors for disease recurrence (Saku et al., 2018; Durel et al., 2016; Comarmond et al., 2013; Sinico et al., 2005; Moosig et al., 2013; Tsurikisawa et al., 2017). The levels of p-ANCA and MPO-ANCA in this case were significantly elevated, which led us to strongly suspect that the patient had EGPA. Additionally, the patient's persistent fever prompted a bone marrow biopsy, which ultimately confirmed the diagnosis of EGPA. ANCA-positive patients seem to be more likely to have vasculitis manifestations. Some studies have found that 43.4% of EGPA patients have ocular complications, some of which are caused by the use of steroids, such as steroid-induced cataract, and others may include neuro-ophthalmic diseases, persistent scleritis, uveitis, etc., which can cause acute damage to visual function, but there are cases of blindness due to this (Turk et al., 2021; Hinojosa-Azaola et al., 2019).

Therefore, in the future when encountering scleritis patients in clinical practice, especially those with scleritis accompanied by systemic abnormalities, a comprehensive screening and evaluation should be conducted to determine any non-ocular conditions related to the diagnosis. In the diagnostic workup of scleritis, a comprehensive hematological analysis is warranted. Complete blood count parameters, namely hemoglobin, platelet, and white blood cell counts, in

conjunction with inflammatory biomarkers such as C-reactive protein (CRP) and erythrocyte sedimentation rate (ESR), possess significant value in signifying the existence of an underlying inflammatory cascade. Furthermore, the assessment of autoimmune serological markers is indispensable. Antinuclear antibody (ANA), extractable nuclear antigens (including anti-ds-DNA, anti-histone, anti-Smith, anti-Ro, anti-La, anti-Jo), rheumatoid factor (RF), complement levels (C3 and C4), antiphospholipid antibodies, as well as the vasculitis autoimmune profile (encompassing c-ANCA, p-ANCA, atypical c-ANCA, atypical p-ANCA, myeloperoxidase p-ANCA, proteinase 3 c-ANCA, glomerular basement membrane antibody), are of crucial importance in formulating a definitive diagnosis of immune-mediated systemic vasculitis concomitant with scleritis. This comprehensive approach to laboratory testing aids in the accurate identification and classification of the disease, facilitating appropriate management strategies and improved patient outcomes.

The treatment of EGPA includes an induction phase and a maintenance phase. The former aims to relieve the disease, while the latter seeks to prevent recurrence. Prospective studies specifically targeting EGPA are rare, and most treatment recommendations for EGPA are directed at symptomatic treatment for specific affected organs. Patients with a confirmed diagnosis of EGPA should be treated with steroids and immunosuppressants as early as possible to improve prognosis (Raffray et al., 2020; Fujimoto et al., 2011). After disease control, steroids need to be tapered, but long-term use of immunosuppressants is still required to reduce the side effects of long-term high-dose steroids. In addition, close follow-up is needed to monitor the dynamic changes of ANCA titers and to detect recurrence of the disease as early as possible (Watanabe et al., 2023; Cottin et al., 2016). For local ocular lesions, in addition to systemic therapy, topical eye drops are more effective. As our understanding of ANCA-related small vessel vasculitis deepens, the diseases it causes in the field of ophthalmology will also be given greater attention.

This case reminds us that when scleritis is accompanied by fever and other systemic symptoms, a thorough physical examination should be performed to determine whether there is a systemic autoimmune disease. When the blood count shows an increase in eosinophils, it is important to perform additional tests, such as ANCA, to consider the possibility of EGPA. Ophthalmologists should be aware of the importance of consulting with internal medicine specialists.

Author Contributions:

Conceptualization, W. H., X. L., X. S.; methodology, W. H., X. L., X. S.; software, W. H., X. L., X. S.; validation, W. H., X. L., X. S.; formal analysis, W. H., X. L., X. S.; investigation, W. H., X. L., X. S.; resources, W. H., X. L., X. S.; data curation, W. H., X. L., X. S.; writing—original draft preparation, W. H., X. L., X. S.; writing — review and editing, W. H., X. L., X. S.; visualization, W. H., X. L., X. S.; supervision, W. H., X. L., X. S.; project administration, W. H., X. L., X. S.; funding acquisition, W. H., X. L., X. S. All authors have read and agreed to the published version of the manuscript.

Funding:

Not applicable.

Institutional Review Board Statement:

The studies were reviewed and approved by the Ethics Committee of the Eye Hospital, China Academy Of Chinese Medical Sciences.

Informed Consent Statement:

Not applicable.

Data Availability Statement:

Not applicable.

Conflict of Interest:

The authors declare no conflict of interest.

References

Berti, A., Boukhlal, S., Groh, M., & Cornec, D. (2020). Eosinophilic granulomatosis with polyangiitis: the multifaceted spectrum of clinical manifestations at different stages of the disease. Expert Review of Clinical Immunology, 16(1), 51-61.

Churg, J., & Strauss, L. (1951). Allergic granulomatosis, allergic angiitis, and periarteritis nodosa. The American journal of pathology, 27(2), 277.

Comarmond, C., Pagnoux, C., Khellaf, M., Cordier, J. F., Hamidou, M., Viallard, J. F., ... & French Vasculitis Study Group. (2013). Eosinophilic granulomatosis with polyangiitis (Churg-Strauss): clinical characteristics and long-term followup of the 383 patients enrolled in the French Vasculitis Study Group cohort. Arthritis & Rheumatism, 65(1), 270-281.

Cottin, V., Bel, E., Bottero, P., Dalhoff, K., Humbert, M., Lazor, R., ... & Cordier, J. F. (2016). Respiratory manifestations of eosinophilic granulomatosis with polyangiitis (Churg–Strauss). European Respiratory Journal, 48(5), 1429-1441.

Durel, C. A., Berthiller, J., Caboni, S., Jayne, D., Ninet, J., & Hot, A. (2016). Long-term followup of a multicenter cohort of 101 patients with eosinophilic granulomatosis with polyangiitis (Churg-Strauss). Arthritis care & research, 68(3), 374-387.

Fujimoto, S., Watts, R. A., Kobayashi, S., Suzuki, K., Jayne, D. R., Scott, D. G., ... & Nunoi, H. (2011). Comparison of the epidemiology of anti-neutrophil cytoplasmic antibody-associated vasculitis between Japan and the UK. Rheumatology, 50(10), 1916-1920.

Furuta, S., Iwamoto, T., & Nakajima, H. (2019). Update on eosinophilic granulomatosis with polyangiitis. Allergology International, 68(4), 430-436.

Hazebroek, M. R., Kemna, M. J., Schalla, S., Sanders-van Wijk, S., Gerretsen, S. C., Dennert, R., ... & Heymans, S. (2015). Prevalence and prognostic relevance of cardiac involvement in ANCA-associated vasculitis: eosinophilic granulomatosis with polyangiitis and granulomatosis with polyangiitis. International journal of cardiology, 199, 170-179.

Hinojosa-Azaola, A., García-Castro, A., Juárez-Flores, A., & Recillas-Gispert, C. (2019). Clinical significance of ocular manifestations in granulomatosis with polyangiitis: association with sinonasal involvement and damage. Rheumatology international, 39(3), 489-495.

Jennette, J. C., Falk, R. J., Bacon, P. A. (2013). 2012 revised international chapel hill consensus conference nomenclature of vasculitides. Arthritis Rheum, 65, 1-11.

Keogh, K. A., & Specks, U. (2006). Churg-Strauss syndrome. In Seminars in respiratory and critical care medicine, 27(02), 148-157.

Kitching, A. R., Anders, H. J., Basu, N., Brouwer, E., Gordon, J., Jayne, D. R., ... & Kain, R. (2020). ANCA-associated vasculitis. Nature reviews Disease primers, 6(1), 71.

Koike, H., Nishi, R., Ohyama, K., Morozumi, S., Kawagashira, Y., Furukawa, S., ... & Katsuno, M. (2022). ANCA-associated vasculitic neuropathies: a review. Neurology and Therapy, 11(1), 21-38.

Lanham, J. G., Elkon, K. B., Pusey, C. D., & Hughes, G. R. (1984). Systemic vasculitis with asthma and eosinophilia: a clinical approach to the Churg-Strauss syndrome. Medicine, 63(2), 65-81.

Lutalo, P. M., & D'Cruz, D. P. (2014). Diagnosis and classification of granulomatosis with polyangiitis (aka Wegener's granulomatosis). Journal of autoimmunity, 48, 94-98.

Moosig, F., Bremer, J. P., Hellmich, B., Holle, J. U., Holl-Ulrich, K., Laudien, M., ... & Gross, W. L. (2013). A vasculitis centre based management strategy leads to improved outcome in eosinophilic granulomatosis and polyangiitis (Churg − Strauss, EGPA): monocentric experiences in 150 patients. Annals of the rheumatic diseases, 72(6), 1011-1017.

Nevares, A., Raut, R., Libman, B., & Hajj-Ali, R. (2020). Noninfectious autoimmune scleritis: recognition, systemic associations, and therapy. Current Rheumatology Reports, 22, 1-10.

Raffray, L., & Guillevin, L. (2020). Updates for the treatment of EGPA. La Presse Médicale, 49(3), 104036.

Saku, A., Furuta, S., Hiraguri, M., Ikeda, K., Kobayashi, Y., Kagami, S. I., ... & Nakajima, H. (2018). Longterm outcomes of 188 Japanese patients with eosinophilic granulomatosis with polyangiitis. The Journal of Rheumatology, 45(8), 1159-1166.

Sinico, R. A., Di Toma, L., Maggiore, U., Bottero, P., Radice, A., Tosoni, C., ... & Buzio, C. (2005). Prevalence and clinical significance of antineutrophil cytoplasmic antibodies in Churg-Strauss syndrome. Arthritis & Rheumatism, 52(9), 2926-2935.

Szczeklik, W., Sokołowska, B. M., Żuk, J., Mastalerz, L., Szczeklik, A., & Musiał, J. (2011). The course of asthma in Churg–Strauss syndrome. Journal of Asthma, 48(2), 183-187.

Tsurikisawa, N., Oshikata, C., Kinoshita, A., Tsuburai, T., & Saito, H. (2017). Longterm prognosis of 121 patients with eosinophilic granulomatosis with polyangiitis in Japan. The Journal of Rheumatology, 44(8), 1206-1215.

Turk, M. A., Hayworth, J. L., Nevskaya, T., & Pope, J. E. (2021). Ocular manifestations in rheumatoid arthritis, connective tissue disease, and vasculitis: a systematic review and metaanalysis. The Journal of Rheumatology, 48(1), 25-34.

Vergouwen, D. P. C., Rothová, A., Ten Berge, J. C., Verdijk, R. M., van Laar, J. A. M., Vingerling, J. R., & Schreurs, M. W. J. (2020). Current insights in the pathogenesis of scleritis. Experimental Eye Research, 197, 108078.

Watanabe, R., & Hashimoto, M. (2023). Eosinophilic granulomatosis with polyangiitis: latest findings and updated treatment recommendations. Journal of Clinical Medicine, 12(18), 5996.

Wechsler, M. E., Akuthota, P., Jayne, D., Khoury, P., Klion, A., Langford, C. A., ... & Gleich, G. J. (2017). Mepolizumab or placebo for eosinophilic granulomatosis with polyangiitis. New England Journal of Medicine, 376(20), 1921-1932.

Advances in World Medical Research, 2025, 1(1), 61-70
https://doi.org/10.71204/s8ksf005

Two-Sample Mendelian Randomization Analysis of the Correlation Between Allergic Rhino-Conjunctivitis and Concomitant Diseases and Peripheral Blood Eosinophil Count

Wei Zhang [1], Guibao Li [2], Jingjing Yuan [3,*]

[1] Eye Hospital, China Academy of Chinese Medical Sciences, Beijing 100040, China

[2] Beijing Language and Culture University, Beijing 100083, China

[3] Dongzhimen Hospital, Beijing University of Chinese Medicine, Beijing 100070, China

*** Correspondence**:

Jingjing Yuan

yuanjingjing85@126.com

Received: 12 April 2025/ Accepted: 12 May 2025/ Published online: 20 May 2025

Abstract

To explore the causal relationship between allergic rhino-conjunctivitis, asthma, and eczema and peripheral blood eosinophil count from the perspective of single nucleotide polymorphisms through two-sample Mendelian randomization analysis. Five methods, including inverse variance weighting, MR-Egger regression, median weighting, simple model, and weighted model, were used to evaluate the relationship between allergic rhino-conjunctivitis, asthma, and eczema and peripheral blood eosinophil count. Sensitivity analysis (pleiotropy, heterogeneity, and leave-one-out test) was used to evaluate the robustness of the results. There was a significant causal association between SNPs of allergic rhinitis , allergic conjunctivitis, asthma, and eczema and SNPs of peripheral blood eosinophil count. The sensitivity analysis of SNP instrumental variables showed no significant heterogeneity or pleiotropy, indicating that the results are robust. Evidence shows that peripheral blood eosinophil count is associated with an increased risk of allergic rhino-conjunctivitis, asthma, and eczema.

Keywords: Mendelian Randomization Analysis; Allergic Rhino-Conjunctivitis; Eosinophil Count

1. Introduction

Allergic rhinitis (AR) is a local allergic reaction disease, predominantly presenting with symptoms such as nasal itching, sneezing, clear nasal discharge, and nasal obstruction. It falls under type IV hypersensitivity reaction mediated by immunoglobulin E (IgE). Studies have demonstrated that in patients with AR, there is an infiltration of mast cells and eosinophils in the local area of the nasal cavity within the peripheral blood. The main pathological changes in the nasal mucosa mainly involve enhanced vascular permeability, tissue edema, and infiltration of

mast cells and eosinophils. Clinically, the infiltration of eosinophils in the peripheral blood can be utilized to predict the hormone resistance status and treatment outcomes of patients.

Allergic diseases are a common category of chronic immune disorders, encompassing AR, allergic conjunctivitis (AC), asthma, eczema (atopic dermatitis), food allergy, and so on. AR is frequently accompanied by diseases such as AC, asthma, and eczema, and this is even more prevalent in seasonal AR. It severely impacts the social life of patients and is often accompanied by emotional disorders. AR and AC are often collectively referred to as allergic rhino-conjunctivitis (ACR). The incidence of AR complicated with asthma ranges from 74% to 100% (Wang et al., 2023), the incidence of AR complicated with AC is between 30% and 71% (Leonardi et al., 2015), and the incidence of AR complicated with eczema is 9.2% (Camilla et al., 2020).

Eosinophilic asthma (allergic asthma) accounts for 70% to 80%. The allergic reaction in the human body mainly refers to the process in which when the same allergen re-enters the body, it specifically binds to the antibodies on the surface of the sensitized basophil granulocytes (BASO), leading to the release of bioactive mediators mainly composed of histamine from these cells. During this process, eosinophils (EOS) among white blood cells exhibit an antagonistic effect with basophil granulocytes (BASO). EOS release histaminase and arylsulfatase to inactivate the histamine and leukotrienes released by BASO, phagocytize the particles expelled by BASO, and simultaneously produce prostaglandin E1 to inhibit the degranulation process of BASO (Ogawa et al., 2024). Research has revealed that EOS is associated with the onset of allergic diseases such as ACR and asthma. The release of extracellular vesicles and DNA traps by EOS affects both local and systemic immune responses, thereby further influencing the pathophysiological processes of allergic diseases such as airway inflammation, chronic sinusitis, and atopic dermatitis (Weihrauch et al., 2024). Animal experiments have found that ribonuclease 2 related to EOS in mice can exacerbate the allergic reaction (Nguyen et al., 2024). The aforementioned studies mainly focus on observational studies and basic experimental research, and lack evidence of causal associations. This study aims to start from Mendel's laws of inheritance, use genetic variations strongly correlated with exposure factors as instrumental variables, and infer the causal effects between exposure and outcomes at the genetic level. In this study, we employ the method of Mendelian randomization (MR) to explore the potential causal relationships between EOS and genetic variations associated with ACR, asthma, and eczema.

2. Methods

2.1. Research Design

This study employed a two-sample Mendelian randomization (MR) method to evaluate the causal effect relationships between eosinophils (EOS) and allergic rhino-conjunctivitis (ACR), asthma, and eczema. The MR analysis adheres to the following three core assumptions (Davey et al., 2020): (1) Association assumption: The instrumental variables of single nucleotide polymorphisms (SNPs) must be closely related to the exposure factors; (2) Independence assumption: Genetic variations are independent of the confounding factors that affect both the

exposure and the outcome; (3) Exclusivity assumption: SNPs can only influence the outcome through the exposure.

2.2. Data Sources

The data for allergic rhinitis (AR), allergic conjunctivitis (AC), asthma, and eczema were derived from the Genome-Wide Association Study (GWAS) summary data. AR included 217,914 European individuals with 16,380,461 SNPs, and the summary data was publicly available from https://gwas.mrcieu.ac.uk/datasets/finn-b-ALLERG_RHINITIS/; AR included 218,792 European individuals with 16,380,466 SNPs, and the summary data was publicly available from https://gwas.mrcieu.ac.uk/datasets/finn-b-H7_ALLERGICCONJUNCTIVITIS/; Asthma included 361,194 European individuals with 10,443,939 SNPs, and the summary data was publicly available from https://gwas.mrcieu.ac.uk/datasets/ukb-d-J10_ASTHMA/; Eczema included 218,792 European individuals with 16,380,466 SNPs, and the summary data was publicly available from https://gwas.mrcieu.ac.uk/datasets/finn-b-L12_DERMATITISECZEMA/. The peripheral blood EOS count was obtained from the GWAS summary data, which included 563,946 European individuals, and the summary data was publicly available from https://gwas.mrcieu.ac.uk/datasets/ieu-b-33/. The research data was sourced from publicly available GWAS databases, and there were no ethical issues involved.

2.3. Selection of Instrumental Variables

The instrumental variables were required to satisfy the condition that the selected SNPs were closely related to AR, AC, asthma, and eczema. The threshold for instrumental variables was set at $P < 5\times10\text{-}8$. Linkage disequilibrium (LD) was removed to ensure that the selected SNPs were independent of each other (Slatkin et al., 2008). The screening criteria were $R2 < 0.001$ and KB = 10,000, and the screening was carried out using the two-sample MR package in R software. The F statistic ($F = \beta2/sx2$) was calculated to further verify the association assumption and to exclude the bias of weak instrumental variables ($F < 10$), so as to determine the final instrumental variables.

2.4. Statistical Methods

2.4.1. Main Causal Relationship Assessment

In this study, five methods, namely inverse variance weighting (IVW), MR-Egger, weighted median, simple model, and weighted mode, were used to evaluate the causal relationships between AR, AC, asthma, eczema, and the peripheral blood EOS count. IVW is the main evaluation method. When all SNPs are valid instrumental variables, the test efficiency of the IVW causal relationship is the highest. The MR-Egger regression slope coefficient is used to evaluate the true causal effect. When there are pleiotropic instrumental variables, the reliability of the causal evaluation will be affected (Bowden et al., 2015). The weighted median method and the IVW method complement each other. Even if half of the instrumental variables are invalid, they can still provide consistent causal relationships. The weighted median method can also be used as a sensitivity analysis to assess the robustness of the causal association (Bowden et al., 2016). The simple model and the weighted mode method can be used as auxiliary methods for the causal

effect test. The results of the causal effect evaluation are usually expressed by the odds ratio (OR) and the 95% confidence interval (CI).

2.4.2. Sensitivity Analysis

In this study, the heterogeneity of the causal effect was evaluated by the Cochran Q test. When the result heterogeneity is large, a random effects model is selected; conversely, a fixed effects model is selected. When $P < 0.1$, it indicates the presence of heterogeneity (Burgess & Bowden, 2017). MR-Egger and MR-PRESSO were used to test the horizontal pleiotropy in the MR analysis. When there is no statistical difference between the MR-Egger intercept and zero, it indicates the absence of pleiotropy (Burgess & Thompson, 2017). The leave-one-out method tests the effect size of the remaining SNPs by removing SNPs one by one to evaluate the robustness of the results (Hemani et al., 2018). All data analyses were performed in R software version 4.2.2, using the Two Sample MR software package (version 4.41).

3. Results

3.1. Determination of Instrumental Variables

The R software was used to screen for single nucleotide polymorphisms (SNPs) that were closely related to the exposure. The fact that all F statistics were > 10 indicated the absence of weak instrumental variables. A total of 448 SNPs were extracted as instrumental variables from the Genome-Wide Association Study (GWAS) data of the peripheral blood eosinophil (EOS) count. Among them, 440 SNPs were significantly associated with allergic rhinitis (AR), 440 SNPs were significantly associated with allergic conjunctivitis (AC), 154 SNPs were significantly associated with asthma, and 145 SNPs were significantly associated with eczema.

3.2. Analysis of Main Results

The results of the inverse variance weighting (IVW) method for the peripheral blood EOS count data suggested a clear causal relationship between allergic rhino-conjunctivitis (ACR), asthma, eczema, and the risk of the peripheral blood EOS count (Odds Ratio [OR] = 1.507, 95% Confidence Interval [CI]: 1.383–1.643; OR = 1.335, 95% CI: 1.249–1.428; OR = 1.228, 95% CI: 1.118–1.350; OR = 1.228, 95% CI: 1.161–1.300). The results of the MR-Egger, weighted median, simple model, and weighted mode methods supported the above conclusions, as shown in Table 1.

Table 1. Results of the Mendelian Randomization (MR) Analysis of the Correlation between Allergic Rhinitis, Allergic Conjunctivitis, Asthma, Eczema, and the Peripheral Blood Eosinophil Count

Indicators	Methods	β	SE	OR（95%CI）	P value
AR	IVW	0.410	0.044	1.507(1.383, 1.643)	<0.01
	MR Egger	0.273	0.110	1.314(1.059, 1.631)	0.014

	Simple Mode	0.319	0.210	1.376(0.912,2.074)	0.129
	Weighted Median	0.365	0.078	1.440(1.235,1.679)	<0.01
	Weighted Mode	0.406	0.132	1.501(1.158,1.946)	0.002
AC	IVW	0.289	0.034	1.335(1.249, 1.428)	<0.01
	MR Egger	0.229	0.084	1.258(1.067,1.483)	0.007
	Simple Mode	0.224	0.176	1.251(0.886,1.768)	0.204
	Weighted Median	0.297	0.062	1.345(1.191,1.519)	<0.01
	Weighted Mode	0.296	0.0987	1.345(1.108,1.632)	0.003
asthma	IVW	0.003	0.000	1.228(1.118,1.350)	<0.01
	MR Egger	0.001	0.001	1.001(0.999, 1.004)	0.301
	Simple Mode	0.003	0.002	1.003(0.999,1.008)	0.108
	Weighted Median	0.003	0.001	1.003(1.002,1.005)	<0.01
	Weighted Mode	0.002	0.002	1.002(0.998,1.006)	0.374
eczema	IVW	0.206	0.029	1.228(1.161,1.300)	<0.01
	MR Egger	0.0979	0.114	1.103(0.882, 1.378)	0.391
	Simple Mode	0.001	0.135	1.001(0.768,1.305)	0.993
	Weighted Median	0.086	0.052	1.090(0.984,1.208)	0.098
	Weighted Mode	0.057	0.085	1.059(0.897,1.251)	0.500

3.3. Results of Sensitivity Analysis

In the Cochran Q heterogeneity test, the Q values of both the inverse variance weighting (IVW) method and the MR-Egger method were greater than 0.1, indicating the absence of heterogeneity, as shown in Table 2. In the leave-one-out method analysis, no single single nucleotide

polymorphism (SNP) that significantly affected the results and undermined the robustness of the results was found, as shown in Figure 1.

Table 2. Results of the Sensitivity, Heterogeneity, and Horizontal Pleiotropy Tests of the Instrumental Variables

Eosinophil	Cochran Q value	P value
AR	702.63	1.462231e-15
AC	672.76	4.501209e-13
asthma	264.44	4.311666e-08
Eczema	388.45	5.272859e-25

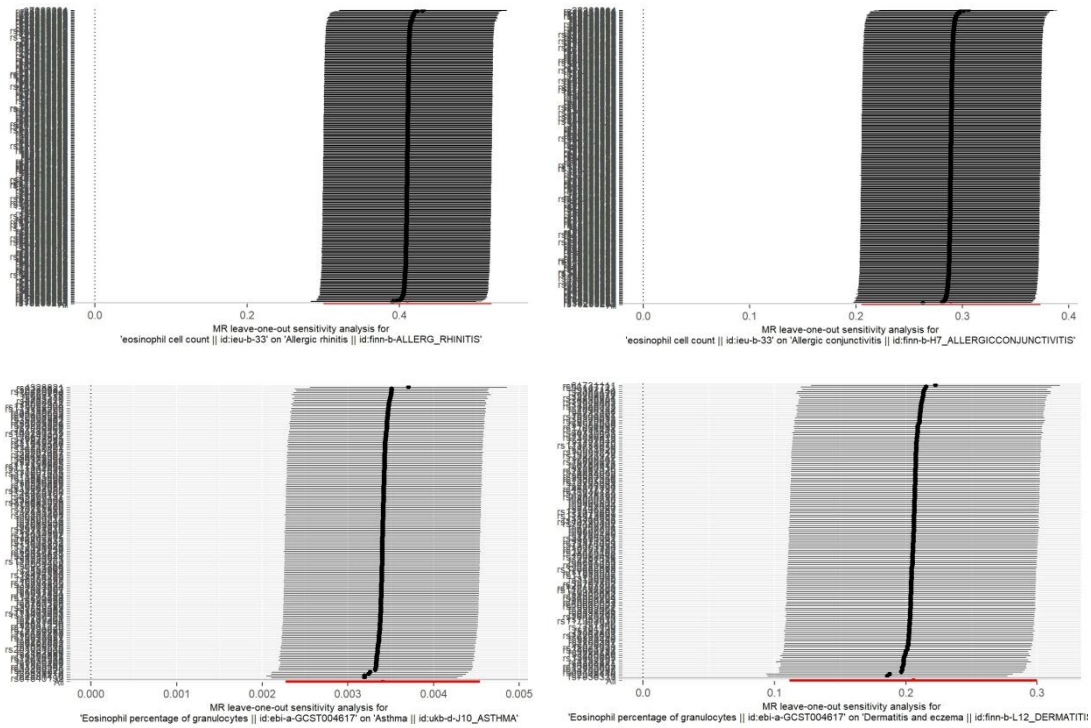

Figure 1. Sensitivity Test by the Leave-One-Out Method

4. Conclusion

In this study, the publicly available data on peripheral blood eosinophil (EOS) count, allergic rhino-conjunctivitis (ACR), asthma, and eczema from the Genome-Wide Association Study (GWAS) database were utilized to conduct a two-sample Mendelian randomization (MR) analysis. The results showed a significant correlation between the peripheral blood EOS count and the occurrence of ACR, asthma, and eczema. A potential causal association was found between the peripheral blood EOS count and the risk of allergic rhinitis (AR), which is consistent with the

results of previous studies on the peripheral blood EOS count and AR (Pranavi et al., 2024), once again verifying the causal effect between the peripheral blood EOS count and AR at the gene level. In this study, the GWAS database was used, and the MR analysis method was adopted to further explore the associations between EOS and allergic conjunctivitis (AC), asthma, and eczema. The results suggested a significant correlation between the peripheral blood EOS count and the occurrence of these three diseases. For the first time, it was proposed that the peripheral blood EOS count is a risk factor for ACR, asthma, and eczema, and it was found that there are also causal effects between the peripheral blood EOS count and ACR, asthma, and eczema at the gene level. The above findings suggest that controlling the peripheral blood EOS count may be beneficial for the prevention and management of the occurrence and development of ACR, asthma, and eczema, providing important evidence for future research on drug interventions for such diseases.

Allergic diseases (such as allergic rhinitis) are caused by the body's abnormal type 2 immune response to harmless antigens in the environment. They include atopic dermatitis, allergic asthma, AR, AC, and allergic urticaria, etc. (Cao et al., 2024). These are inflammatory comorbidities with a genetic predisposition and a chronic and recurrent manifestation. Currently, in the fields of genomics, transcriptomics, proteomics, epigenetics, metagenomics, and metabolomics, some biomarkers and potential targets of reference value have been discovered (Hao et al., 2025). EOS and mast cells are key effector cells in allergies (Gangwar et al., 2021). If the late phase of the allergic reaction does not subside, it can develop into the chronic stage, that is, the stage of allergic inflammatory reaction. This involves a large number of mast cells and EOS coexisting in the inflamed tissues during the late phase and chronic stage. The bidirectional interaction between them is mediated through cell surface receptors (such as CD48, 2B4 and their respective ligands), intercellular contact, and the release of mediators (such as various specific granular mediators, metabolites of arachidonic acid, cytokines, and chemokines), which keeps the allergic inflammation in a continuous cycle. The latest research has found that the degranulation of EOS is regulated by the miR-223-3p/FBXW7 targeting, thereby enhancing the allergic inflammation of AR. The miR-223-3p/FBXW7 axis related to EOS provides a new method for the treatment of AR (Wu et al., 2023). Observational studies (Fernandez et al., 2022) have shown that EOS plays a central role in the pathophysiology of chronic ocular allergies such as AC in spring and in maintaining the immune response. Therefore, research on EOS-related cell subtypes, receptors, and mediator release is helpful for the precise treatment of allergic diseases. The activation state of EOS in the blood and airways and its state after encountering inflammatory mediators determine the multiple roles of EOS in type 2 inflammation. Airway epithelial cells play a sentinel role, which can guide the aggregation and migration of EOS and play an important role in the pathogenesis of asthma (Steffan et al., 2024). Different from clinical observational studies and laboratory studies, the GWAS data used in this study has the advantages of a large sample size and being unaffected by external confounding factors. Therefore, the results are reliable. This study explains the causal relationship between EOS and ACR, asthma, and eczema at the gene level, and further confirms the relationship between EOS and allergic diseases as well as the relevance of the pathological mechanisms. It is a powerful complement to clinical observations and laboratory research.

Author Contributions:

Conceptualization, W. Z and J. Y.; methodology, G. L.; software, G. L.; validation, W. Z.; formal analysis, G. L.; investigation, W. Z.; resources, W. Z and G. L.; data curation, G. L.; writing—original draft preparation, W. Z.; writing—review and editing, J. Y.; visualization, W. Z.; supervision, G. L.; project administration, W. Z., G. L.; funding acquisition, W. Z., J. Y. All authors have read and agreed to the published version of the manuscript.

Funding:

This research was funded by National Population Health Science Data Center of Chinese Academy of Medical Sciences, grant number NCMI202409A08; National Natural Science Foundation of China, grant number 82205206; Talent Training Project of Dongzhimen Hospital of Beijing University of Chinese Medicine, grant number DZMG-ONGG0006.

Institutional Review Board Statement:

Not applicable.

Informed Consent Statement:

Not applicable.

Data Availability Statement:

Not applicable.

Acknowledgments:

The authors acknowledge for efforts of the authors.

Conflict of Interest:

The authors declare no conflict of interest.

References

Bowden, J., Davey Smith, G., & Burgess, S. (2015). Mendelian randomization with invalid instruments: effect estimation and bias detection through Egger regression. International journal of epidemiology, 44(2), 512-525.

Bowden, J., Davey Smith, G., Haycock, P. C., & Burgess, S. (2016). Consistent estimation in Mendelian randomization with some invalid instruments using a weighted median estimator. Genetic epidemiology, 40(4), 304-314.

Burgess, S., & Thompson, S. G. (2017). Interpreting findings from Mendelian randomization using the MR-Egger method. European journal of epidemiology, 32, 377-389.

Burgess, S., Bowden, J., Fall, T., Ingelsson, E., & Thompson, S. G. (2017). Sensitivity analyses for robust causal inference from Mendelian randomization analyses with multiple genetic variants. Epidemiology, 28(1), 30-42.

Cao, Z., Li, Q., Li, Y., & Wu, J. (2024). Identification of plasma protein markers of allergic disease risk: a mendelian randomization approach to proteomic analysis. BMC genomics, 25(1), 503.

Davey Smith, G., Holmes, M. V., Davies, N. M., & Ebrahim, S. (2020). Mendel ' s laws, Mendelian randomization and causal inference in observational data: substantive and nomenclatural issues. European journal of epidemiology, 35(2), 99-111.

Fernandez, A., Asbell, P., & Roy, N. (2022). Emerging therapies targeting eosinophil-mediated inflammation in chronic allergic conjunctivitis. The Ocular Surface, 26, 191-196.

Gangwar, R. S., Pahima, H., Puzzovio, P. G., & Levi-Schaffer, F. (2021). Update on eosinophil interaction with mast cells: the allergic effector unit. Eosinophils: Methods and Protocols, 221-242.

Hao, Y., Yang, Y., Zhao, H., Chen, Y., Zuo, T., Zhang, Y., ... & Song, X. (2025). Multi-omics in Allergic Rhinitis: Mechanism Dissection and Precision Medicine. Clinical Reviews in Allergy & Immunology, 68(1), 19.

Hemani, G., Zheng, J., Elsworth, B., Wade, K. H., Haberland, V., Baird, D., ... & Haycock, P. C. (2018). The MR-Base platform supports systematic causal inference across the human phenome. elife, 7, e34408.

Jøhnk, C., Høst, A., Husby, S., Schoeters, G., Timmermann, C. A. G., Kyhl, H. B., ... & Jensen, T. K. (2020). Maternal phthalate exposure and asthma, rhinitis and eczema in 552 children aged 5 years; a prospective cohort study. Environmental Health, 19, 1-10.

Leonardi, A., Castegnaro, A., Valerio, A. L. G., & Lazzarini, D. (2015). Epidemiology of allergic conjunctivitis: clinical appearance and treatment patterns in a population-based study. Current opinion in allergy and clinical immunology, 15(5), 482-488.

Nguyen, L. M., Kanda, A., Kamioka, Y. (2024). Mouse eosinophil-associated ribonuclease-2 exacerbates the allergic response. Allergy,79(8), 2251-2255.

Ogawa, T., Maki, Y., Takahashi, S., Ono, T., Sato, K., Kawana, A., & Kimizuka, Y. (2025). Airway Epithelium-derived CXCL14 Promotes Eosinophil Accumulation in Allergic Airway Inflammation. American Journal of Respiratory Cell and Molecular Biology, 72(2), 39141567.

Pranavi, V., Kulkarni, K. D., & KULKARNI, K. D. (2024). Allergen Sensitivity Patterns and Their Correlation With Total Serum IgE Levels and Absolute Eosinophil Counts Among Patients With Allergic Rhinitis and Asthma in North Karnataka. Cureus, 16(8), e67183.

Slatkin, M. (2008). Linkage disequilibrium—understanding the evolutionary past and mapping the medical future. Nature Reviews Genetics, 9(6), 477-485.

Steffan, B. N., Townsend, E. A., Denlinger, L. C., & Johansson, M. W. (2024). Eosinophil-epithelial cell interactions in Asthma. International Archives of Allergy and Immunology, 185(11), 1033-1047.

Wang, M., Gong, L., Luo, Y., He, S., Zhang, X., Xie, X., ... & Feng, X. (2023). Transcriptomic analysis of asthma and allergic rhinitis reveals CST1 as a biomarker of unified airways. Frontiers in Immunology, 14, 1048195.

Weihrauch, T., Melo, R. C., Gray, N., Voehringer, D., Weller, P. F., & Raap, U. (2024). Eosinophil extracellular vesicles and DNA traps in allergic inflammation. Frontiers in Allergy, 5, 1448007.

Wu, S., Wang, Z., Zhu, Y., Zhu, X., Guo, L., Fu, Y., ... & Liu, Y. (2023). MiR-223-3p regulates the eosinophil degranulation and enhances the inflammation in allergic rhinitis by targeting FBXW7. International Immunopharmacology, 118, 110007.

Advances in World Medical Research, 2025, 1(1), 71-77
https://doi.org/10.71204/qbn44528

Analysis of 43 Cases of Difficulties in Removing Artificial Nasolacrimal Duct Stents after Implantation

Jiaxin Chen [1], Jinxin Chen [1], Licong Nie [1], Yonggang Liu [1,*]

[1] Eye Hospital, China Academy of Chinese Medical Sciences, Beijing 110000, China

*** Correspondence**:

Yonggang Liu

ygliu0208@163.com

Received: 15 April 2025/ Accepted: 16 May 2025/ Published online: 20 May 2025

Abstract

To explore the causes of difficulties in removing artificial nasolacrimal duct stents after implantation, analyze the bony structural characteristics of the nasolacrimal duct and its impaction causes, and study the structural features of the nasolacrimal duct under paranasal sinus CT, so as to provide references for clinical practice. The clinical data of 43 patients (44 sides) with difficulties in removing artificial nasolacrimal ducts after implantation from October 2018 to June 2022 were retrospectively analyzed, including the patients' age, concurrent diseases, catheterization time, etc. The removal of the nasolacrimal duct was performed under nasal endoscopy, and 40 patients underwent paranasal sinus CT examination. Among the 44 cases of difficult tube removal, 43 cases were successfully removed, and 1 case was not removed. The reasons for the difficulties included the detachment or inversion of the traction wire (30 cases), the impaction of the tube head ring (11 cases), the fracture of the nasolacrimal duct due to long - term catheterization (1 case), and suture fixation during the catheterization operation (1 case). The difficulties in removing artificial nasolacrimal duct stents are related to factors such as the position of the traction wire, the impaction of the tube body, the degeneration of the nasolacrimal duct, and nasal diseases. Feasible solutions were also explored. The bony structural characteristics of the nasolacrimal duct, such as narrowness, curvature, and the influence of surrounding bones, increase the difficulty of tube removal. The paranasal sinus CT of 40 cases can show that the structure of the some nasolacrimal duct is different from that of the normal nasolacrimal duct. The research suggests that clinicians should comprehensively consider various factors to optimize the treatment strategy, providing a reference for clinical surgeries.

Keywords: Artificial Nasolacrimal Duct; Difficulties in Tube Removal; Nasal Endoscopy; Bony Structure; Paranasal Sinus CT

1. Introduction

Artificial nasolacrimal duct implantation surgery is a common treatment for lacrimal duct stenosis caused by chronic dacryocystitis and other reasons. It can make the lacrimal duct unobstructed and relieve symptoms such as epiphora, inflammation, and empyema (Nitin et al., 2022; Xie et al., 2017; Kim et al., 2007; Farat et al., 2021; Fayet et al., 2021). At an appropriate time after nasolacrimal duct implantation, if the function of the lacrimal duct returns to normal, in order to reduce complications and prevent the aging of the nasolacrimal duct, the artificial nasolacrimal duct needs to be removed (Karaca et al., 2019; Deosthale et al., 2023). The difficulties in removing the nasolacrimal duct may be related to multiple factors. This article analyzes and summarizes the cases of difficult nasolacrimal duct removal in our department as follows.

2. Materials and Methods

A retrospective analysis was performed on 43 cases (44 sides) of patients who came to our department with difficulties in removing artificial nasolacrimal ducts after implantation from October 2018 to June 2022. The patients' ages ranged from 23 to 72 years old, with an average age of 43 ± 8.1 years old. There were 23 cases with rhinitis, 12 cases with sinusitis, 20 cases with nasal septum deviation, and 33 cases with inferior turbinate hypertrophy.

The catheterization time of the artificial nasolacrimal duct ranged from 3 months to 30 years. Three types of catheters were involved, namely silicone - material nasolacrimal ducts, metal - material nasolacrimal ducts, and artificial synthetic polymer nasolacrimal ducts. The catheterization methods included traction through the lacrimal punctum and retrograde implantation through the nose, with standardized lacrimal duct irrigation (Figure 1).

The removal of the nasolacrimal duct was performed under nasal endoscopy in the otolaryngology department. The nasal cavity was contracted to fully expose the inferior meatus. The tail end of the artificial nasolacrimal duct in the inferior meatus was searched for under a 0 - degree endoscope, and it was clamped and removed with alligator forceps. During the tube - removal process, the force and direction were adjusted according to the resistance (Figure 2). According to the increasing difficulty of tube removal, there were the following four situations: ① The traction wire at the tail end of the nasolacrimal duct fell off or drooped backward, and the tube wall was not impacted. It could be clamped and removed smoothly; ② The tube head or tube body was impacted with resistance. The impacted ring of the nasolacrimal duct was pulled to the nasal meatus, and the ring was cut and removed; ③ The nasolacrimal duct became deformed and broken due to long - term catheterization, and it was removed in segments (Figure 3).

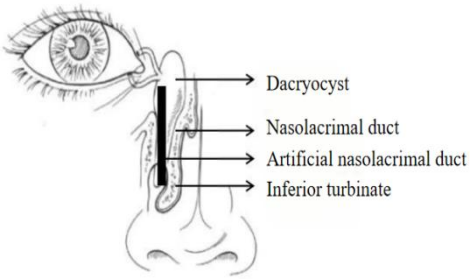

Figure 1. Schematic diagram of nasolacrimal duct implantation

Figure 2. Schematic diagram of nasolacrimal duct removal

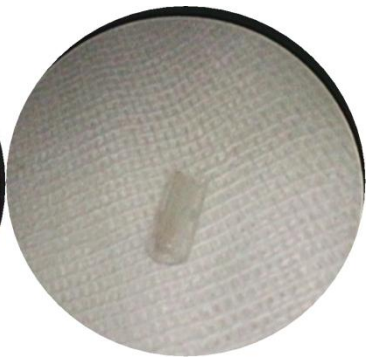

Figure 3. Schematic diagram of removal after nasolacrimal duct rupture

3. Results

Among the 44 cases of difficult tube removal of the artificial nasolacrimal duct, 43 cases were successfully removed, and 1 case was not removed. In 28 cases, the traction wire at the end of the nasolacrimal duct fell off, and it could not be directly removed through the nostril. It was removed under endoscopy. In 2 cases, the traction wire at the end of the nasolacrimal duct drooped backward to the posterior nostril and could not be directly removed through the anterior nostril. It was removed under endoscopy. In 11 cases, the ring at the head of the nasolacrimal duct was impacted and was removed after being cut under endoscopy. In 1 case, the tube body of the nasolacrimal duct that had been catheterized for more than 30 years was broken into 3 segments and was removed under endoscopy. In 1 case, the nasolacrimal duct was sutured and fixed during the catheterization operation, and it could not be removed through the nose. It was removed by incising the lacrimal punctum.

4. Discussion

4.1. Causes of Difficult Tube Removal and Feasible Solutions

The removal of the nasolacrimal duct often faces various challenges in clinical practice. In this study, the removal of the nasolacrimal duct was mainly related to the position of the traction wire, the impaction of the tube body, and the fracture of the nasolacrimal duct due to degeneration. In this study, in 28 cases, the traction wire fell off, and in 2 cases, it drooped backward to the posterior nostril, making it impossible to directly remove the tube through the nostril. This was related to the catheterization time and operation. Long - term catheterization was likely to cause the traction wire to loosen, and improper operation might also damage the traction wire. However, a change in the position of the traction suture does not directly lead to difficulties in removing the nasolacrimal duct.In 11 cases, the ring at the head of the nasolacrimal duct was impacted with resistance, resulting in difficulties in tube removal. Most patients had nasal diseases, which also affected the removal of the nasolacrimal duct. In 1 case, the nasolacrimal duct that had been catheterized for more than 30 years was broken. Due to long - term catheterization, the material of

the nasolacrimal duct aged, and with the erosion of tears and tissue friction, its structure was damaged, increasing the difficulty of tube removal. Previous studies have shown that the nasolacrimal duct itself can cause granulation hyperplasia of the surrounding soft tissues and is prone to adhere to lacrimal duct secretions, increasing the difficulty of removal, which is consistent with the viewpoints of this study (Deosthale et al., 2023).Among the 43 patients, there were 23 cases with rhinitis, 12 cases with sinusitis, 20 cases with nasal septum deviation, and 33 cases with inferior turbinate hypertrophy. These diseases could cause swelling of the nasal mucosa, increased secretions, change the micro - environment around the nasolacrimal duct, affect the operation field of tube removal, and might also cause the nasolacrimal duct to be compressed, deformed, and adhered and impacted (Schleimer, 2017).

Removing the nasolacrimal duct within an appropriate time can prevent complications and material aging. Some studies have also shown that the implantation of artificial nasolacrimal duct stents can cause changes in the position of the eyelid (Vu et al., 2022). At present, the use of new biodegradable nasolacrimal ducts can reduce complications, but the long - term efficacy is still controversial (Zhan et al., 2017). If preparations with anti - inflammatory and immunosuppressive effects are used, such as ophthalmic ointment and low - dose mitomycin used by previous teams, it may reduce the possibility of difficult removal (Masoomian et al., 2021).

4.2. Analysis of the Bony Structural Characteristics of the Nasolacrimal Duct and its Impaction Causes

The physiological stenosis, curved course, non - uniform thickness of the nasolacrimal duct, and excessive insertion depth of the nasolacrimal duct are the causes of impaction during difficult tube removal. Its course is not only curved, but also its diameter is not uniform. It is usually the widest at the lacrimal sac and gradually becomes thinner when passing through the maxilla. This feature needs to be paid special attention to during tube removal (Ali, 2023).

In this study, the impaction during the removal of the nasolacrimal duct in 11 cases might be due to individual anatomical variations, resulting from the special structural problem that the ring at the head of the nasolacrimal duct is larger than the lumen of the human nasolacrimal duct. However, impaction is not only a problem of the structure of the tube head of the nasolacrimal duct, but also related to anatomical depth, physiological stenosis, improper catheterization, and interference from surrounding tissues. If the angle and position are inaccurate during catheterization, impaction is likely to occur.Some studies believe that primary acquired nasolacrimal duct obstruction can lead to changes in the thickness of the periosteum and fibrosis, which may also be one of the causes of impaction during the removal of the artificial nasolacrimal duct (Ali, 2021). Long - term inflammatory stimulation can cause thickening and adhesion of the soft tissues around the artificial nasolacrimal duct, also resulting in impaction of the nasolacrimal duct (Yazici et al., 2002; Prasad & Ghosh, 2020; Orsolini et al., 2020).

4.3. Analysis and Characteristics of the Nasolacrimal Duct Structure in 40 Cases of Paranasal Sinus CT

In 12 patients with a history of sinusitis surgery, the mucosa in the paranasal sinuses was thickened, showing a soft - tissue density shadow. In a small number of patients, the bones around

the nasolacrimal duct were blurred and thickened due to inflammation. On CT, it was manifested as the dilation of the nasolacrimal duct, increased density in the lumen, and the spread of inflammation in the paranasal sinuses to the surrounding area of the nasolacrimal duct, indicating that sinusitis might cause inflammation and adhesion, affecting the structure and function of the nasolacrimal duct (Desai et al., 2022; Campos-Navarro et al., 2023). In 23 patients with a history of rhinitis surgery, there were no obvious changes in the paranasal sinus CT. In 20 patients with a history of nasal septum deviation surgery, the paranasal sinus CT showed that the deviated part of the nasal septum compressed the ipsilateral nasal cavity structure, causing different displacements and deformations of the attachment of the nasolacrimal duct on the lateral wall of the nasal cavity due to different degrees of compression. In 33 cases with inferior turbinate hypertrophy, the CT suggested that part of the nasolacrimal duct was locally compressed and deformed.

Author Contributions:

Jiaxin Chen and Yonggang Liu designed the work; Jinxin Chen and Nie Licong contributed to the acquisition, analysis, and interpretation of data; Jiaxin Chen and Yonggang Liu wrote the main manuscript and prepared all the figures. Jiaxin Chen and Yonggang Liu revised the manuscript. All authors reviewed the manuscript.

Funding:

This work was supported by the grant of Project in Eye Hospital China Academy of Chinese Medical Science (No.202015/No.202026), Central High-Level Traditional Chinese Medicine Hospital Project of eye Hospital China Academy of Chinese medical science (No.GSP5-36/No.GSP5-80), Fundamental Research Funds for the Central Public Welfare Research Institutes No. ZZ17-XRZ-085).

Institutional Review Board Statement:

The studies were reviewed and approved by the Ethics Committee of the Eye Hospital of the China Academy of Chinese Medical Sciences.

Informed Consent Statement:

Not applicable.

Data Availability Statement:

Not applicable.

Acknowledgments:

The authors acknowledge for the support and technical comments of all reviewers.

Conflict of Interest:

The authors declare no conflict of interest.

References

Ali, M. J. (2023). Etiopathogenesis of primary acquired nasolacrimal duct obstruction (PANDO). Progress in Retinal and Eye Research, 96, 101193.

Ali, M. J., Mishra, D. K., & Bothra, N. (2021). Lacrimal fossa bony changes in chronic primary acquired nasolacrimal duct obstruction and acute dacryocystitis. Current Eye Research, 46(8), 1132-1136.

Campos-Navarro, L. A., Ibarra-Macari, M. E., Barrón-Campos, A. C., Moreno-Martínez, J. M., & Almeyda-Farfán, J. A. (2023). Hallazgos nasosinusales por tomografía computada en dacriocistitis crónica pediátrica. Cirugía y cirujanos, 91(1), 87-93.

Deosthale, N., Garikapati, P., Choudhary, S., Khadakkar, S., Deshpande, A., Mangade, S., & Dhote, K. (2023). Surgical Outcome of Endoscopic Dacryocystorhinostomy with and Without Prolene Stent in Chronic Dacryocystitis: A Randomized Controlled Trial. Indian Journal of Otolaryngology and Head & Neck Surgery, 75(4), 3443-3448.

Desai, A. B., Vibhute, P., & Bhatt, A. A. (2022). Obliterative sinusitis: an underreported clinical entity. Clinical Imaging, 81, 72-78.

Farat, J. G., Schellini, S. A., Dib, R. E., Santos, F. G. D., Meneghim, R. L. F. S., & Jorge, E. C. (2021). Probing for congenital nasolacrimal duct obstruction: a systematic review and meta-analysis of randomized clinical trials. Arquivos Brasileiros de Oftalmologia, 84(1), 91-98.

Fayet, B., Racy, E., Ruban, J. M., Katowitz, J. A., Katowitz, W. R., & Brémond-Gignac, D. (2021). Preloaded Monoka (Lacrijet) and congenital nasolacrimal duct obstruction: initial results. Journal Français d'Ophtalmologie, 44(5), 670-679.

Karaca, U., Genc, H., & Usta, G. (2019). Canalicular laceration (cheese wiring) with a silicone tube after endoscopic dacryocystorhinostomy: when to remove the tube?. GMS ophthalmology cases, 9, 31728262.

Kim, N. J., Kim, J. H., Hwang, S. W., Choung, H. K., Lee, Y. J., & Khwarg, S. I. (2007). Lacrimal silicone intubation for anatomically successful but functionally failed external dacryocystorhinostomy. Korean Journal of Ophthalmology, 21(2), 70-73.

Masoomian, B., Eshraghi, B., Latifi, G., & Esfandiari, H. (2021). Efficacy of probing adjunctive with low-dose mitomycin-C irrigation for the treatment of epiphora in adults with nasolacrimal duct stenosis. Taiwan Journal of Ophthalmology china, 11(3), 287-291.

Nitin, T., Uddin, S., & Paul, G. (2022). Endonasal Endoscopic Dacryocystorhinostomy with and Without Stents−A Comparative Study. Indian Journal of Otolaryngology and Head & Neck Surgery, 74(Suppl 2), 1433-1441.

Orsolini, M. J., Schellini, S. A., Souza Meneguim, R. L. F., & Catâneo, A. J. M. (2020). Success of endoscopic dacryocystorhinostomy with or without stents: systematic review and meta-analysis. Orbit, 39(4), 258-265.

Prasad, B. K., & Ghosh, K. K. (2020). Evaluation and comparison of the outcomes of endoscopic dacryocystorhinostomy with and without silicone stent. Bengal Journal of Otolaryngology and Head Neck Surgery, 28(3), 221-227.

Schleimer, R. P. (2017). Immunopathogenesis of chronic rhinosinusitis and nasal polyposis. Annual Review of Pathology: Mechanisms of Disease, 12(1), 331-357.

Vu, Q. A., Youn, J. M., & Baek, S. (2022). Changes in Eyelid Position Following Silicone Tube Insertion and Removal in Dacryocystorhinostomy. Journal of Craniofacial Surgery, 33(3), e223-e226.

Xie, C., Zhang, L., Liu, Y., Ma, H., & Li, S. (2017). Comparing the success rate of dacryocystorhinostomy with and without silicone intubation: a trial sequential analysis of randomized control trials. Scientific reports, 7(1), 1936.

Yazici, Z., Yazici, B., Parlak, M., Tuncel, E., & Ertürk, H. (2002). Treatment of nasolacrimal duct obstruction with polyurethane stent placement: long-term results. American Journal of Roentgenology, 179(2), 491-494.

Zhan, X., Guo, X., Liu, R., Hu, W., Zhang, L., & Xiang, N. (2017). Intervention using a novel biodegradable hollow stent containing polylactic acid-polyprolactone-polyethylene glycol complexes against lacrimal duct obstruction disease. PLoS One, 12(6), e0178679.